Seismically imaging (continental) magma reservoirs

Rhyolitic magmatism at Yellowstone, Long Valley

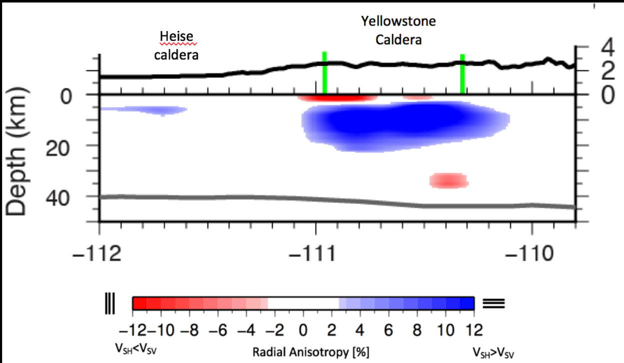

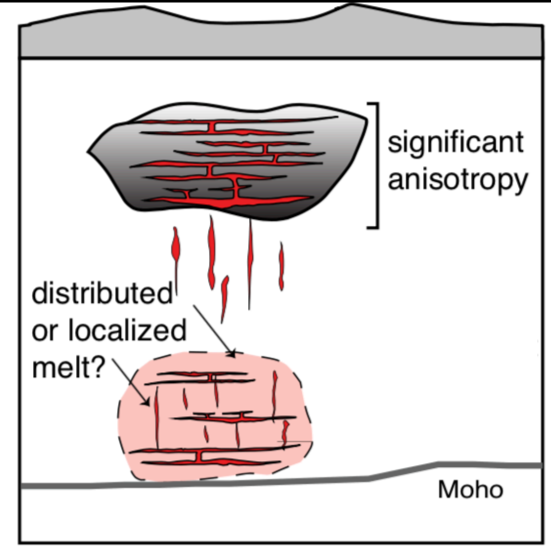

Chengxin Jiang et al., 2018

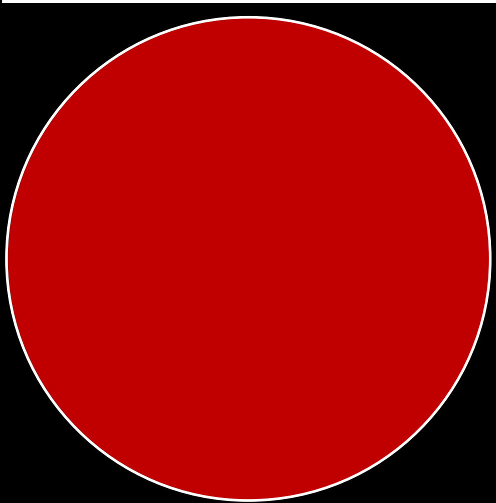

Yellowstone 0.64 Ma
Eruptive volume

Dacitic arc magmatism at Mount St. Helens

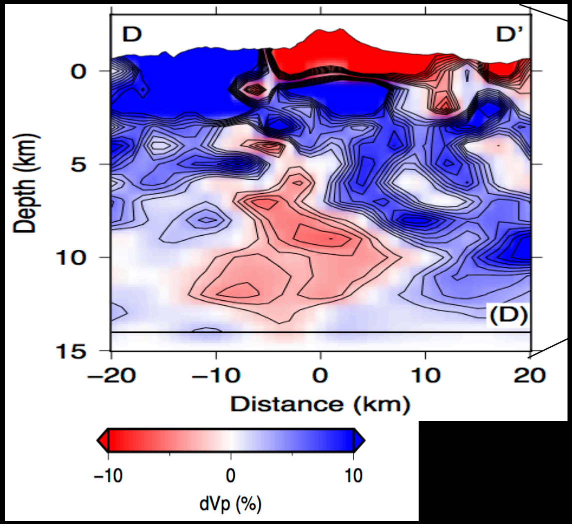

Eric Kiser et al., 2018

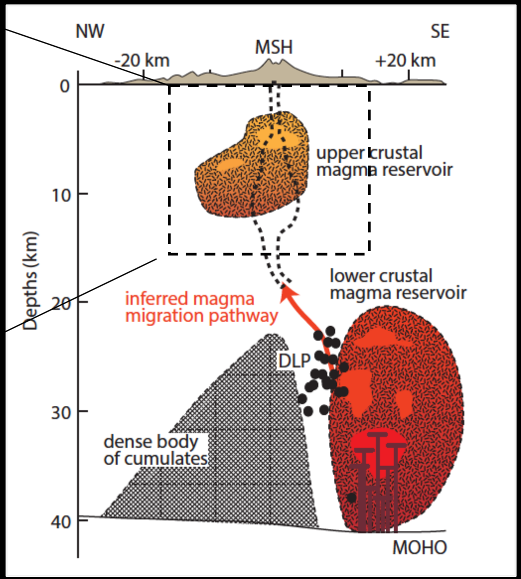

Maren Wanke, Olivier Bachmann

Mount St. Helens 1980
Eruptive volume

THE UNIVERSITY of NEW MEXICO

Brandon Schmandt, Chengxin Jiang[1], Steven Hansen[2]

[1]now at Harvard University; [2]now at Macquarie University

Geo PRISMS earthscope NSF

Seismically imaging (continental) magma reservoirs

Why?

Voluminous silicic eruptions require extensive geochemical evolution in the crust, which should leave an expression in seismic properties.

- How to identify the current life-cycle stage?
    - Where and how much magma is stored?
    - Geometry of transport pathways?

- Guidance for physical models
- Differences in magmatic system structure underlying eruptive characteristics (e.g., smaller and larger volume systems)?

Mount St. Helens

Long Valley & Yellowstone

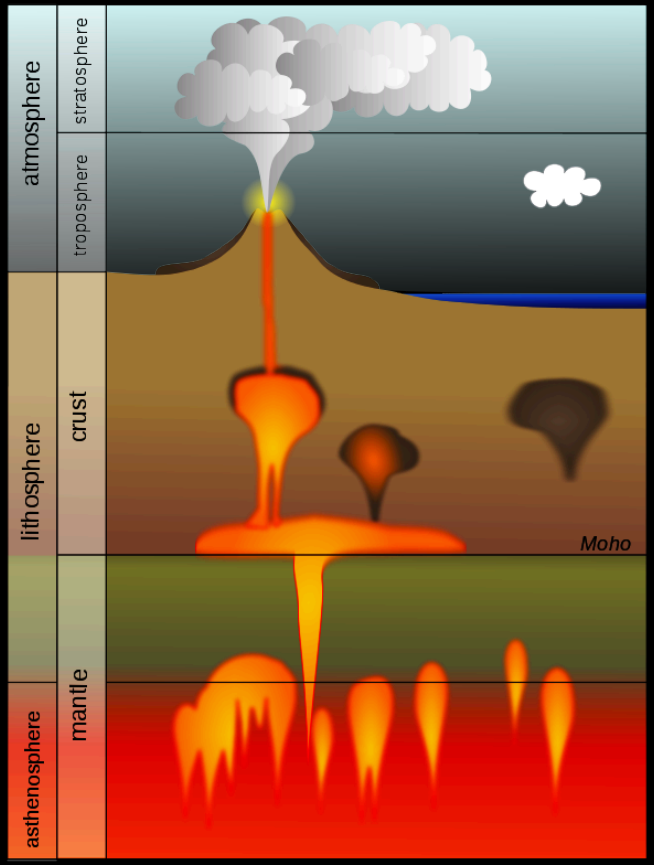

(USGS)

Getting data – Broadband 3-C Seismographs

Justin Wilgus, Margaret Glasgow, Steve Hansen

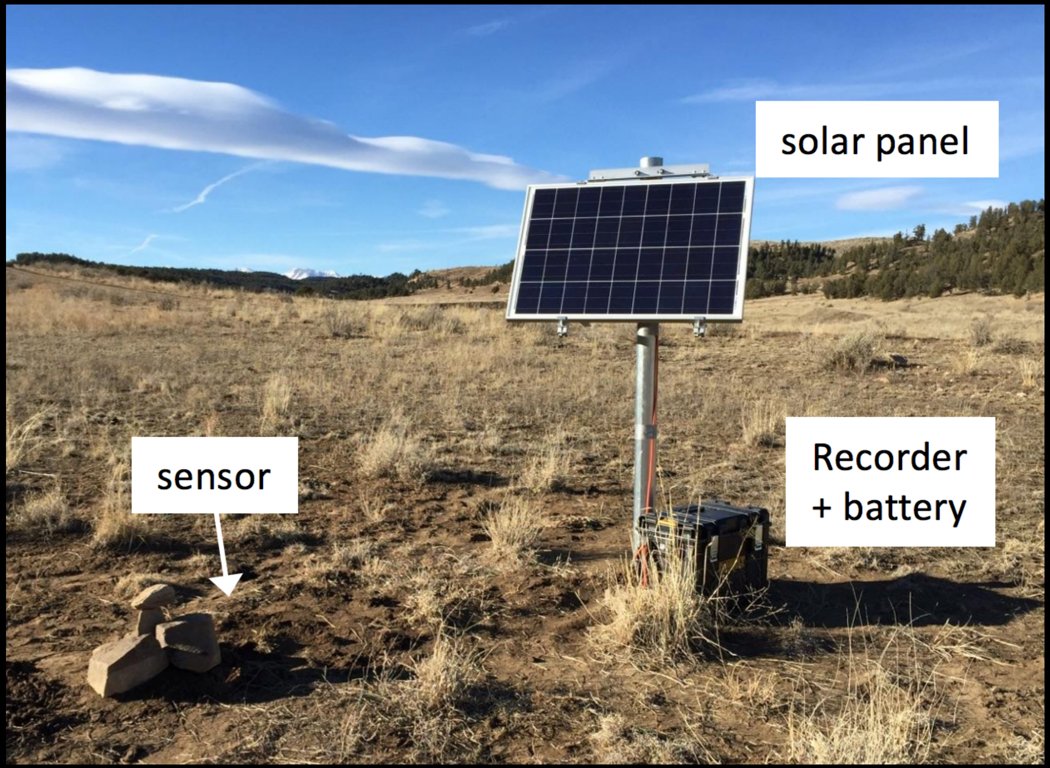

Data are very versatile due to broadband and 3-C, but expensive and can only install a few per day at most.
Once running, can collect long continuous time series

Rapidly deployable short-period and cable-free seismographs

Autonomous seismographs or 'nodes':
-cable-free
-GPS clock
-24-bit digitizer
- ~1 month battery life

Fairfield Nodal Zland

Steve Hansen and Wes Thelen on the new dome at Mount St. Helens

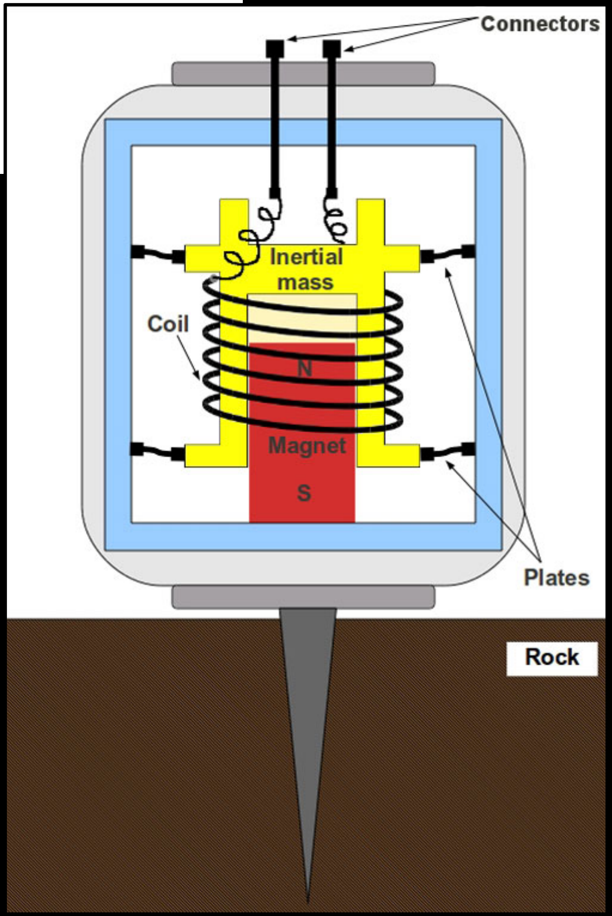

The other way to deploy
1,000’s of sensors…

Cabled geophones

Not feasible in rugged topography, urban areas, or areas that require low-impact

1,000 nodes

13 Students from U. New Mexico
and Portland State University
2 field techs from NodalSeismic

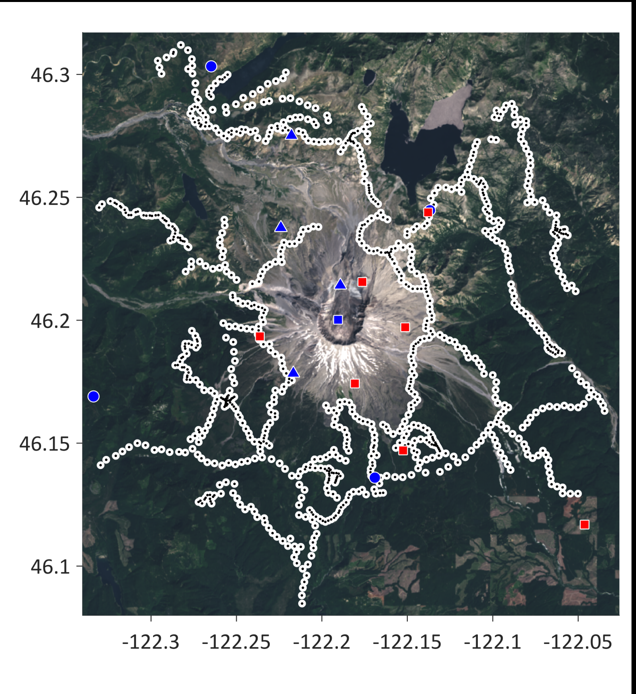

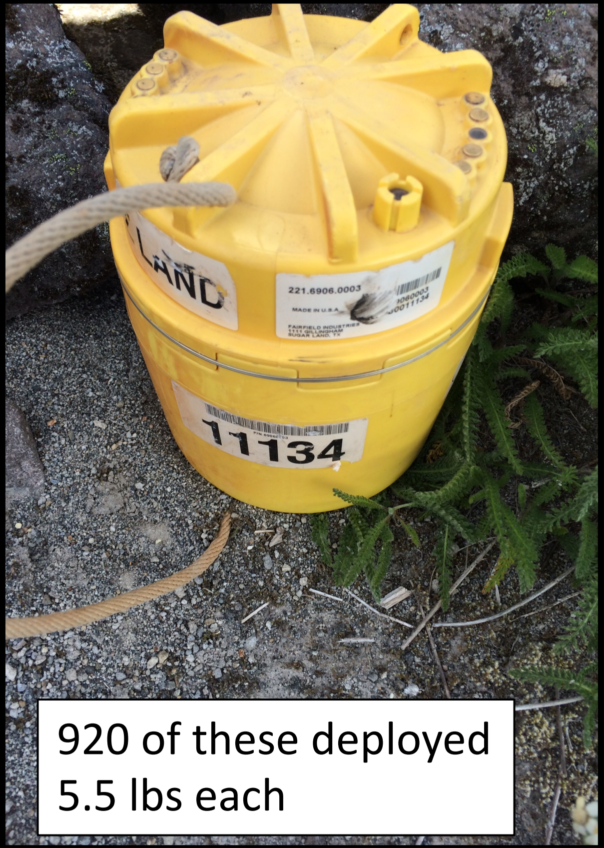

Mount St. Helens Node Array in 2014

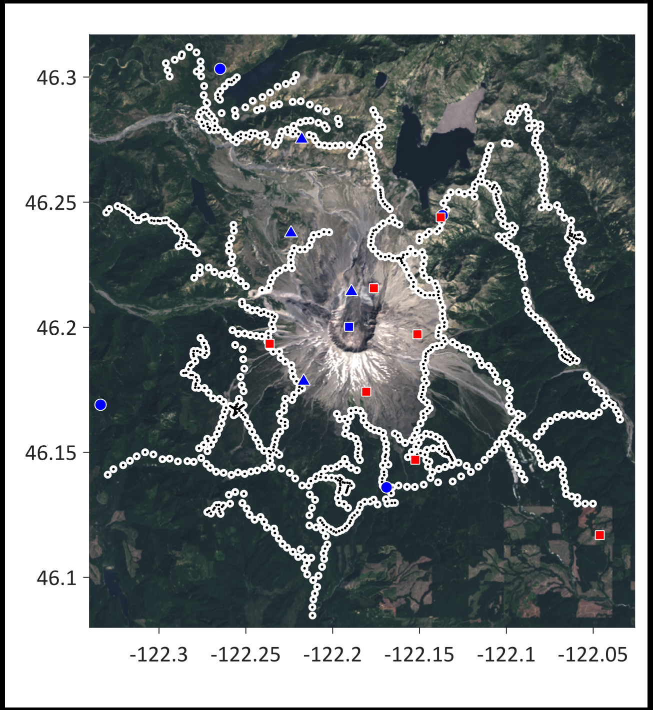

What are the measurable seismic wave properties that tell us about magmatic/volcanic structures?

- Speed (isotropic) from body wave travel times or group/phase speed
- Directionally dependent speed = anisotropic velocities
- Scattering – parent phase gives rise to new transmitted/reflected waves at sharp gradients in Vp, Vs
- Energy dissipation due to intrinsic attenuation

$$v_p = \sqrt{\frac{k + \frac{4\mu}{3}}{\rho}} = \sqrt{\frac{\lambda + 2\mu}{\rho}}$$

$$v_s = \sqrt{\frac{\mu}{\rho}}$$

k = Bulk modulus

μ = Shear modulus

ρ = density

$$\lambda = k - \frac{2}{3}\mu$$

λ = Lame's lambda constant

What are the measurable seismic wave properties that tell us about magmatic/volcanic structures?

How to translate seismic properties into magmatic properties (bulk composition, temperature, melt, volatiles, etc)?

$$Vp = \sqrt{\frac{k + \frac{4\mu}{3}}{\rho}} = \sqrt{\frac{\lambda + 2\mu}{\rho}}$$

$$Vs = \sqrt{\frac{\mu}{\rho}}$$

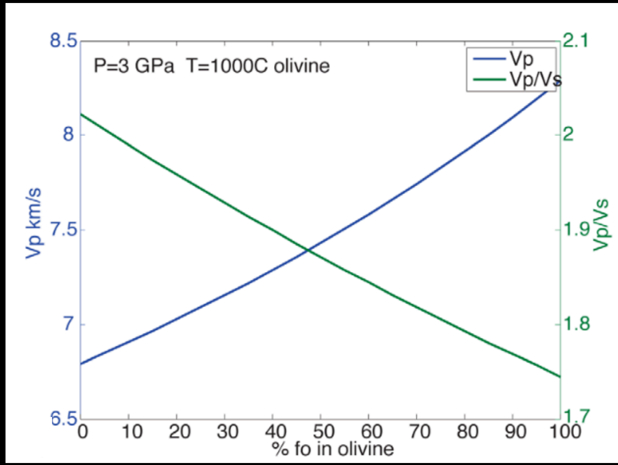

Abers and Hacker, 2016 – open scripts

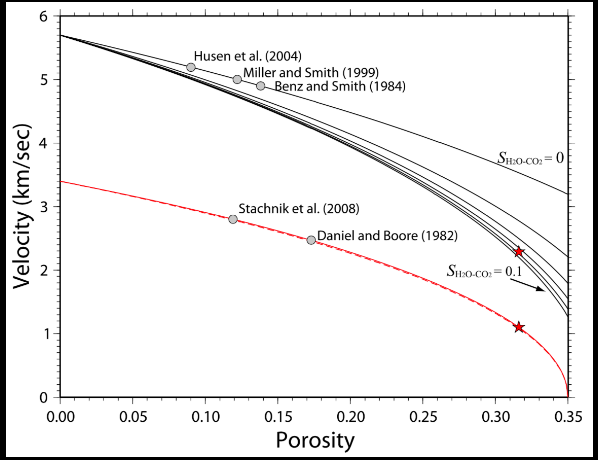

Chu et al. 2010 – melt effects tuned for Yellowstone

k = Bulk modulus

μ = Shear modulus

ρ = density

$$\lambda = k - \frac{2}{3}\mu$$

λ = Lame's lambda constant

Tomography

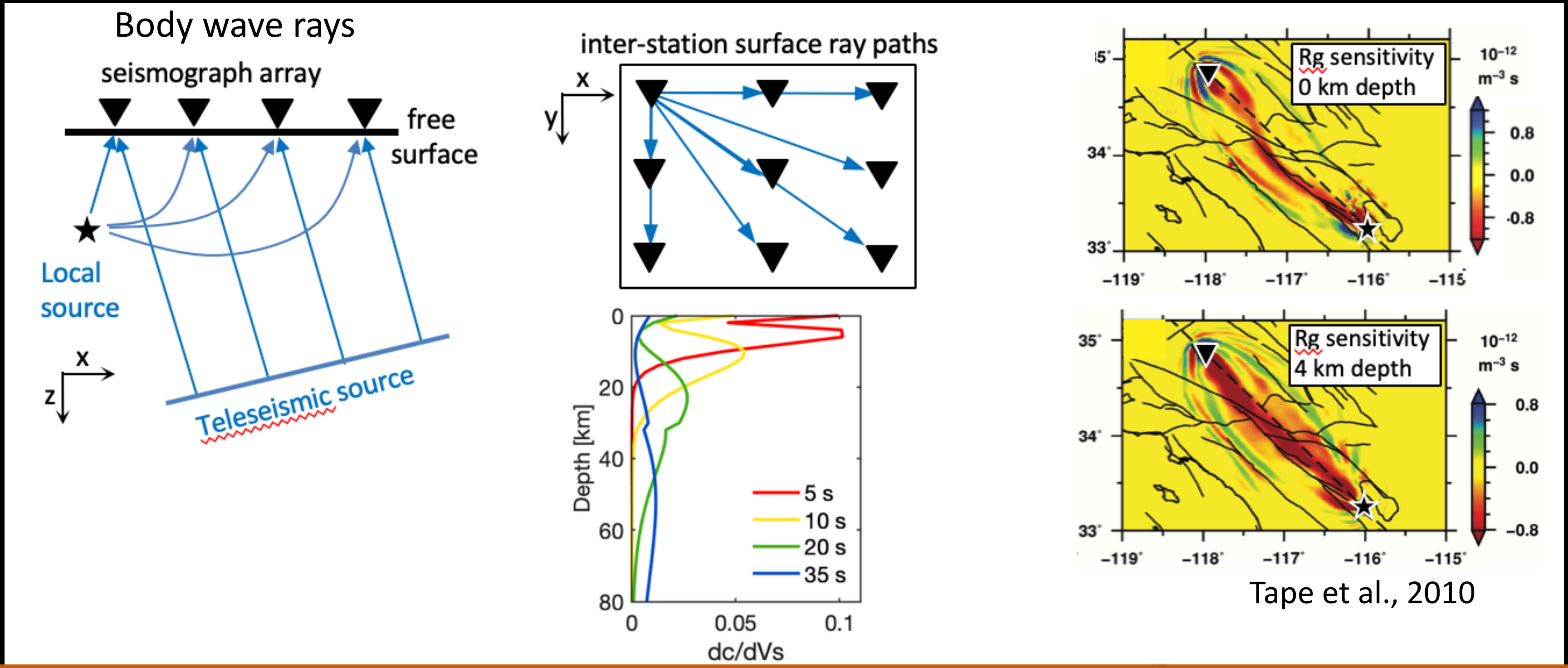

Scattered wave imaging

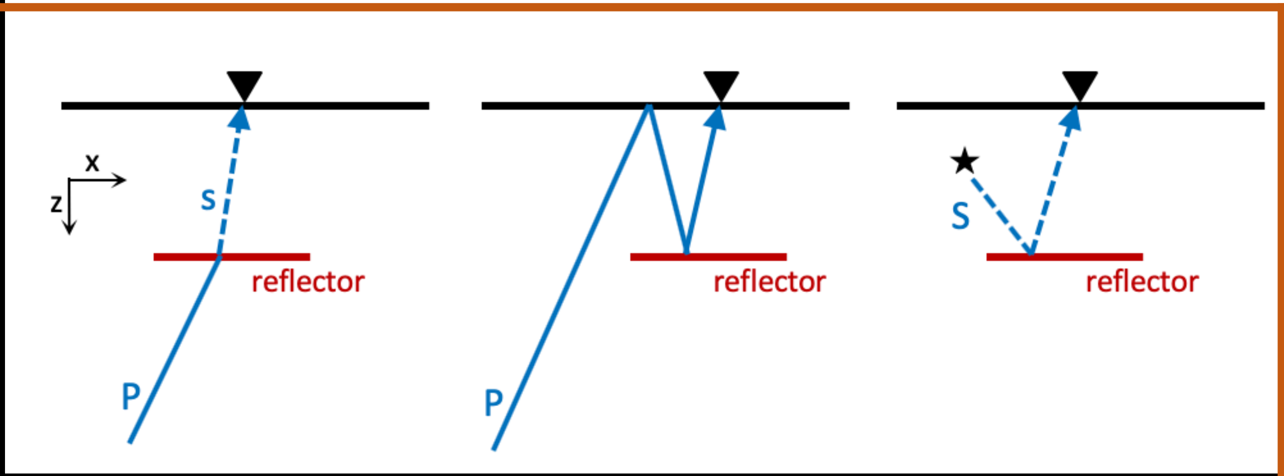

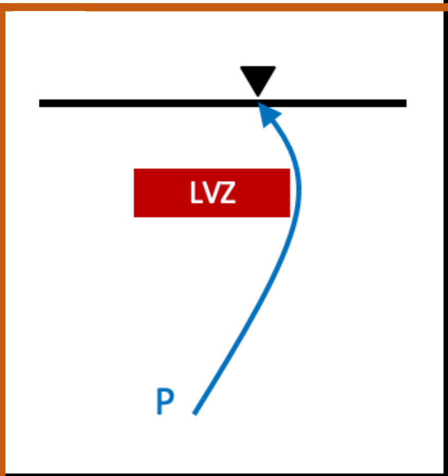

Polarization analysis

Approaches to seismic tomography - travel times and ray theory

$$d = Gm$$

Typically approached as an iterative linear inverse problem

d = vector of travel time observations
G = partial derivatives of each travel time with respect to a small change in each model parameter
m = vector of model parameters, slowness (1/velocity) in discrete volumes

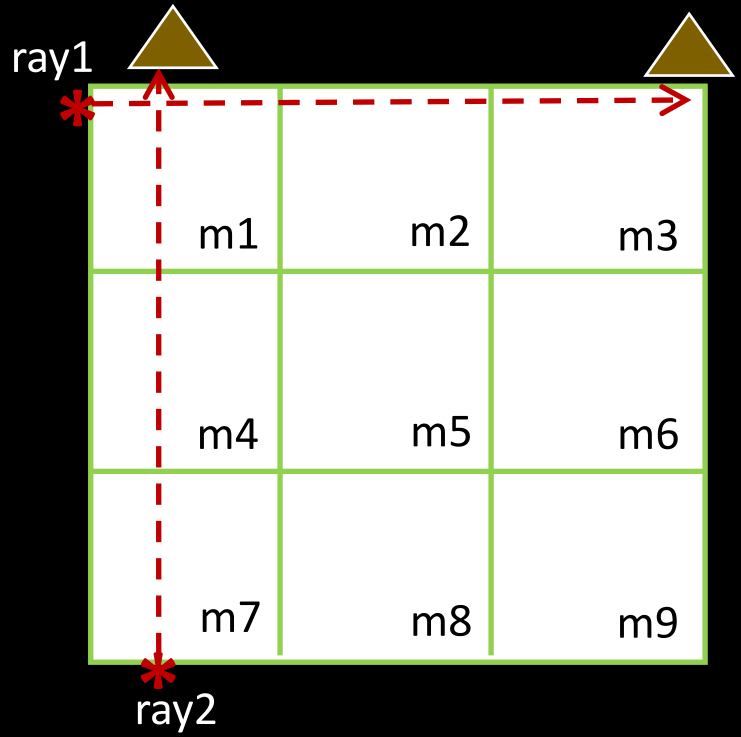

Here, two ray paths sample a 3x3 model space

Approaches to seismic tomography - travel times and ray theory

$$d = Gm$$

d = vector of travel time observations
G = partial derivatives of each travel time with respect to a small change in each model parameter
m = vector of model parameters, slowness (1/velocity) in discrete volumes

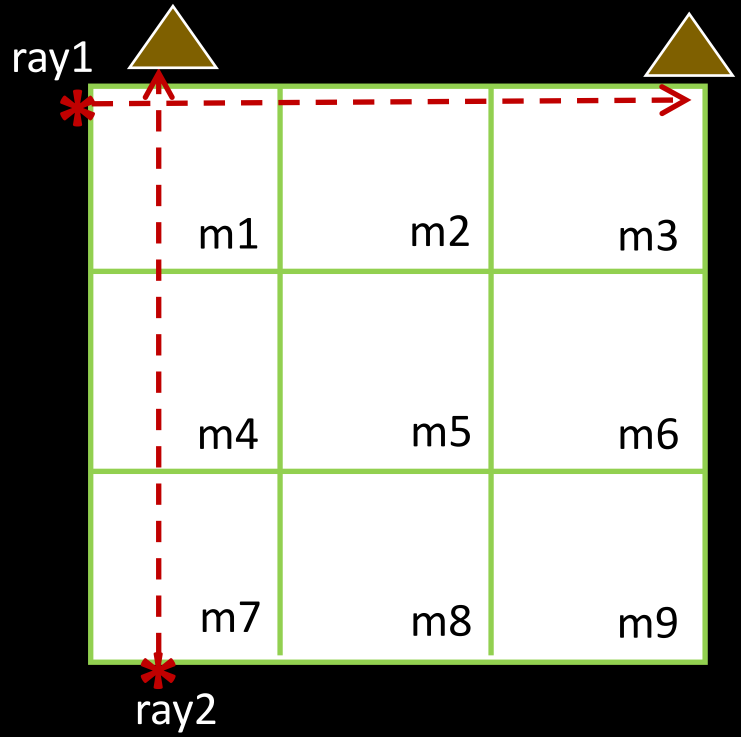

Simple fake data

d = [3.5 2.5] travel time in seconds

$$G = \begin{bmatrix} 1 & 1 & 1 & 0 & 0 & 0 & 0 & 0 & 0 \\ 1 & 0 & 0 & 1 & 0 & 0 & 1 & 0 & 0 \end{bmatrix}$$

Rows = 2 observational ray paths
Columns = 9 model parameters
Length of ray path in each block controls sensitivity or $\delta t/\delta m$

m = 9 x 1 vector of slowness values

Least-squares optimal solutions can be found rapidly for very large systems

Approaches to seismic tomography - travel times and ray theory

$$d = Gm$$

Typically approached as an iterative linear inverse problem

d = vector of travel time observations
G = partial derivatives of each travel time with respect to a small change in each model parameter
m = vector of model parameters, slowness (1/velocity) in discrete volumes

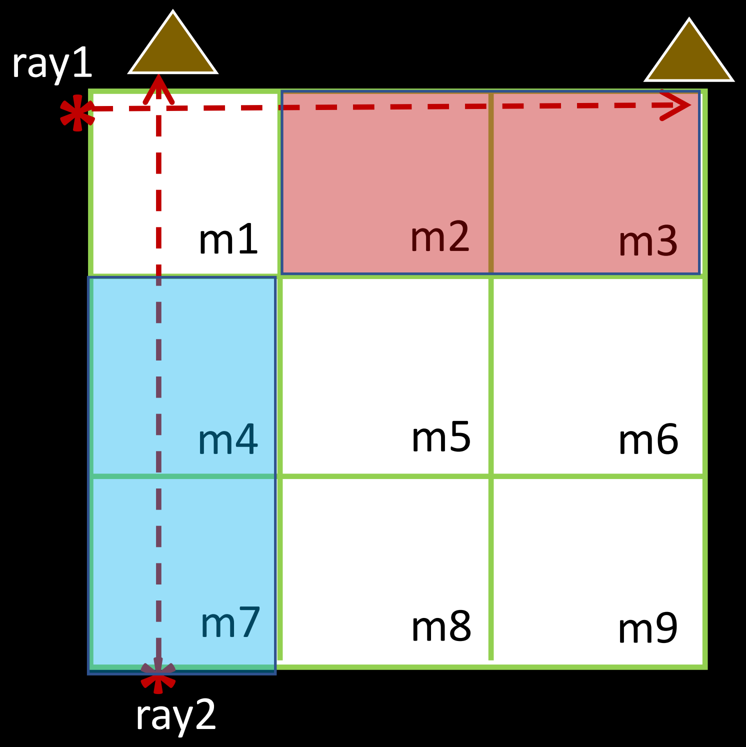

d = [3.5 2.5] travel time in seconds

$$G = \begin{bmatrix} 1\ 1\ 1\ 0\ 0\ 0\ 0\ 0\ 0 \\ 1\ 0\ 0\ 1\ 0\ 0\ 1\ 0\ 0 \end{bmatrix}$$

Rows = 2 observational ray paths
Columns = 9 model parameters
Length of ray path in each block controls sensitivity or $\delta t/\delta m$

m = 9 x 1 vector of slowness values

Least-squares optimal solutions can be found rapidly for very large systems

Approaches to seismic tomography - travel times and ray theory

$$d = Gm$$

Length of ray path in each block controls sensitivity or $\delta t/\delta m$

This simplification has proven useful, but such a severe approximation that sensitivity is limited to the source-receiver path is not accurate for most earthquake observations

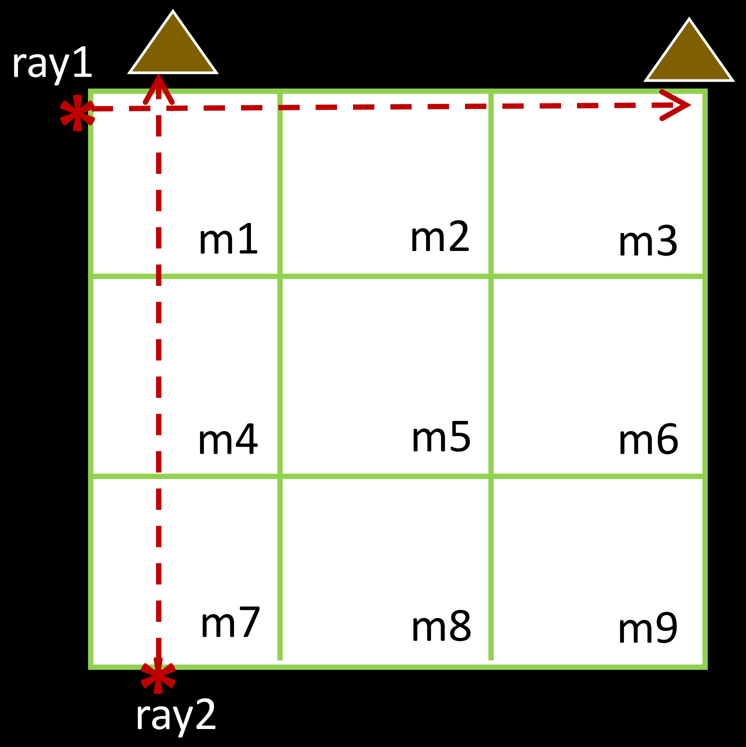

Usually many more than 9 model parameters, especially for 3D

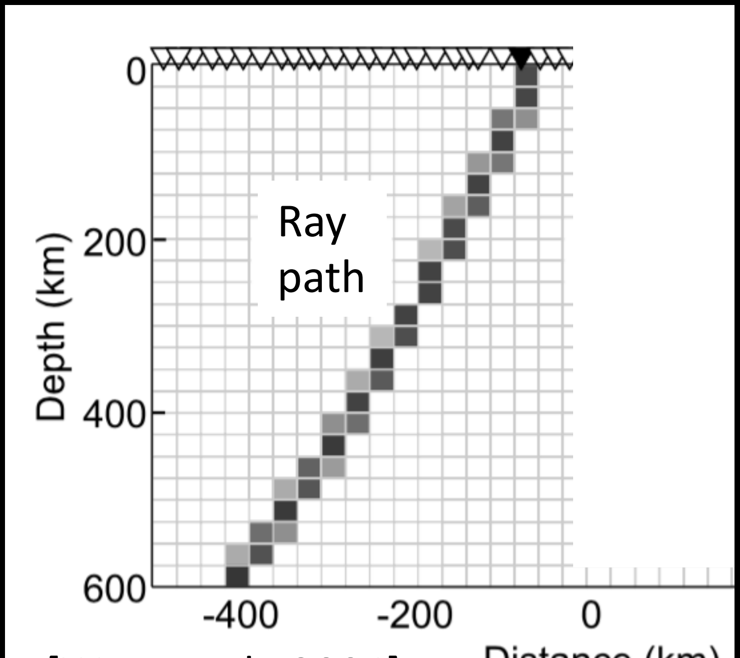

[West et al., 2004]

Global mantle scale example of P wave travel time sensitivity

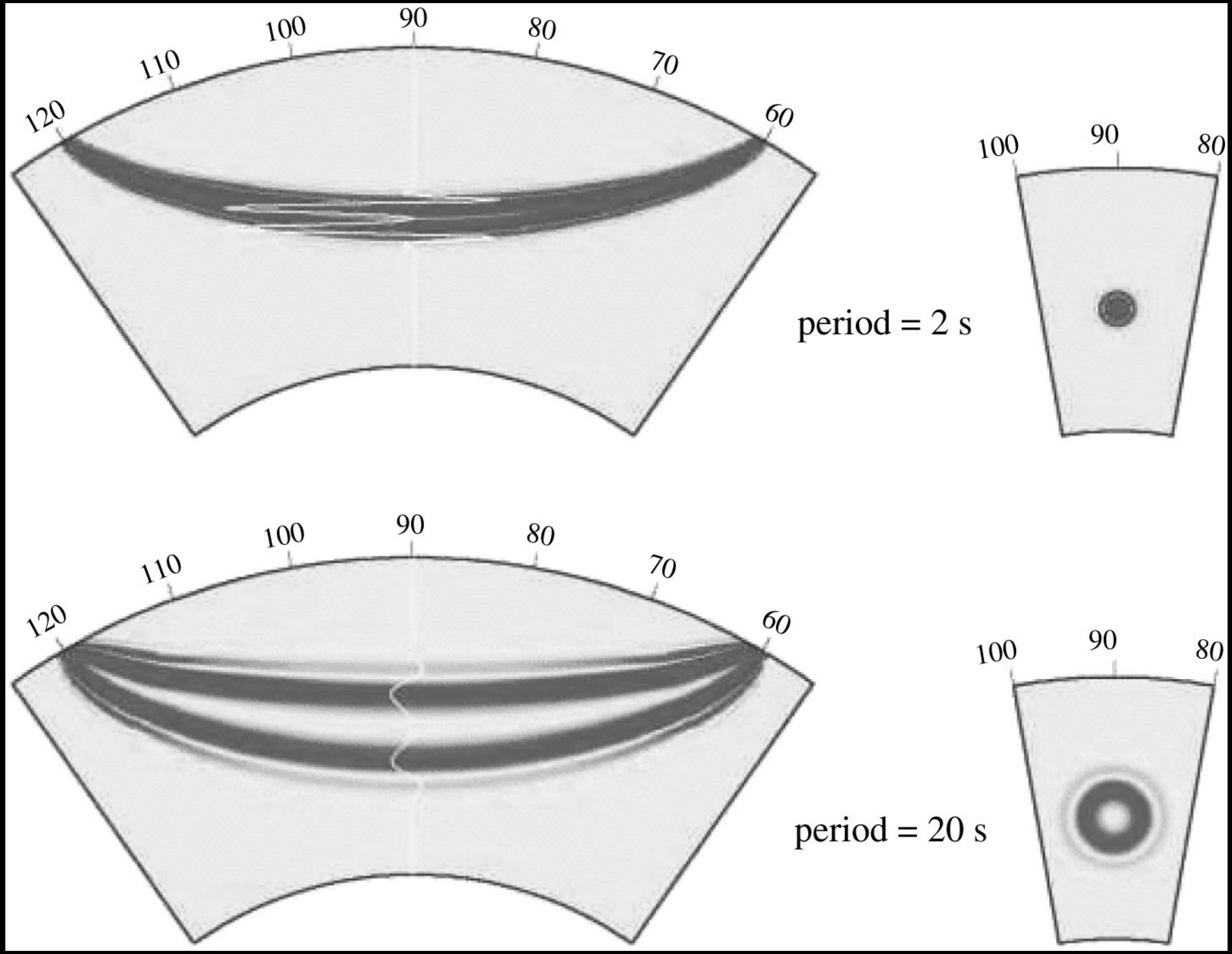

(Dahlen et al., 2000; Hung et al., 2000)

For global scale tomography at period of ~2 s, sensitivity is ray-like given realistic dimensions of model parameters

At 20 s, the distribution of travel time sensitivity is substantially different and ray theory is a weaker approximation

Global mantle scale example of P wave travel time sensitivity

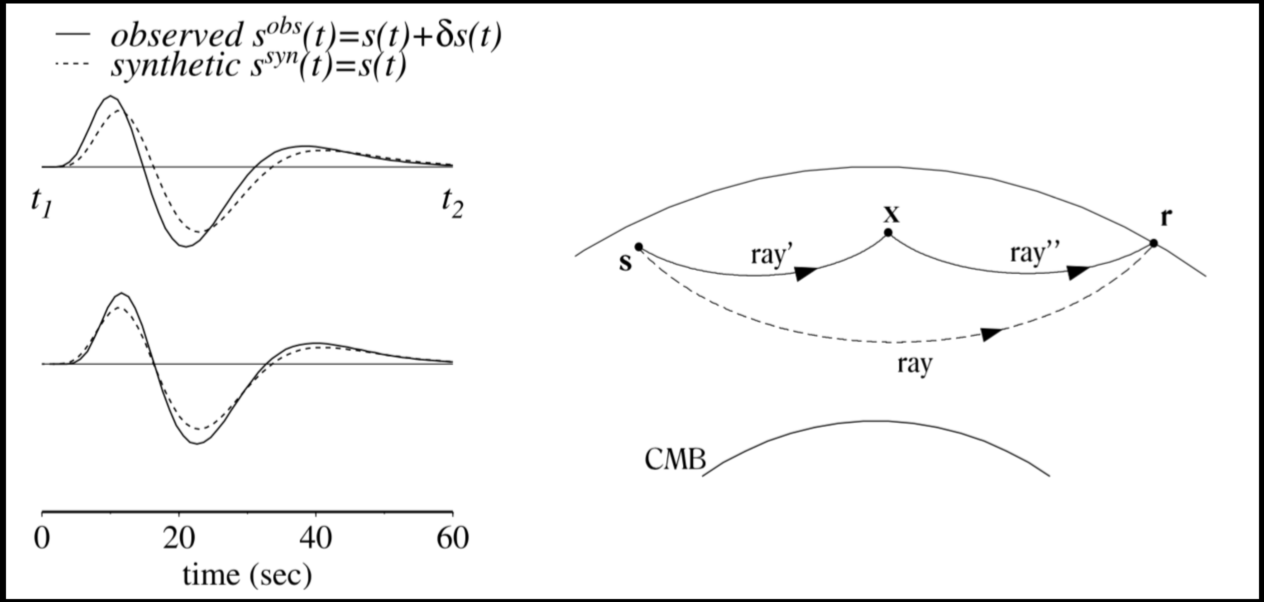

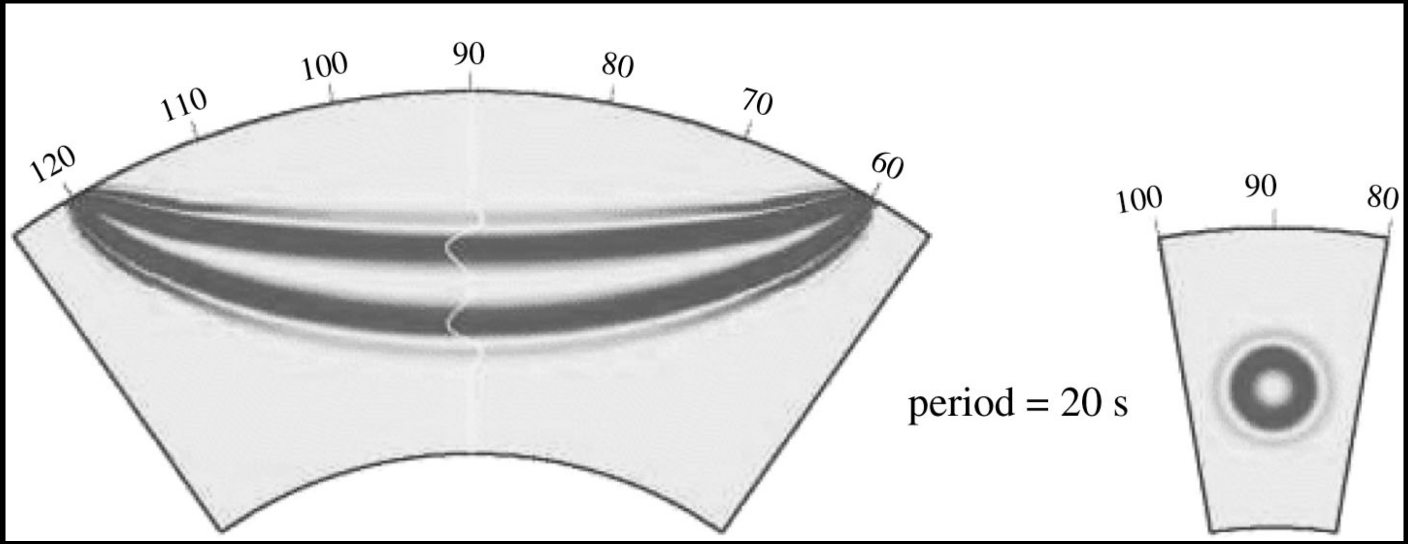

(Dahlen et al., 2000; Hung et al., 2004)

Off-path scattered energy can arrive close enough in time to the direct arrival to distort the waveform and influence the measured travel time (Assumes single-scattering)

Here sensitivity is calculated for a small perturbation to 1D reference model

It is more demanding to update these calculations of sensitivity with respect to a 3D reference model

Approaches to seismic tomography - travel times and finite frequency sensitivity kernels

$d = Gm$

moderate increase
in accuracy of G

Finite-frequency sensitivity kernels calculated for 1D reference models, rather than ray-theoretical sensitivity

Allows use of multiple frequency body wave travel times to be meaningful

Reduces reliance on ad hoc smoothing constraints

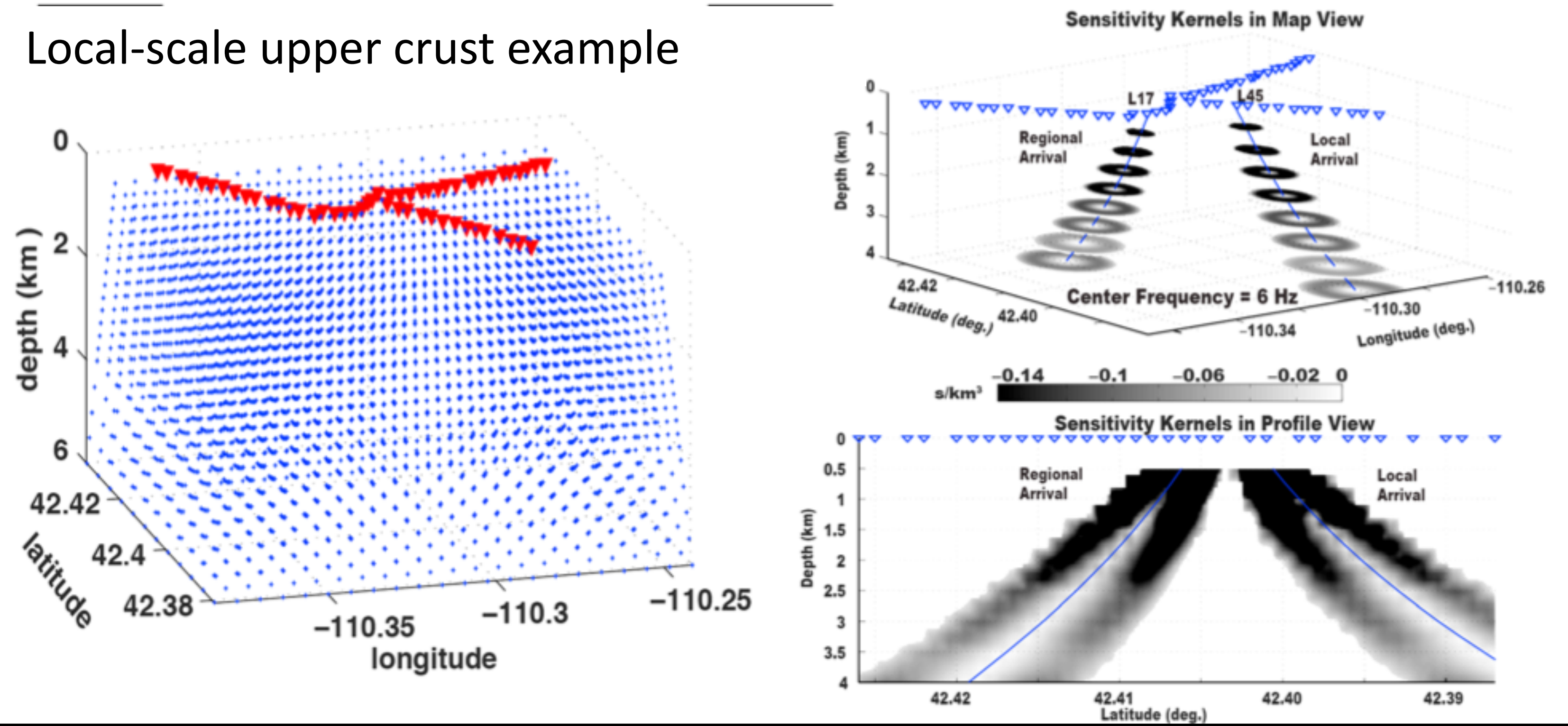

Biryol et al., 2013

Recent/ongoing advances in tomography have largely proceeded in two different directions:

1. Retain simple 1D assumptions for forward problem, but use computing power to sample highly multi-dimensional parameter space. Major benefit is uncertainty constraints.

2. Retain gradient based inversion, but use computing power to compute accurate 3D forward problem iteratively updating sensitivity kernels

Approaches to seismic tomography – Guided searching of parameter space

$d = f(m)$

Alternatively we can try MANY forward models and see which ones provides fit the data within their uncertainties

1D problems often need ~10 model parameters so this is a powerful way to obtain probabilistic results with simple forward problems

3D body wave problems often need $10^4 – 10^6$ parameters so this may be impractical or marginally possible with HPC (Burdick and Lekic, 2017)

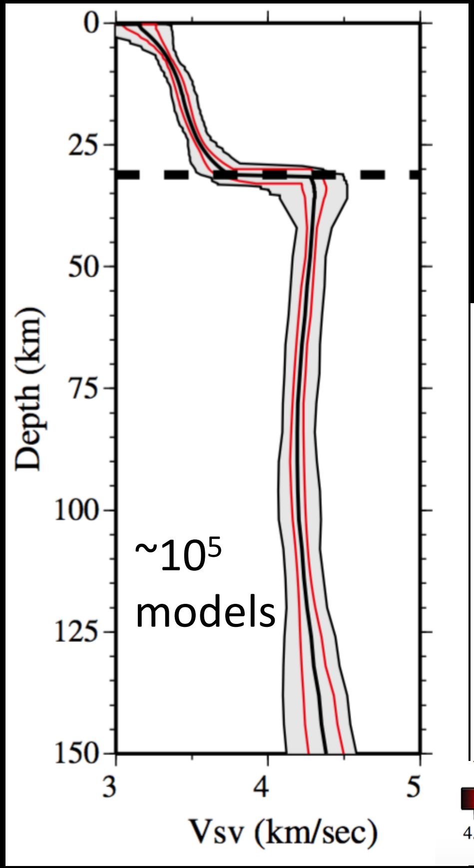

Here f(m) is a locally 1D dispersion calculation

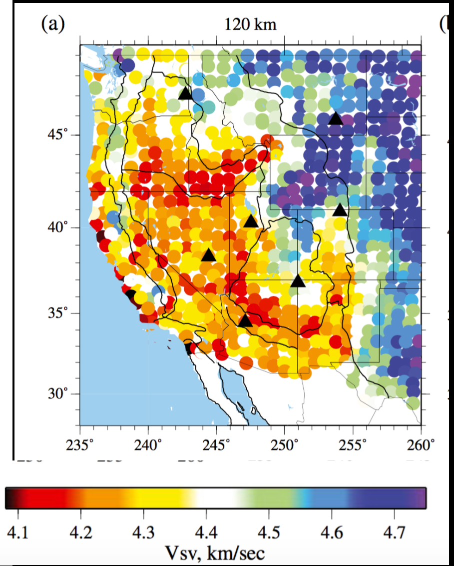

[Shen et al., 2013]

Here f(m) is a ray-tracing travel time calculation

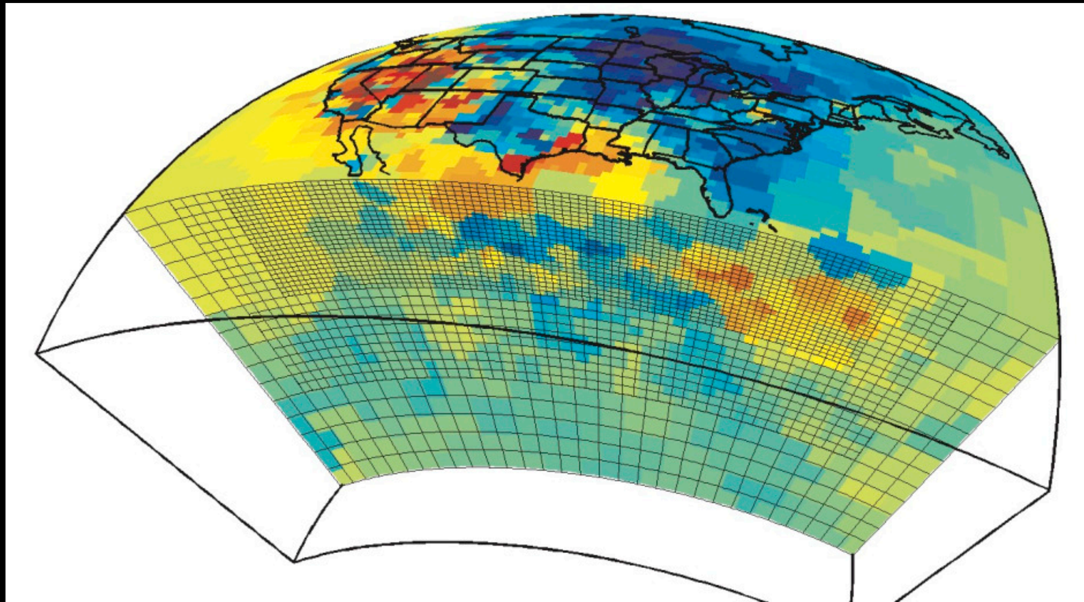

Burdick and Lekic, 2017

Approaches to seismic tomography – Full Waveform Inversion

$$d = Gm$$

Compromise is usually increased wavelengths for d

Dramatic increase in accuracy of G

Here the sensitivity matrix G is updated with numerical calculation of full ~elastic wavefield. Each iteration is a HPC problem.

Application to southern California crust by Tape et al., 2009, 2010

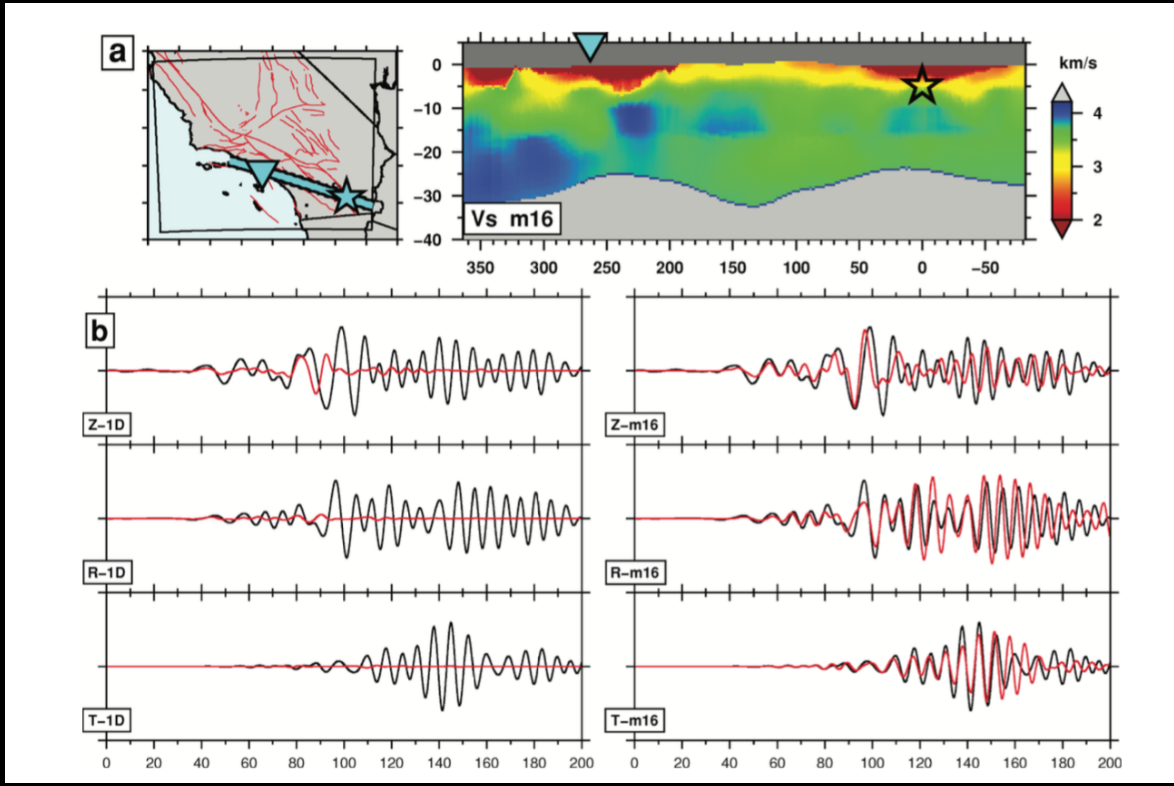

Updated 3D sensitivity kernels can differ strongly from 1D case

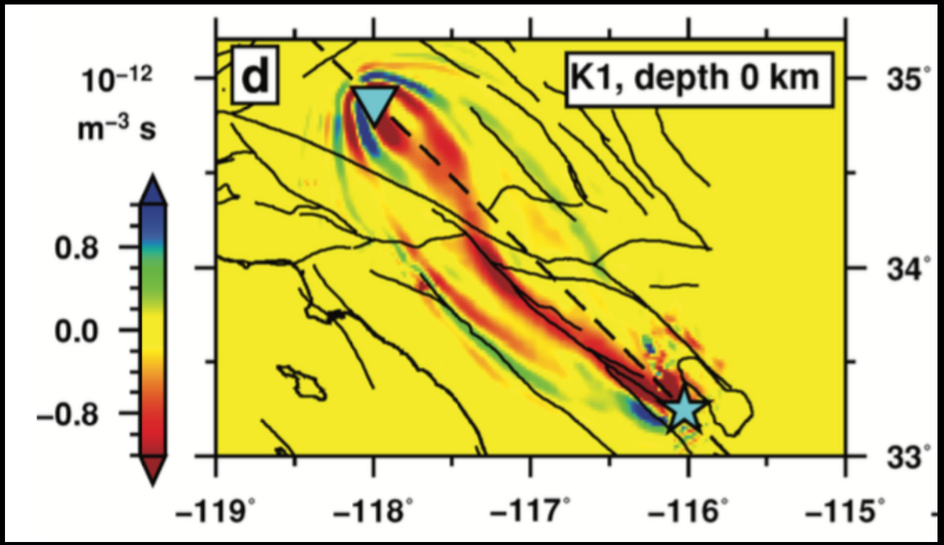

[Tape et al., 2010]

Approaches to seismic tomography – Full Waveform Inversion

$$d = Gm$$

Compromise is usually increased wavelengths for d

Dramatic increase in accuracy of G

So far, early applications to continental magmatic systems just aim to fit surface wave dispersion at relatively long periods (e.g., Flinders et al., 2018) compared to signals generated by local earthquakes and controlled sources.

Lots of room to grow toward approaches more similar to those of the resource exploration industry (e.g., Yuan and Simons, 2014)

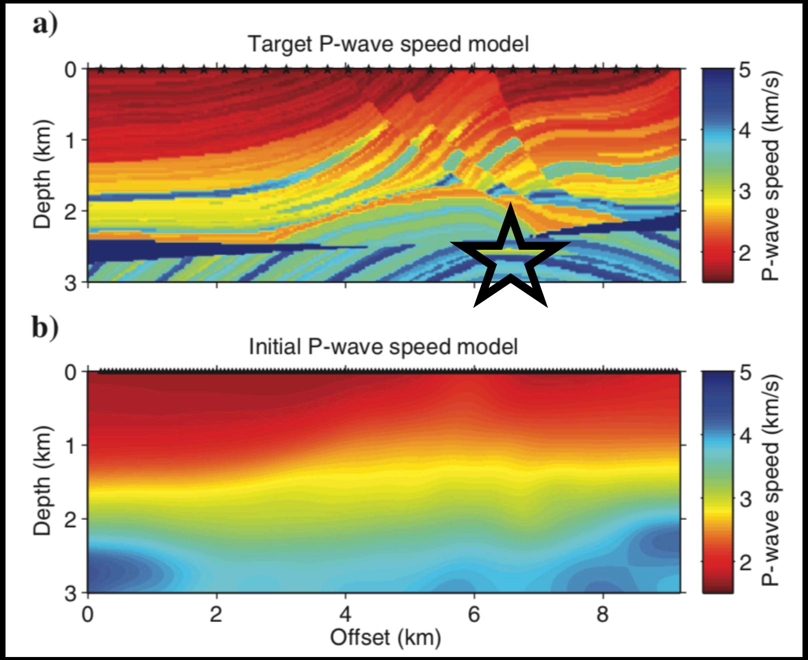

Industry benchmark model

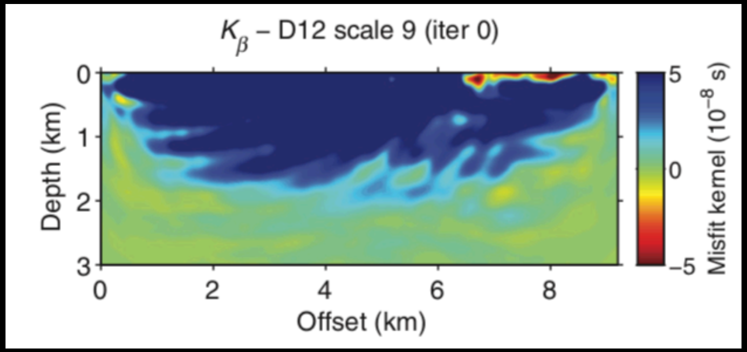

Early, larger scale iteration updates smooth structure

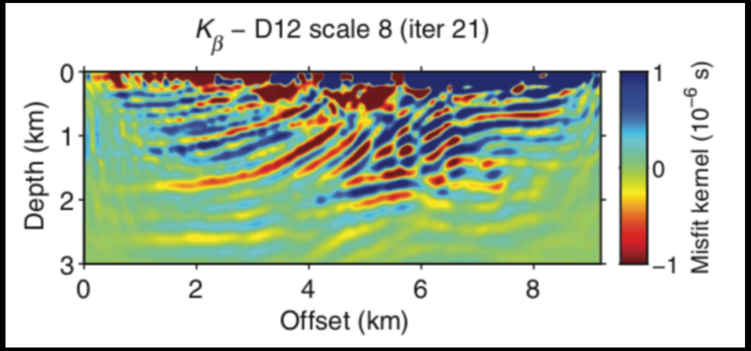

Later iterations to fit finer scale body waves

Yuan and Simons, 2014

Seismically imaging magma reservoirs,

starting with large systems at

Yellowstone and Long Valley

Mantle melt supply beneath Long Valley caldera

- Localized low-Vs uppermost mantle beneath LVC indicates continued source of partial melts from the mantle
- Inboard localization of plate boundary driven transtension drives mantle ascent

Joint S and Rayleigh wave tomography

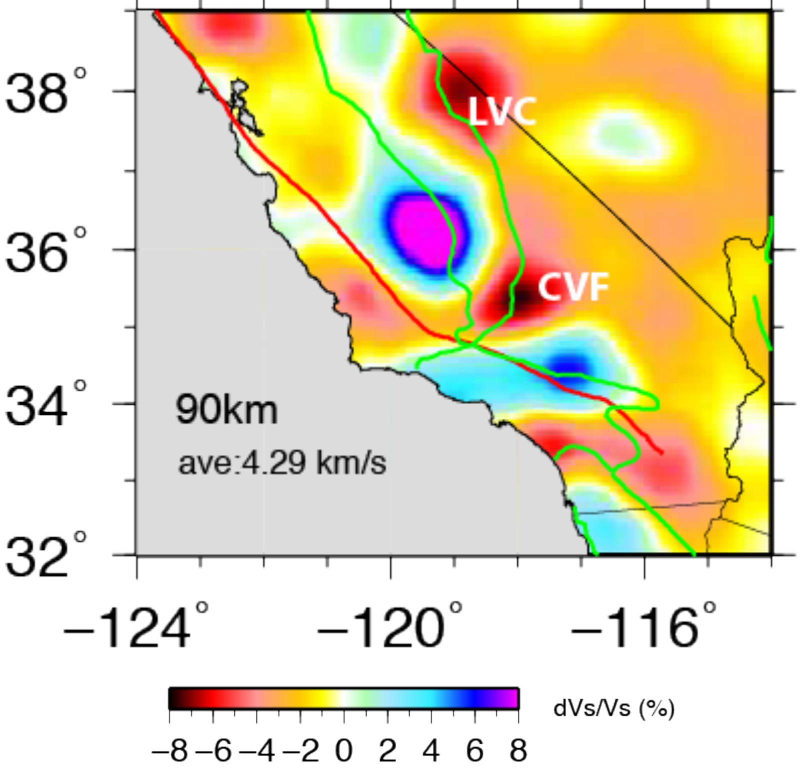

Jiang et al., 2018

2nd Invariant strain rate map from GPS

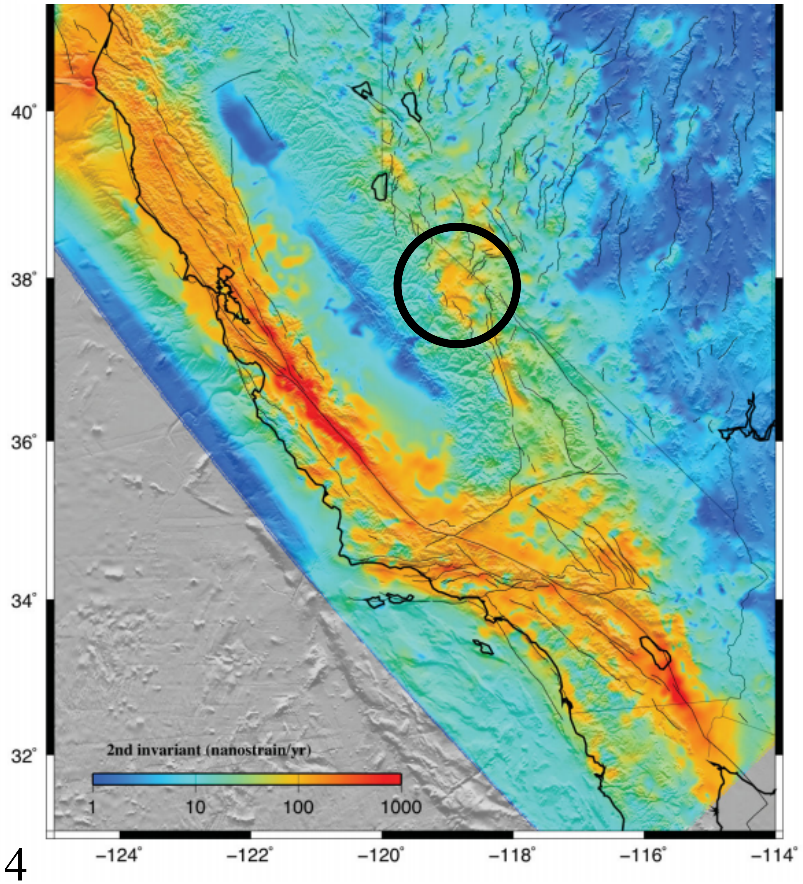

Kreemer et al., 2014

Mantle melt supply beneath Long Valley caldera

- Localized low-Vs uppermost mantle (<4.0 km/s) beneath LVC indicates continued source of partial melts from the mantle
- Inboard localization of plate boundary transtension drives mantle ascent

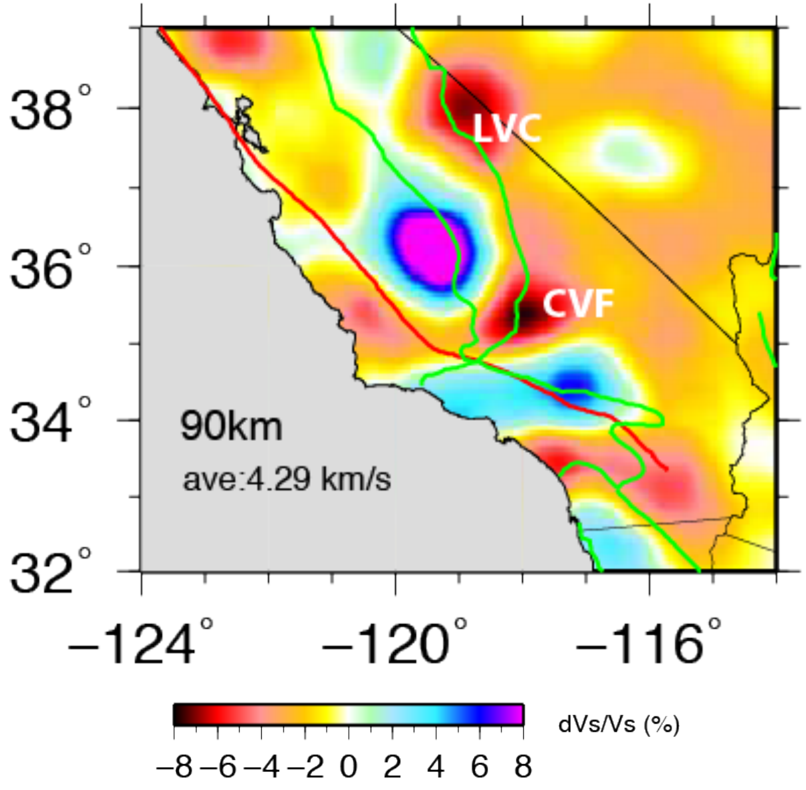

Jiang et al., 2018

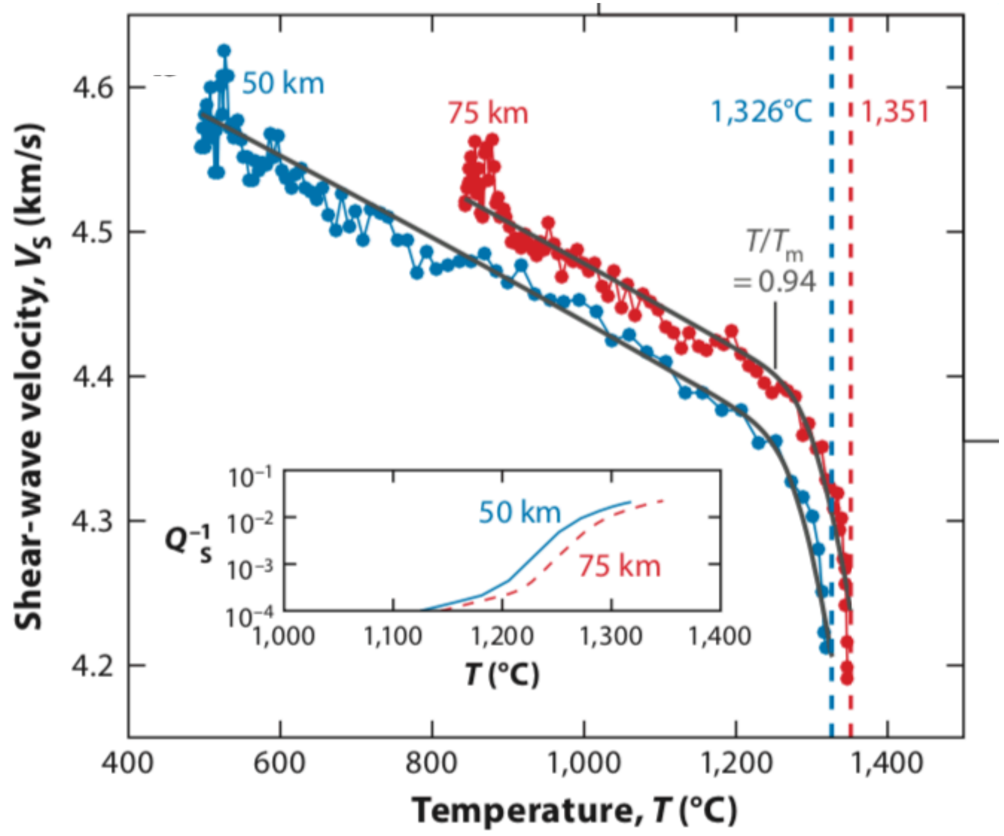

Near solidus Vs drop from ~4.4 – 4.2 km/s

Takei, 2017

P wave tomography at Long Valley

- Teleseismic P wave tomography with 3-D ray tracing
- Dense short-period array

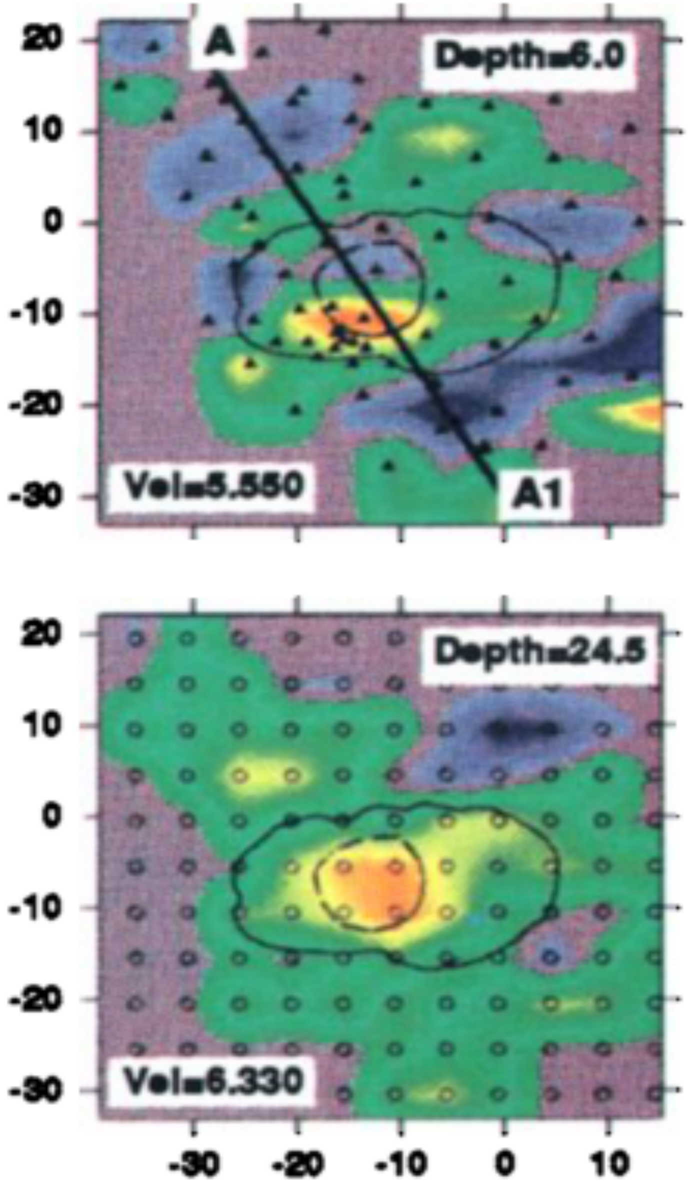

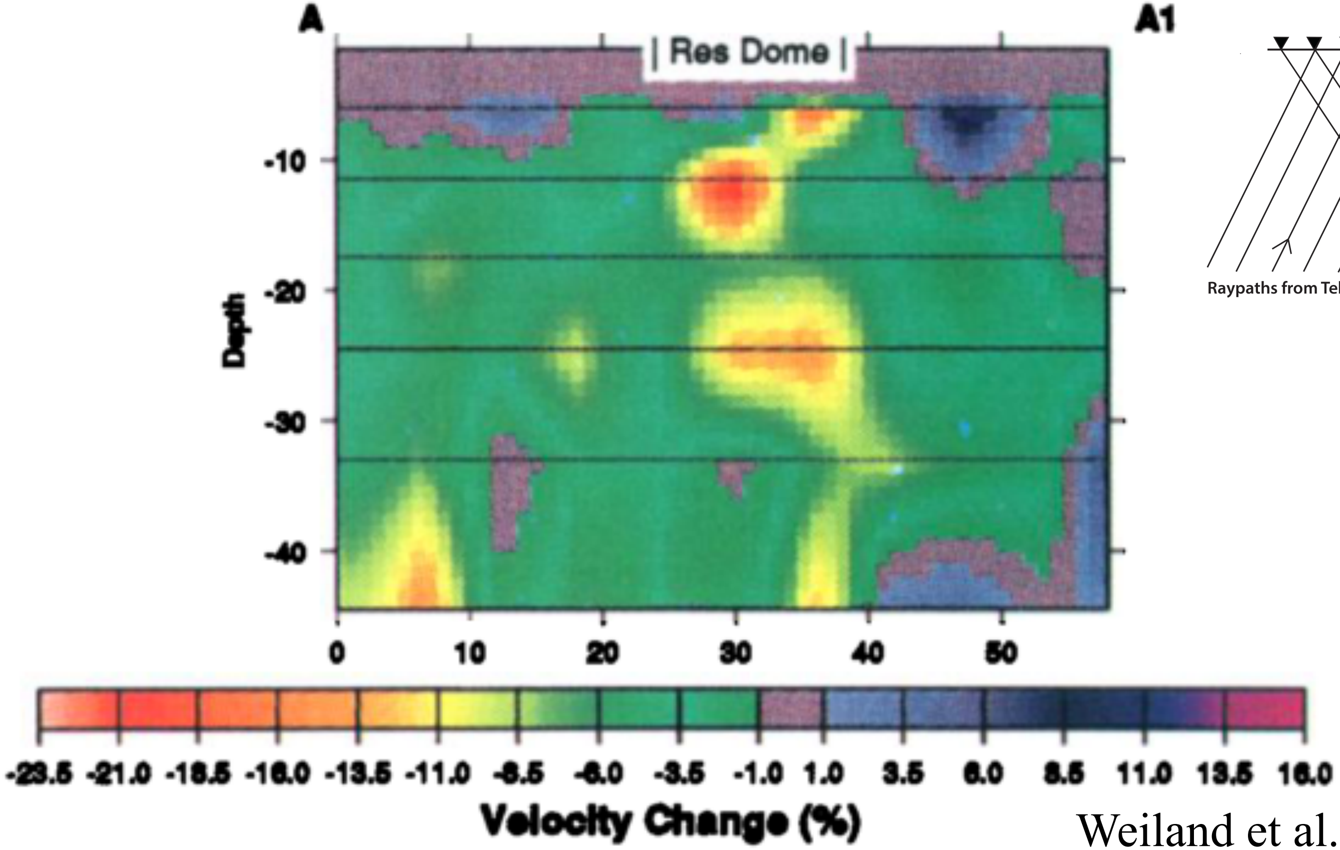

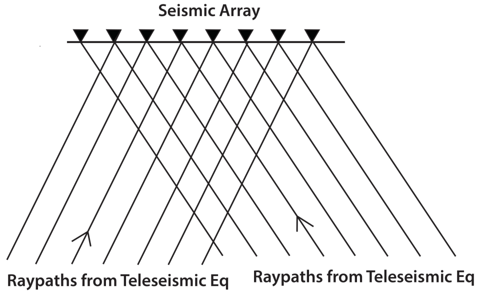

Weiland et al.,1995

Teleseismic P wave polarization evidence for very low velocity anomaly in upper-to-middle crust

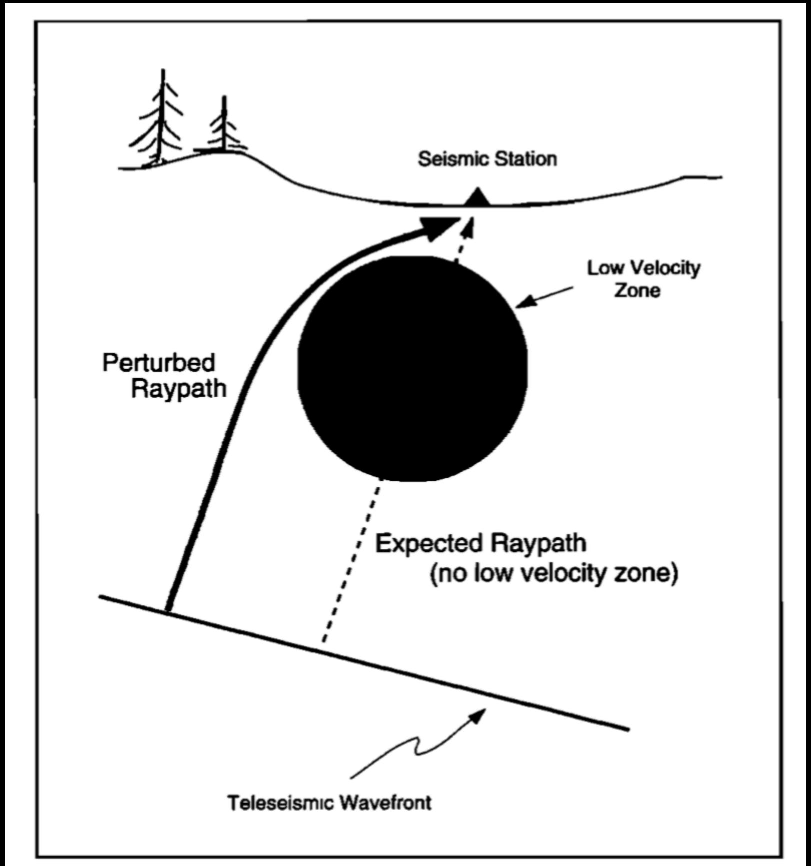

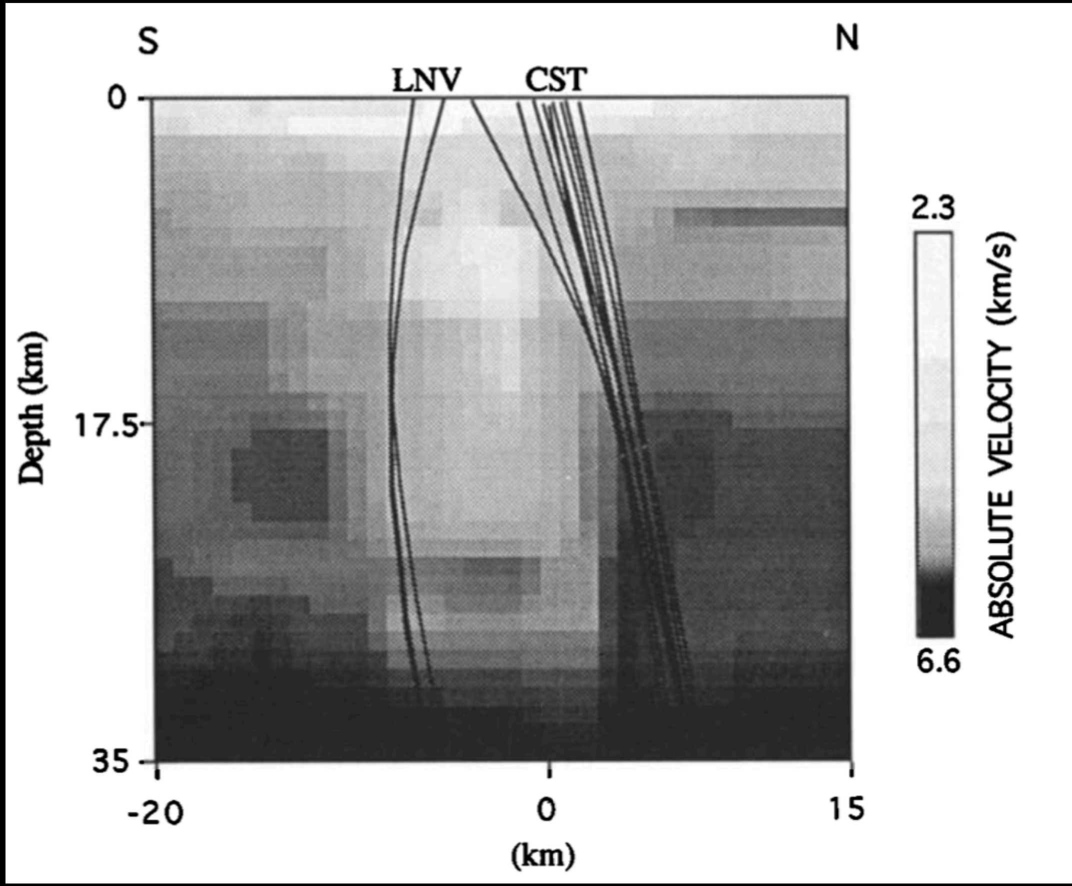

Steck and Prothero, 1994

Long Valley cross-sections, different methods

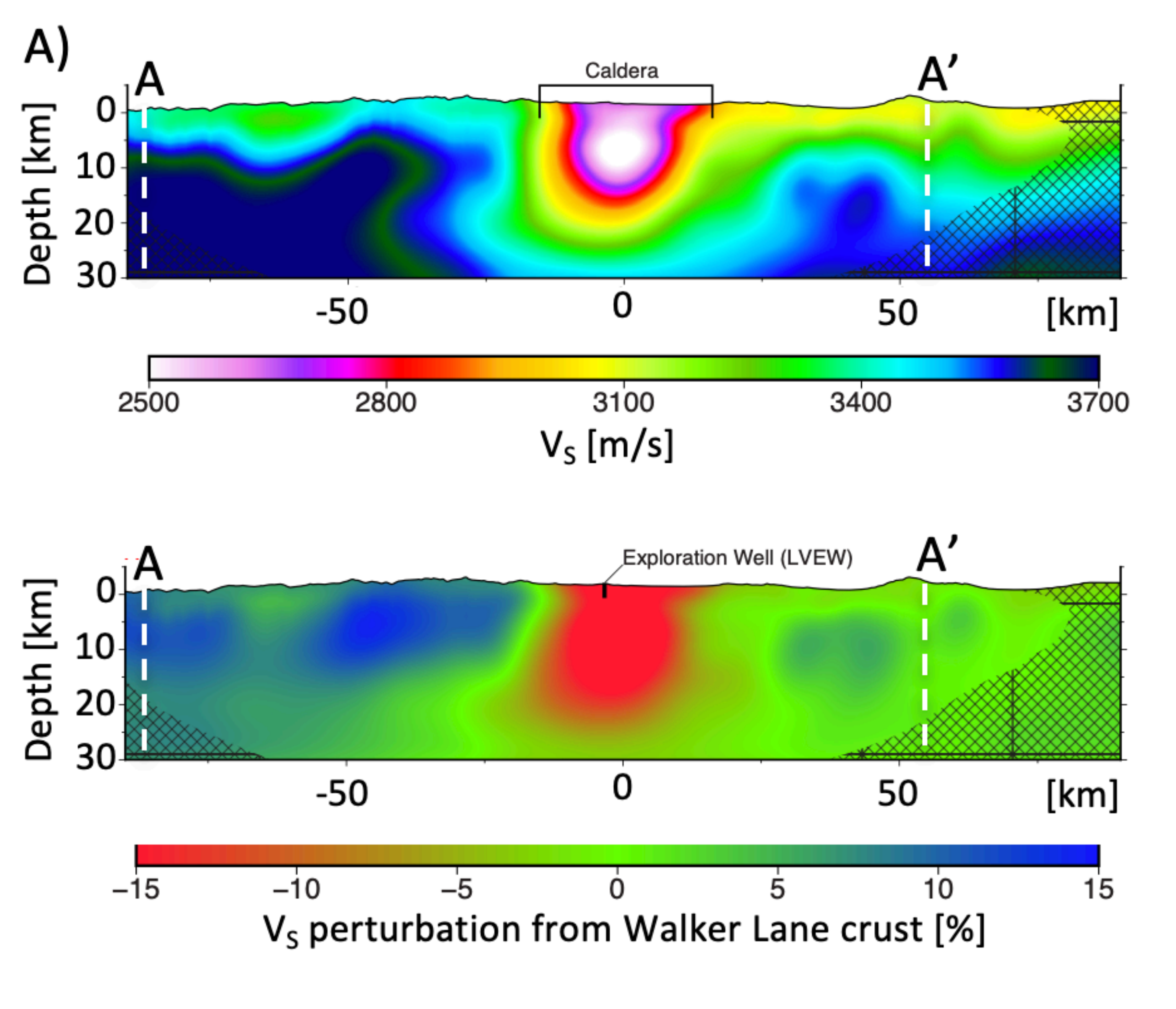

Flinders et al. 2018

Full wave forward calculation

Inverts dispersion measurements for vertical component inter-station Greens function

Vsv reductions of ~20-30%, min Vs ~2.5 km/s (Flinders et al., 2018)

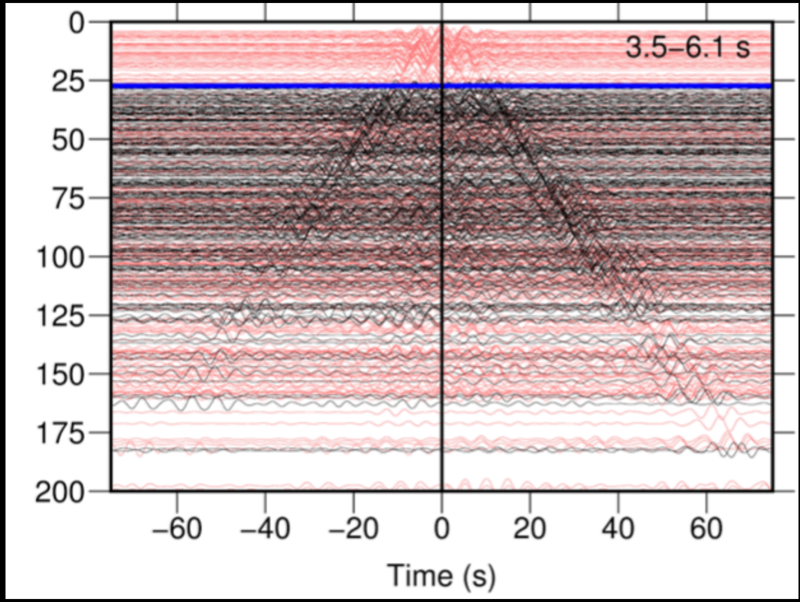

Mantle source of Yellowstone

- Hot spot track with migrating onset of silicic magmatism
- Teleseismic S wave tomography
- Multi-scale broadband arrays

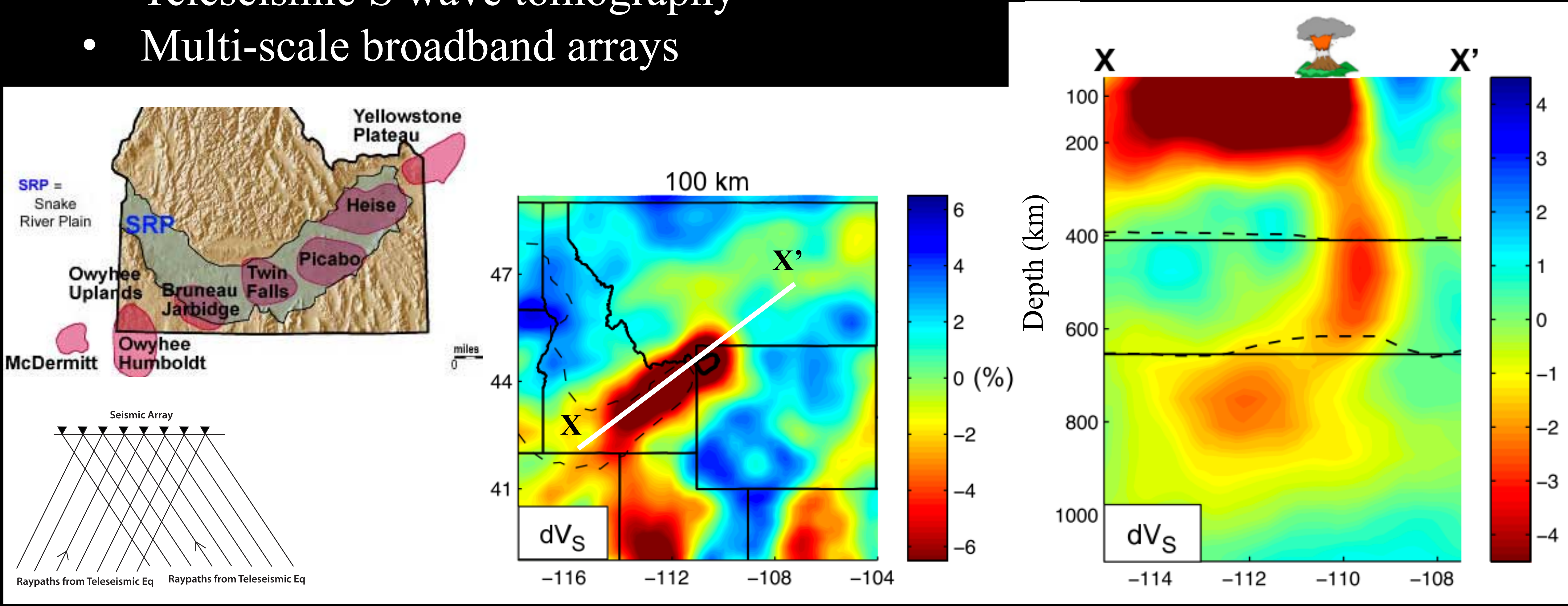

Schmandt et al., 2012

Mantle source of Yellowstone

- Hot spot track with migrating onset of silicic magmatism
- Teleseismic S wave tomography

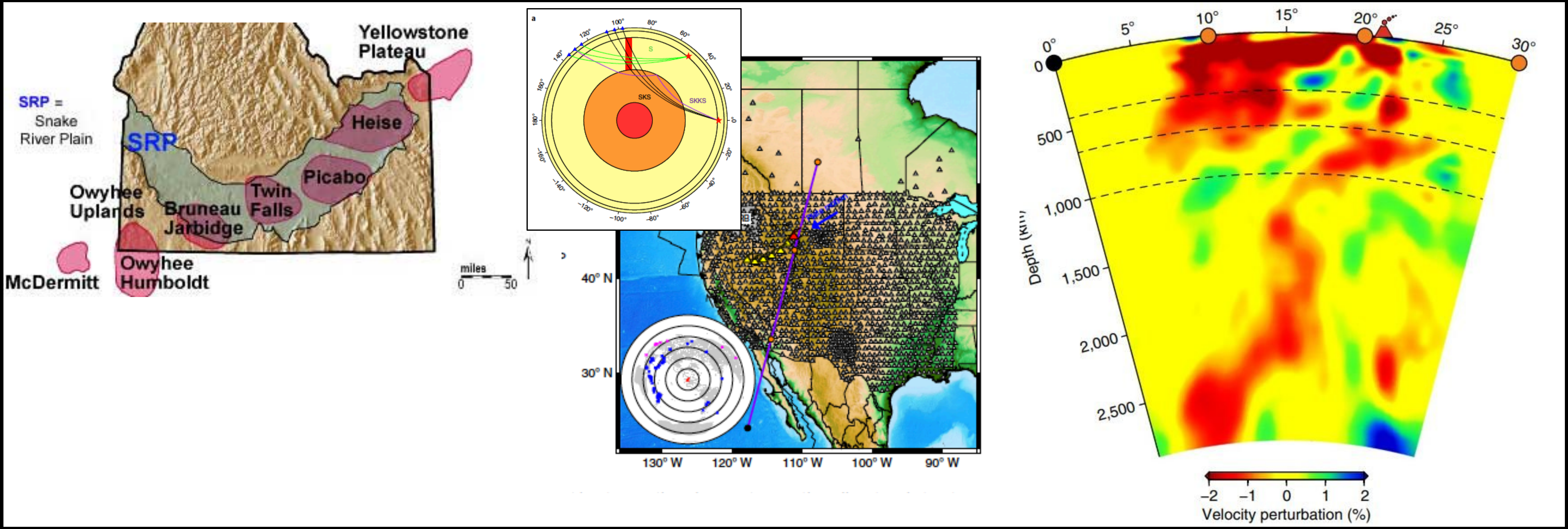

Nelson and Grand, 2018

Yellowstone hotspot's crustal magmatic system

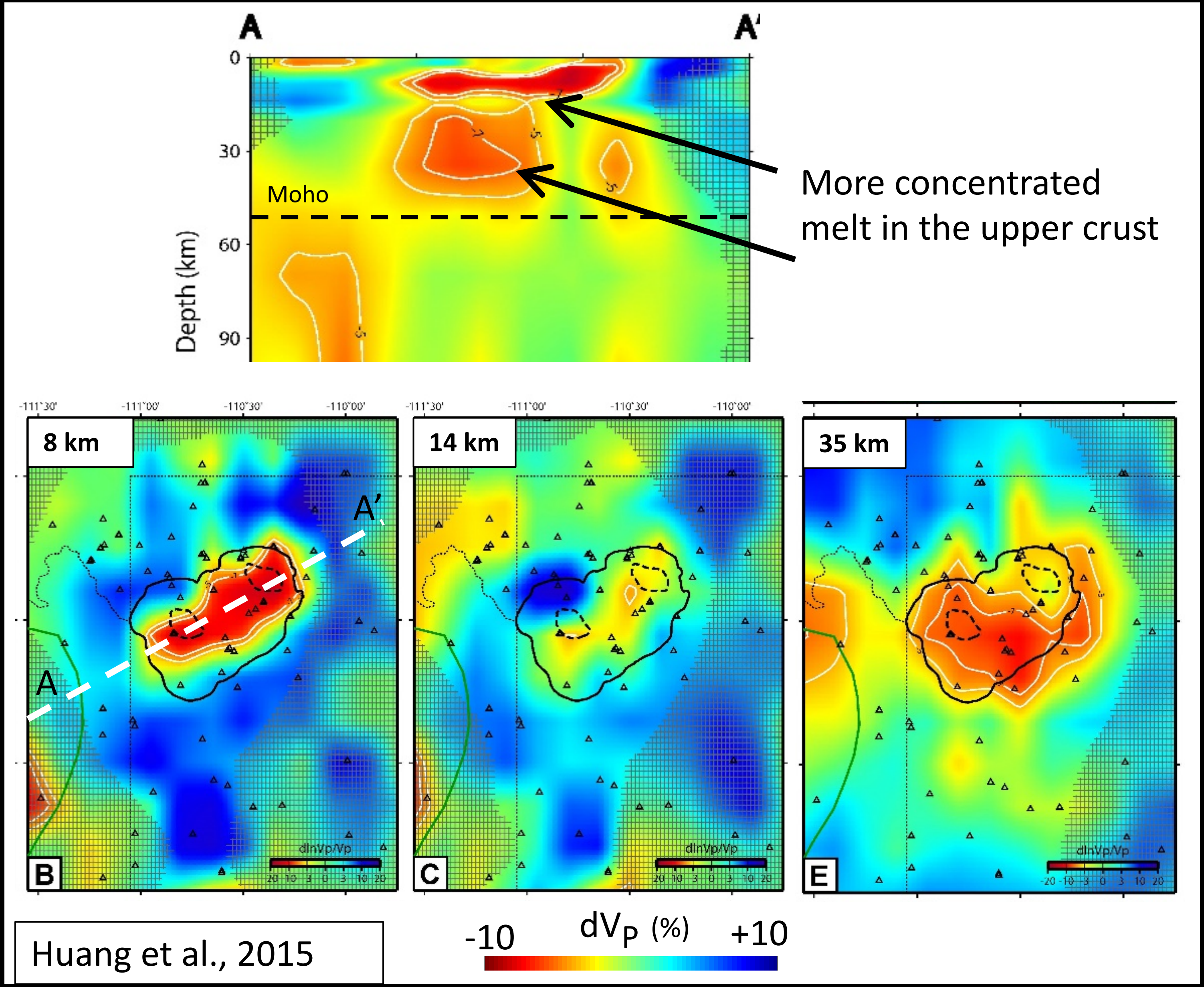

Combining local and teleseismic P wave travel time tomography [Huang et al., 2015]

Integrates a long history of broadband and short-period deployments

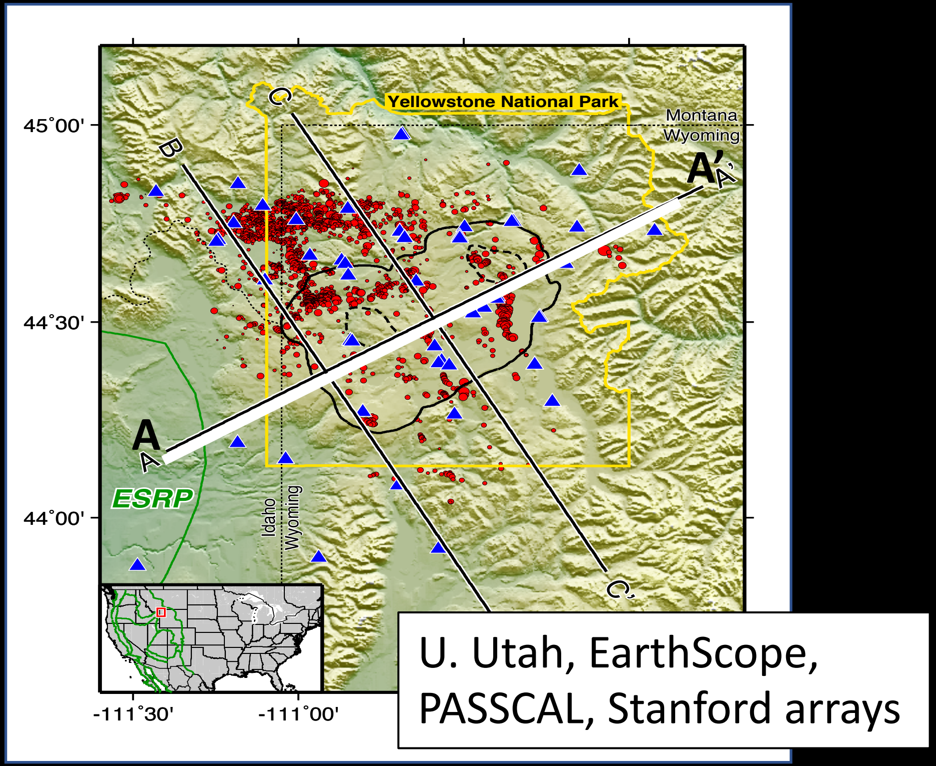

Yellowstone hotspot's crustal magmatic system

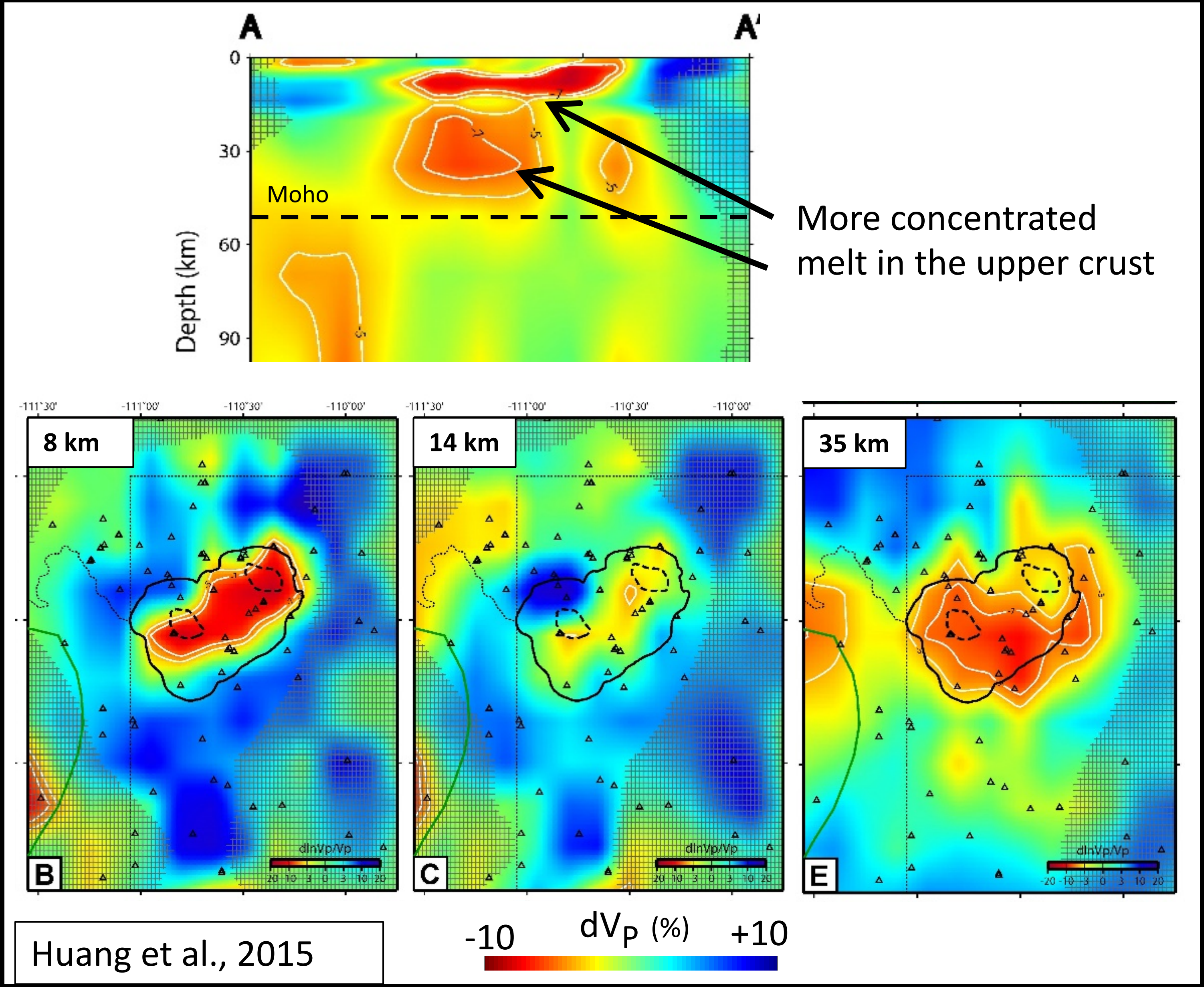

Two local minima in Vp perturbation as a function of depth

Low-mobility crystal-dominated mush with ~2-10% melt may be sufficient

Some waveform evidence for locally higher melt fractions of up to ~30% [Chu et al., 2010]

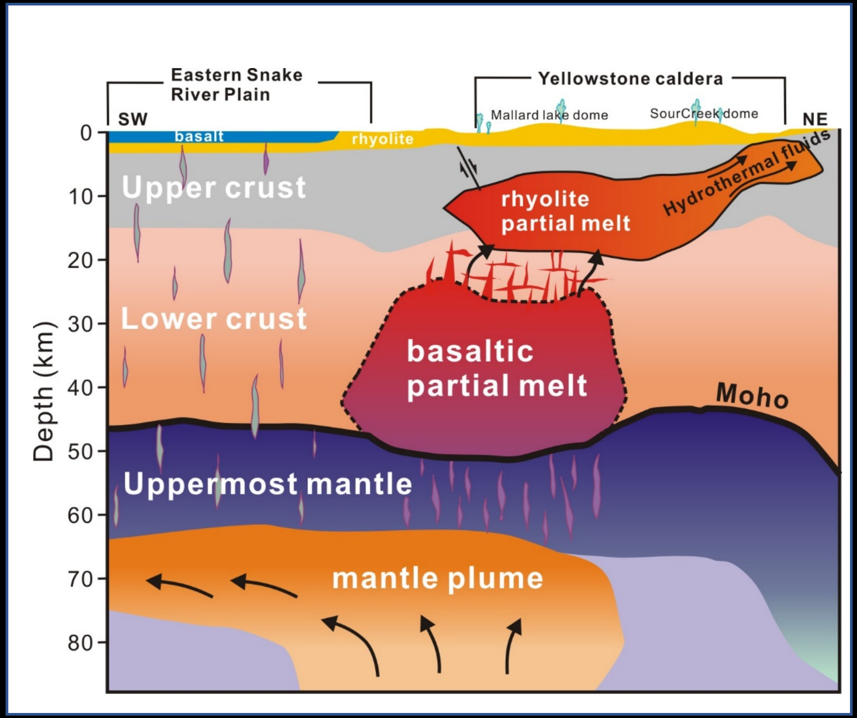

Polarization and waveform fitting in 2-D beneath Yellowstone caldera

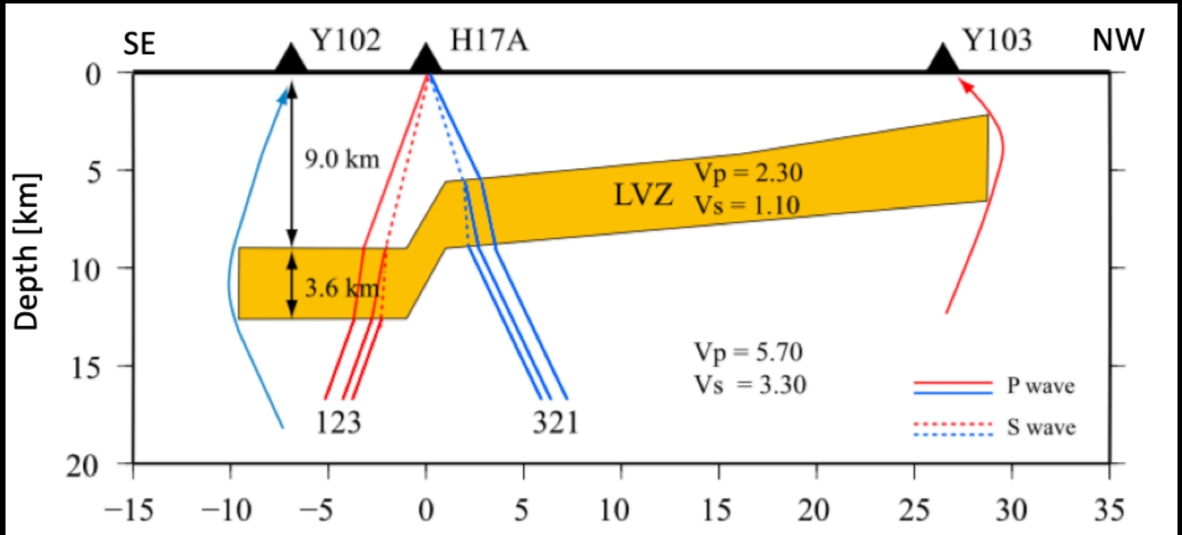

Chu et al., 2010

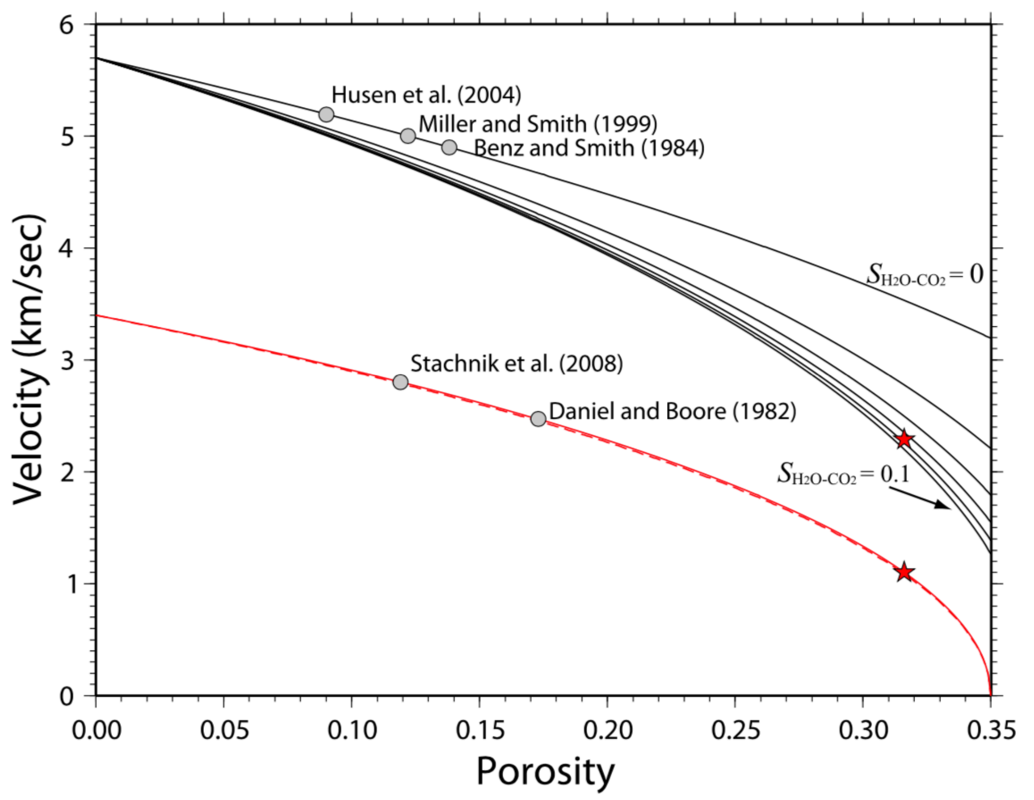

Chu et al. 2010

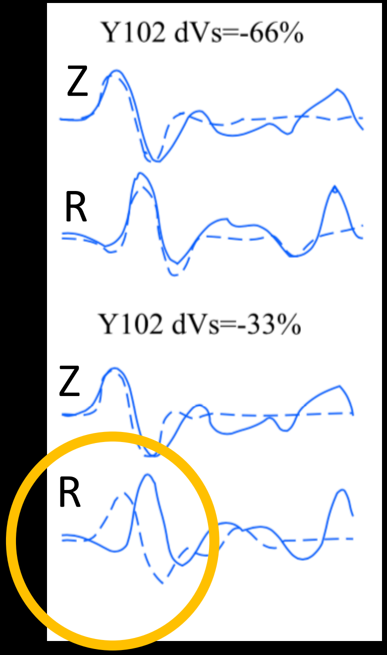

Estimated structure from 2-D forward modeling

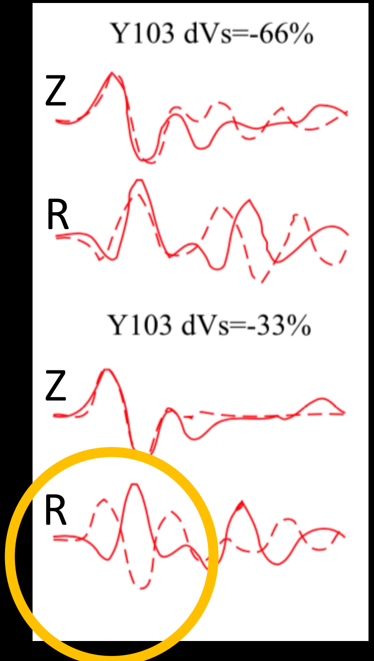

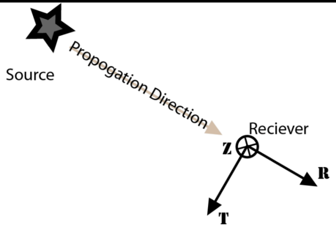

Yellowstone hotspot's crustal magmatic system

Are these melt reservoirs uniform and well-mixed?

How does transport occur within and between them?

Does the mean velocity from tomography provide a good estimate of melt content and mobility?

Two local minima in Vp perturbation as a function of depth

Low-mobility crystal-dominated mush with ~2-10% melt may be sufficient

Some waveform evidence for locally higher melt fractions of up to ~30% [Chu et al., 2010]

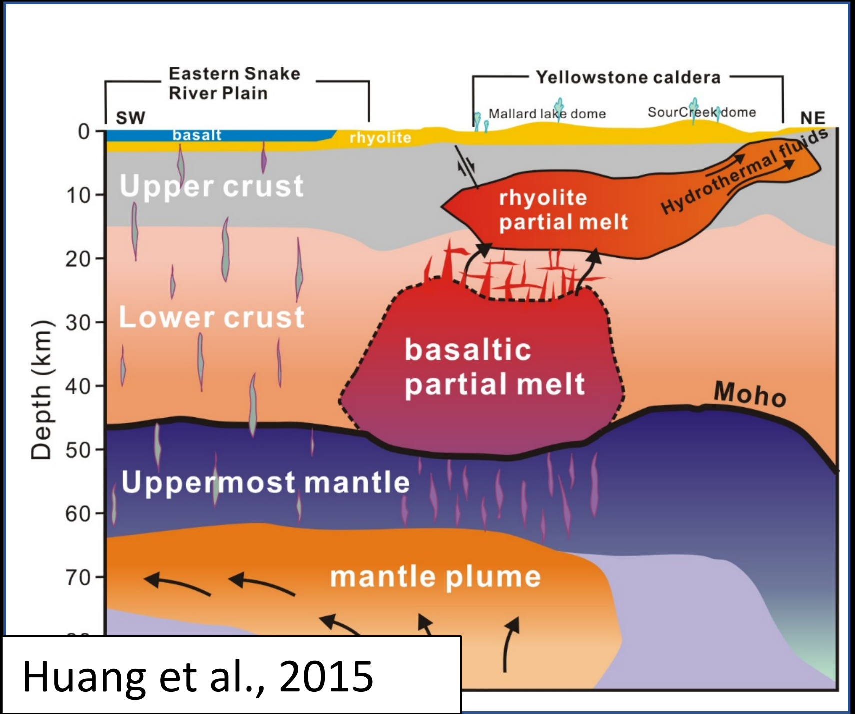

Huang et al., 2015

Rayleigh and Love waves

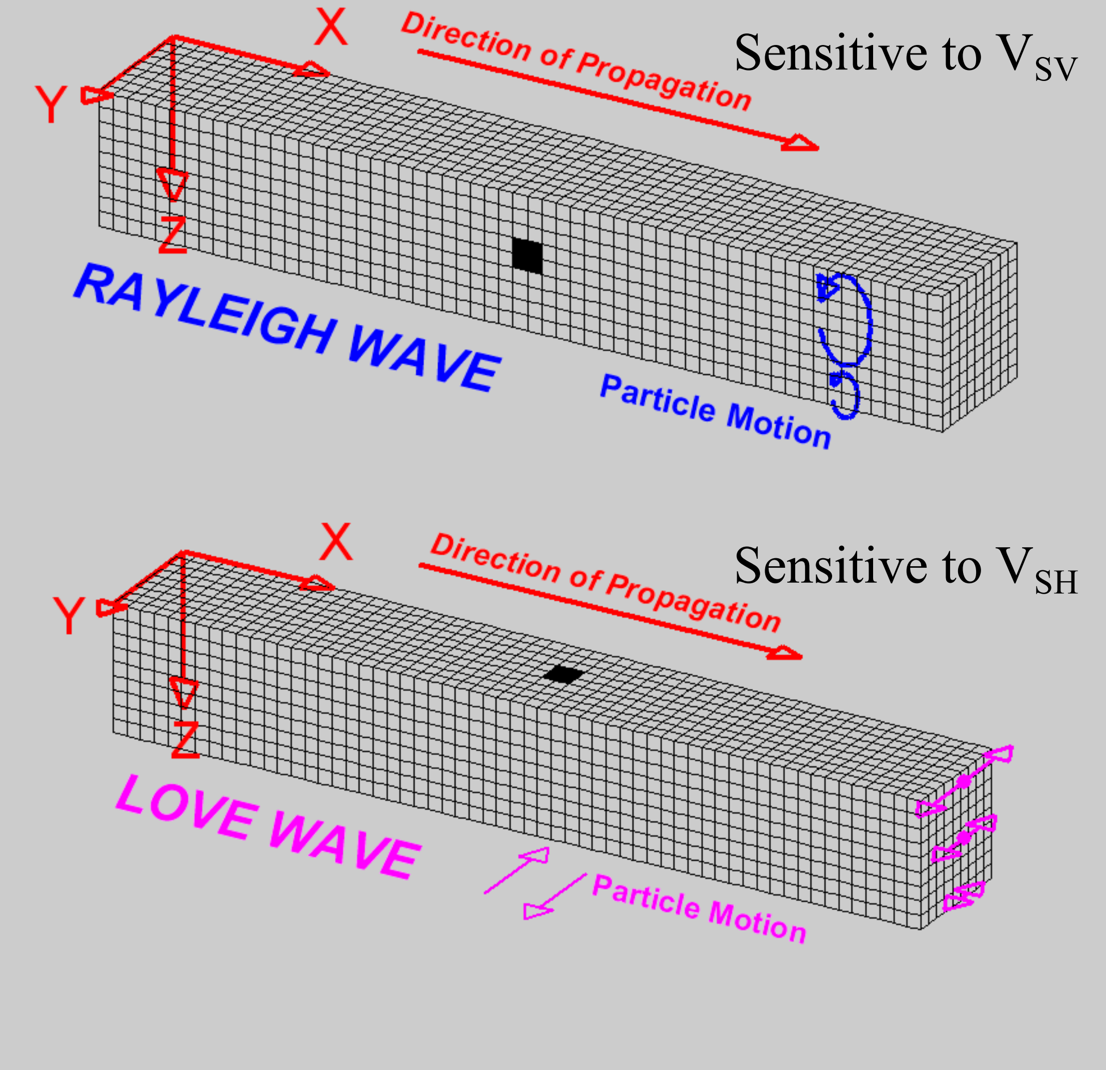

L. Braile

- V_{SV} & V_{SH} depend on the physical properties of rocks
- Inconsistency of Rayleigh and Love with a common Vs model indicates seismic anisotropy

Radial anisotropy and surface waves

- Oriented horizontally → sills/lenses in magmatic context
- Oriented vertically → dikes in magmatic context

Apparent anisotropy from layered isotropic media (e.g., Postma, 1955; Backus, 1962)

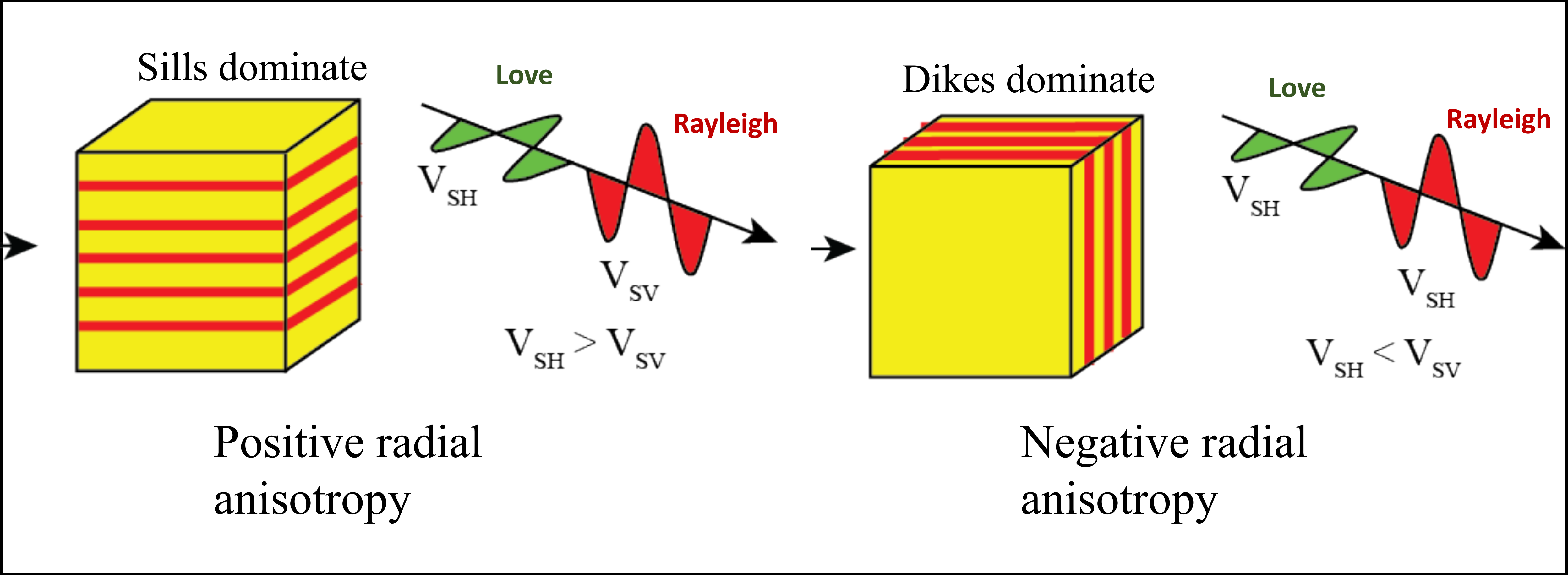

Seismic noise interferometry

Seismic station

Time window of signal recorded at A

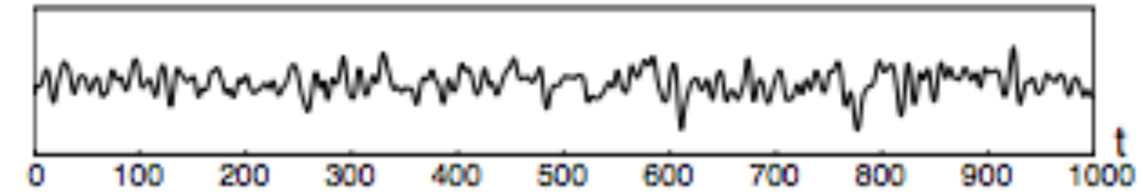

Time window of signal recorded at B

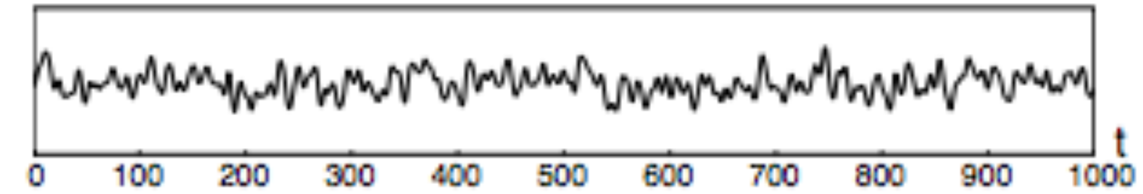

Cross-correlations of A & B

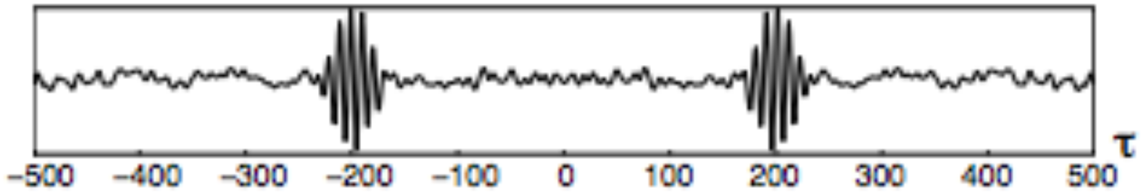

$$\int u_1(t)\,u_2(t+\tau)\;dt = C(\tau)$$

Signals emerge from longer-term averaging of cross-correlation functions

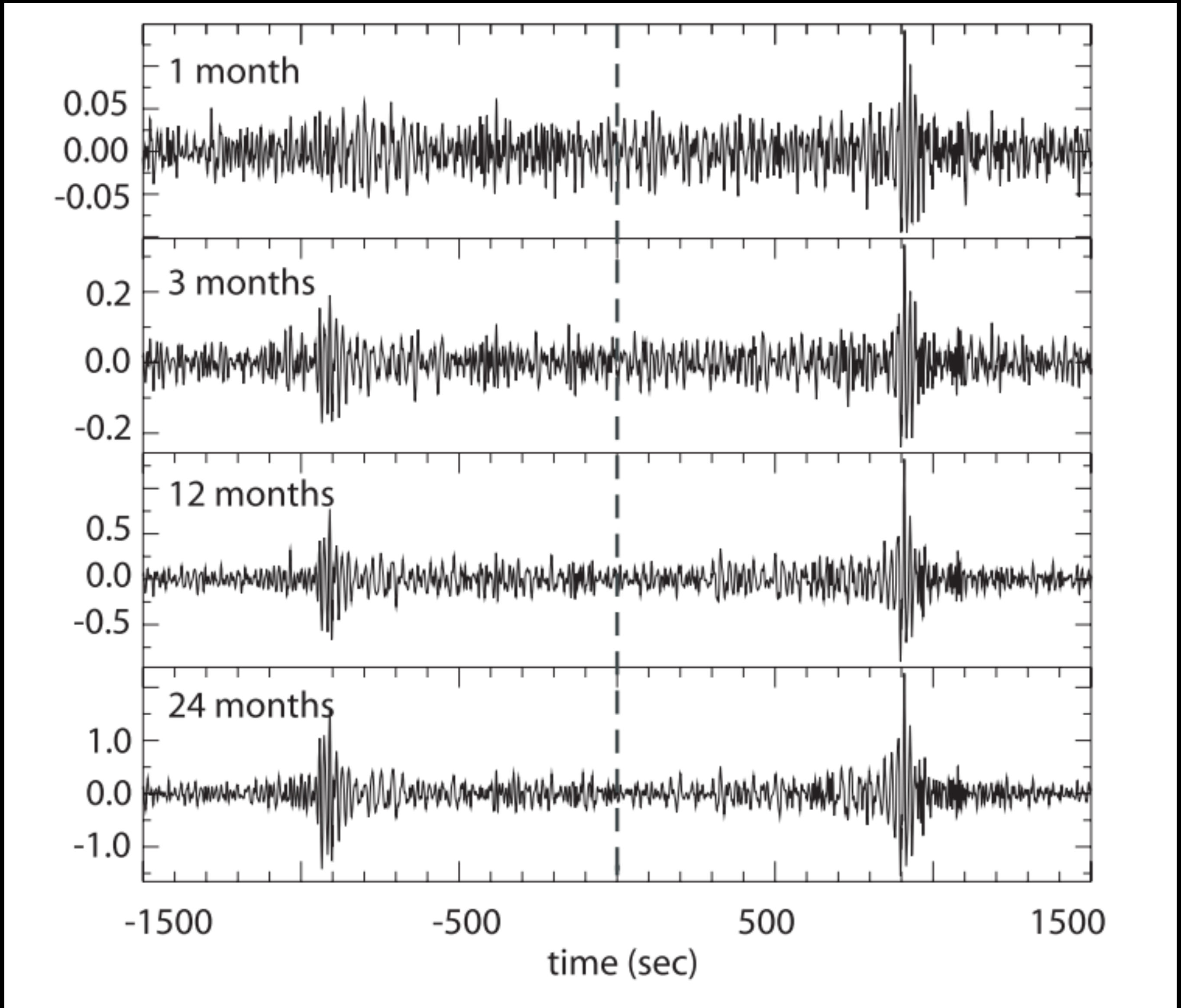

Empirical estimate of Green’s function for a surface source

Bensen et al., GJI, 2007

Vertical and Transverse noise correlations at Long Valley

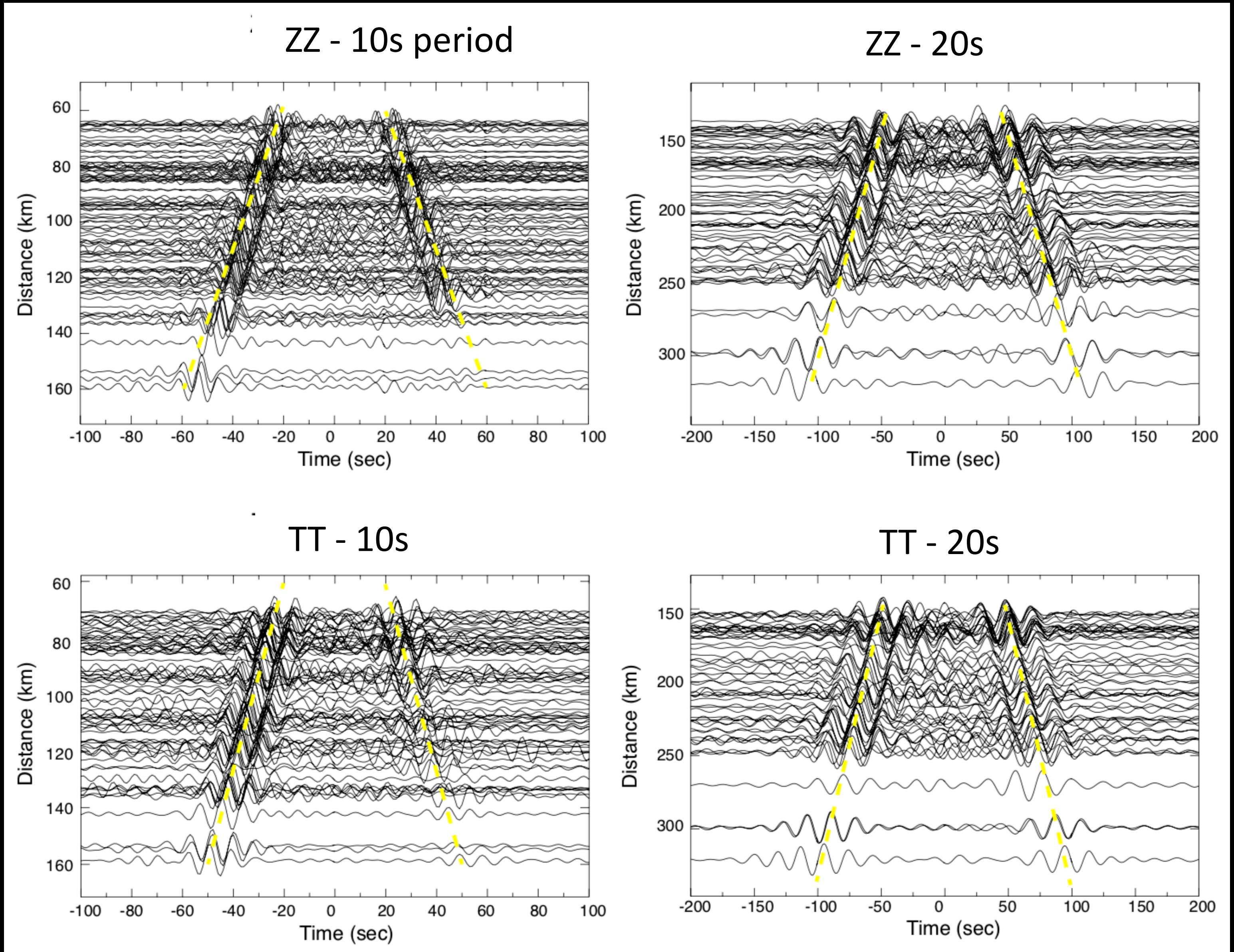

Wavefield from a ‘virtual source’

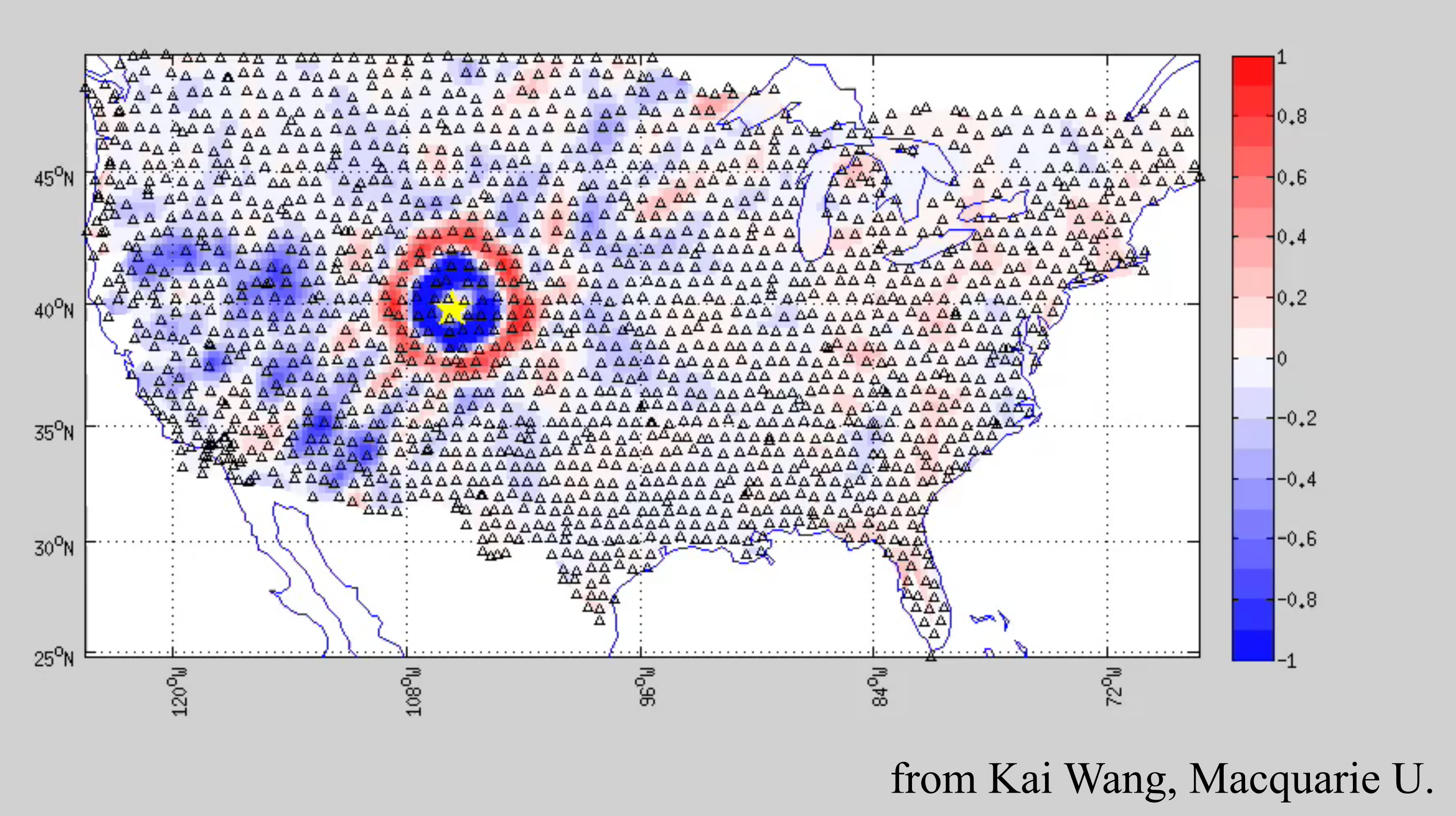

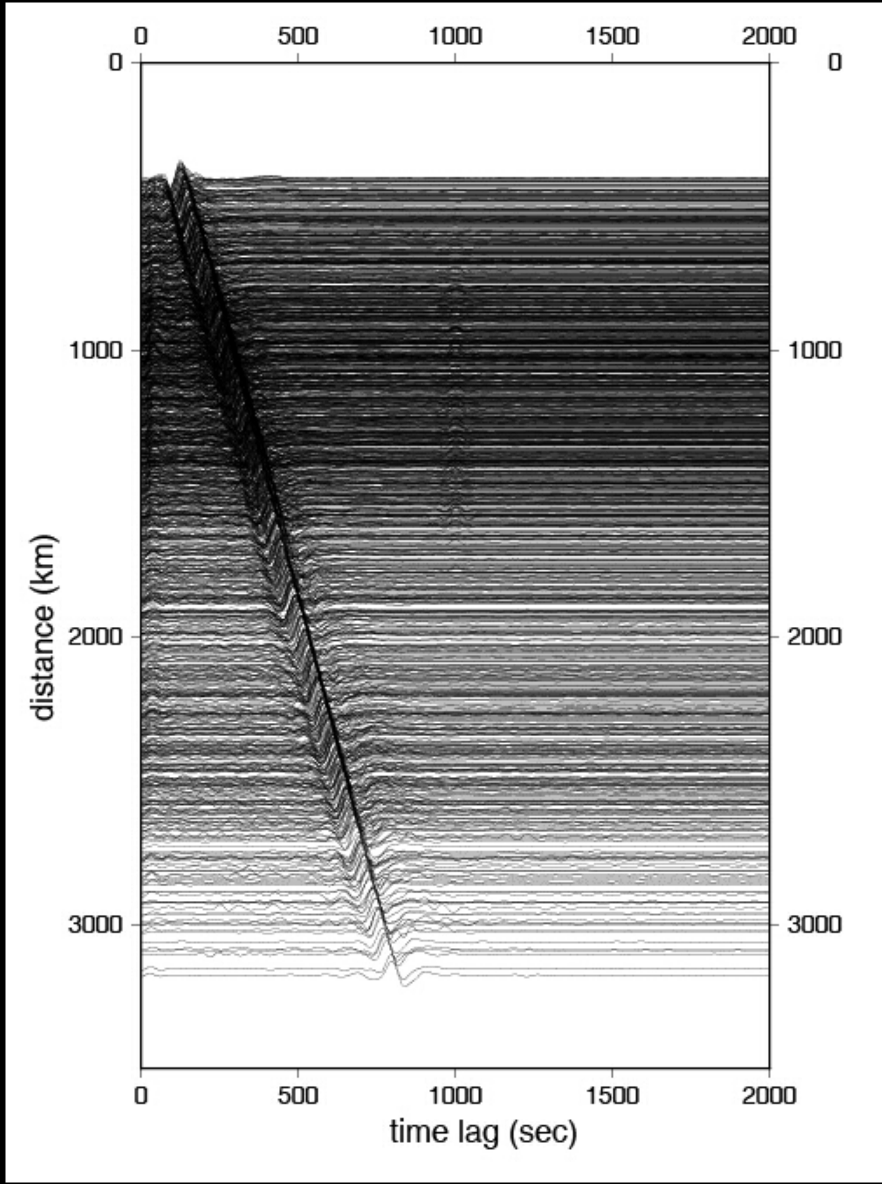

~2000 broadband seismographs from EarthScope and permanent networks

Wavefield from a 'virtual source'

7 x 10 km scale with 5200 nodes

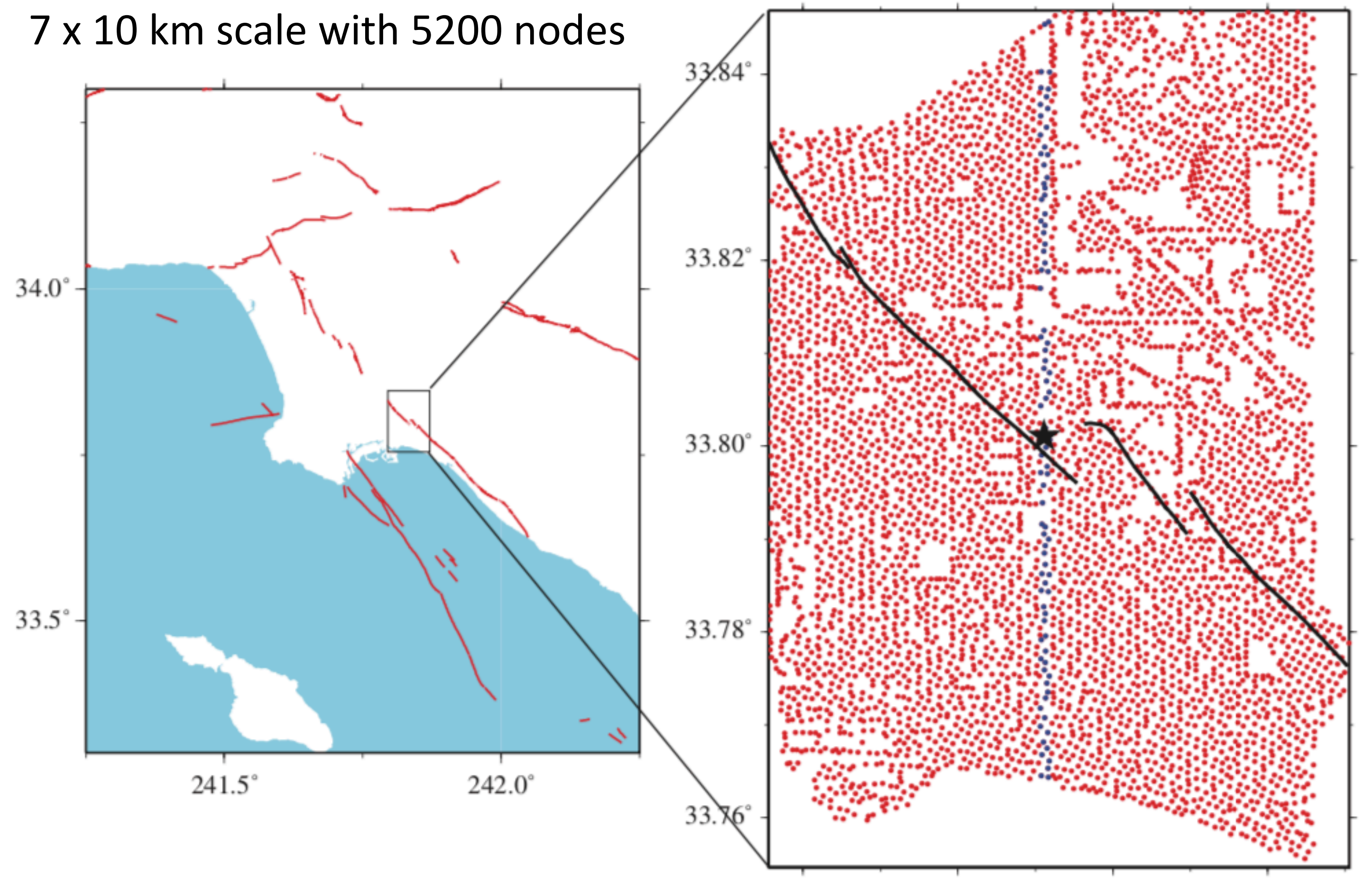

Lin et al., 2013

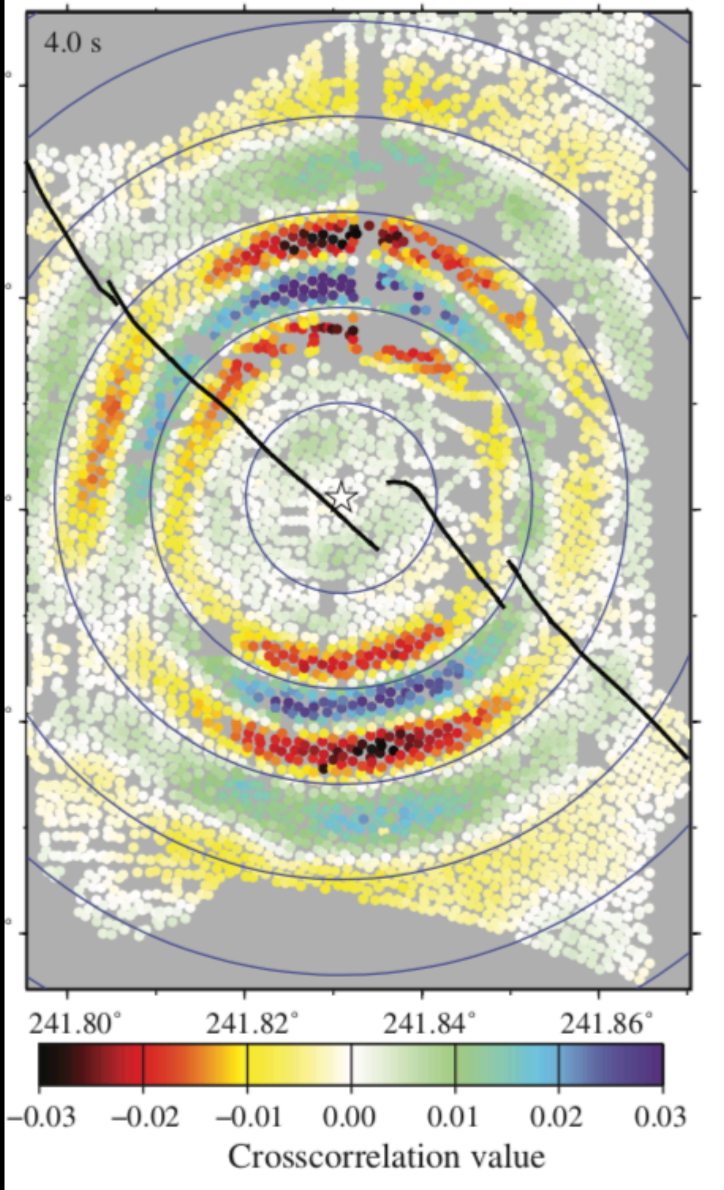

Focus on radial anisotropy in surface wave tomography
(mostly skipping earlier surface wave tomography steps)

Main steps:

1) Estimate empirical Green's function for ZZ and TT (using EE, NN, EN, NE)
2) Measure dispersion between station pairs for Rayleigh and Love waves
3) Invert dispersion curves for 2-D phase velocity maps
4) <u>Invert phase velocities for (an)isotropic Vs as a function of depth</u>

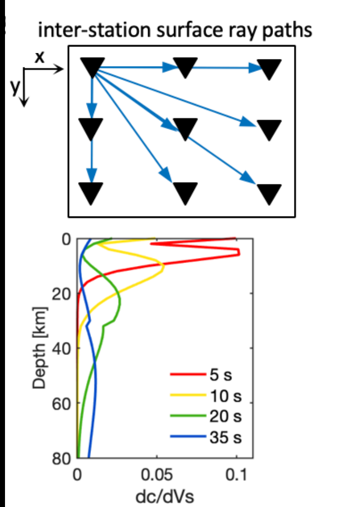

1)

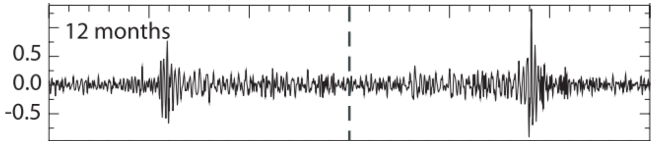

Bensen et al., 2007

2)

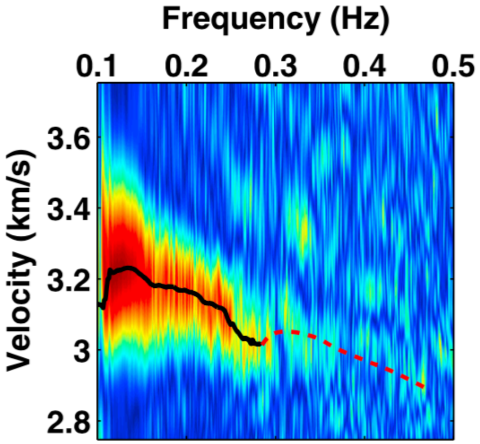

van Wijk et al., 2011

3)

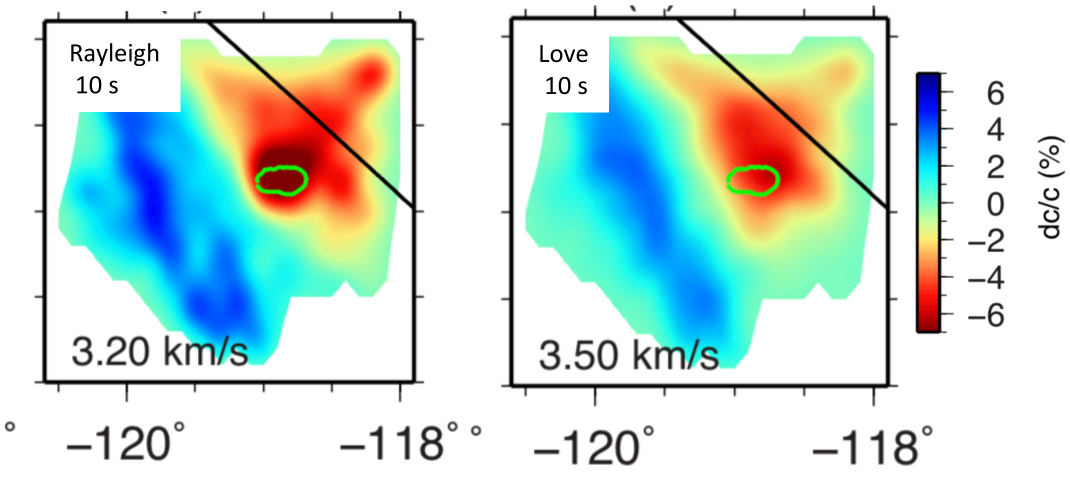

Inverting dispersion measurements for Vs(depth)

1,500,000 iterations per model point (based on tests of stability of posterior for anisotropic terms)

Posterior distribution defined as best 1,000 models at each location

Identify anisotropic parameters that are non-zero at 2-sigma

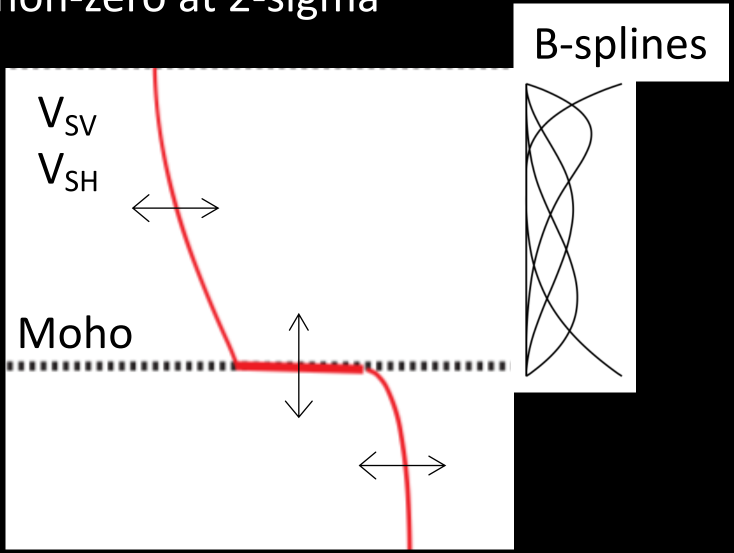

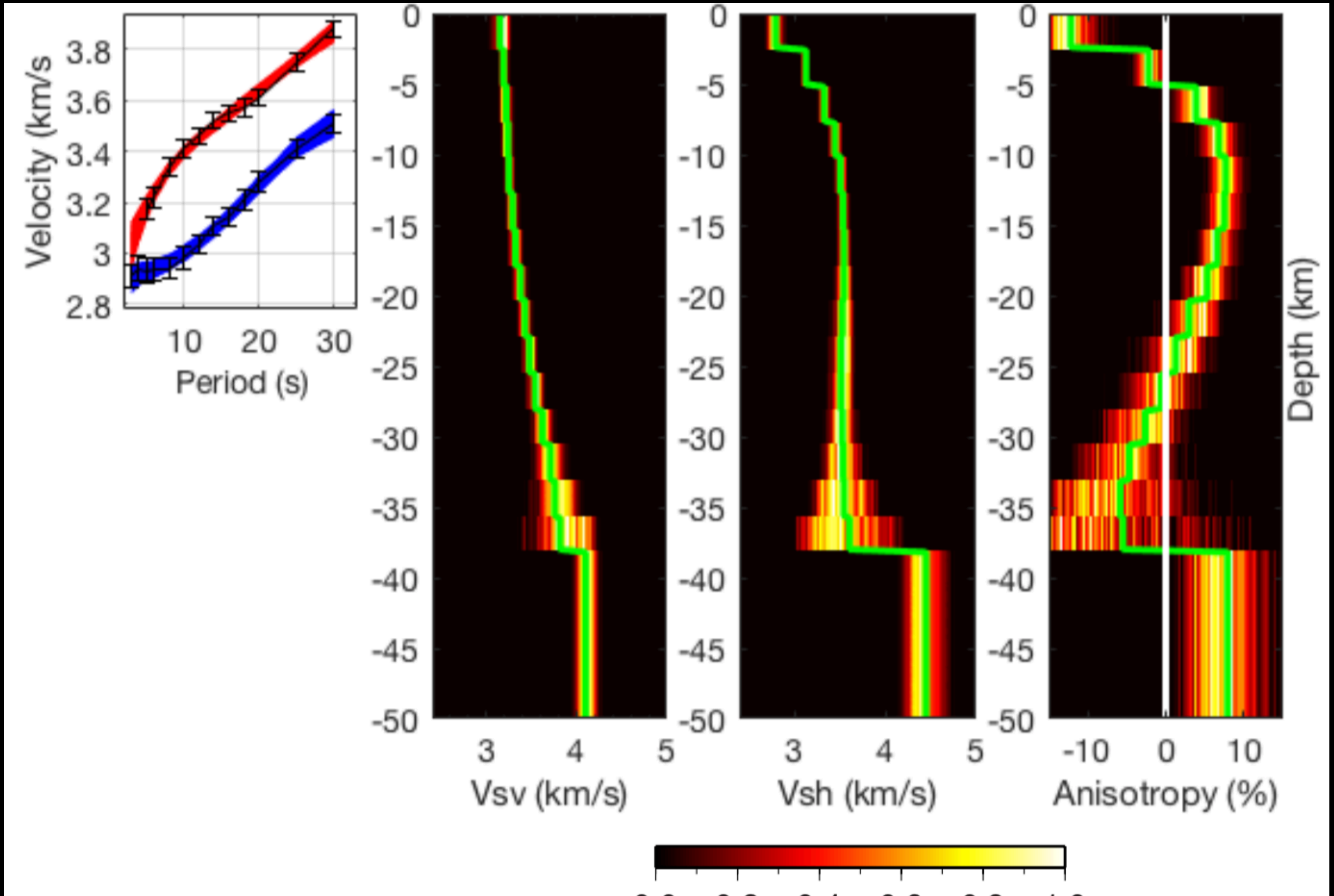

Example point near LVC

Influence of radial anisotrop parameters

Introduction of radial anisotropy leads to major improvements in fit to the dispersion data compared to isotropic inversions

Improvements are found in many areas, but some of the strongest are found beneath the calderas

Observed phase velocity

Predicted phase velocity

$$\chi^2 = \sum_i \frac{(O_i - C_i)^2}{\sigma_i^2}$$

Phase velocity uncertainty
From repeated inversion with bootstrap resampling

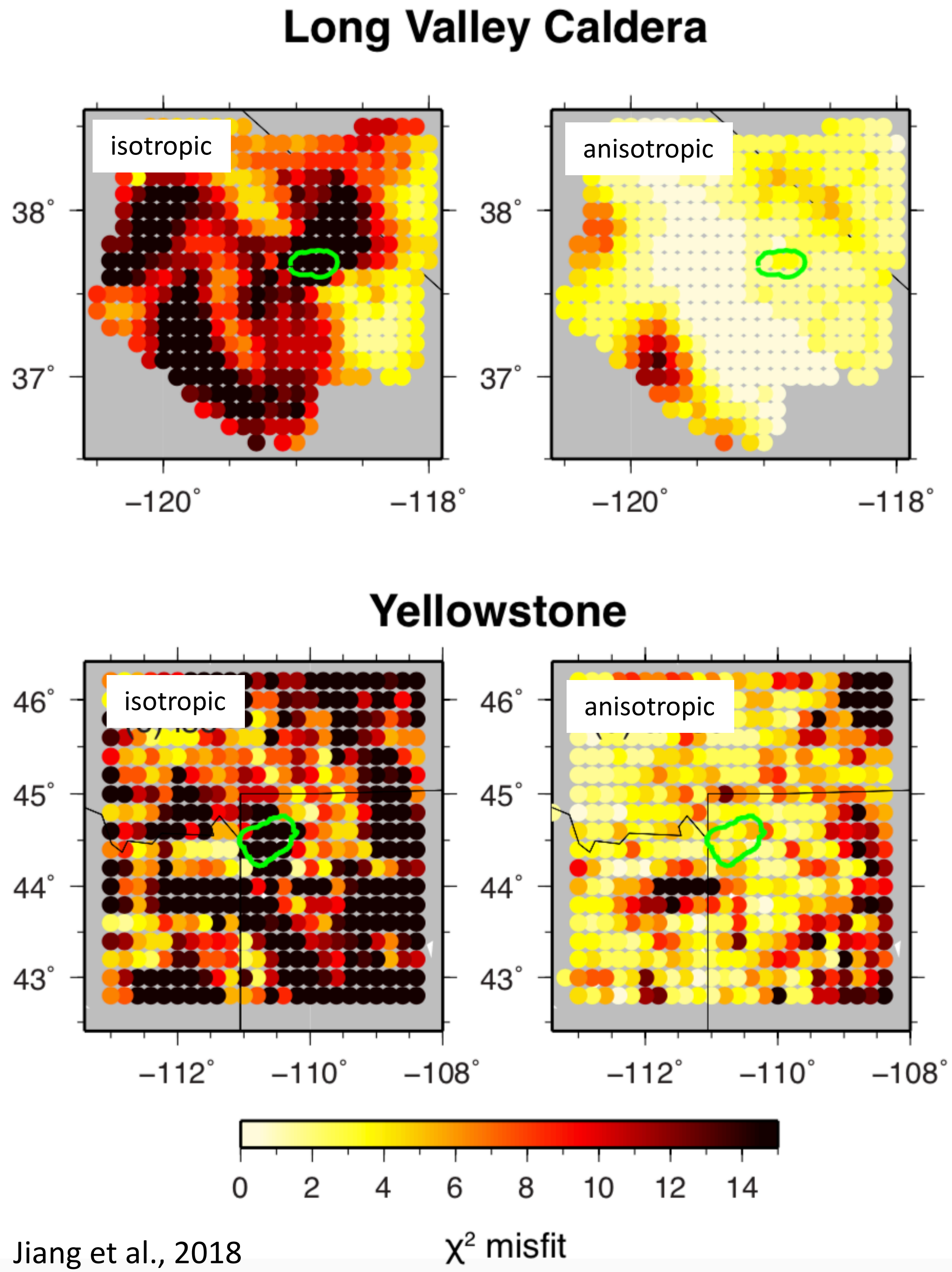

Jiang et al., 2018

Influence of radial anisotropy parameters

Introduction of radial anisotropy leads to major improvements in fit to the dispersion data compared to isotropic inversions

Improvements are found in many areas, but some of the strongest are found beneath the calderas

Observed phase velocity

Predicted phase velocity

$$\chi^2 = \sum_i \frac{(O_i - C_i)^2}{\sigma_i^2}$$

Phase velocity uncertainty
From repeated inversion with bootstrap resampling

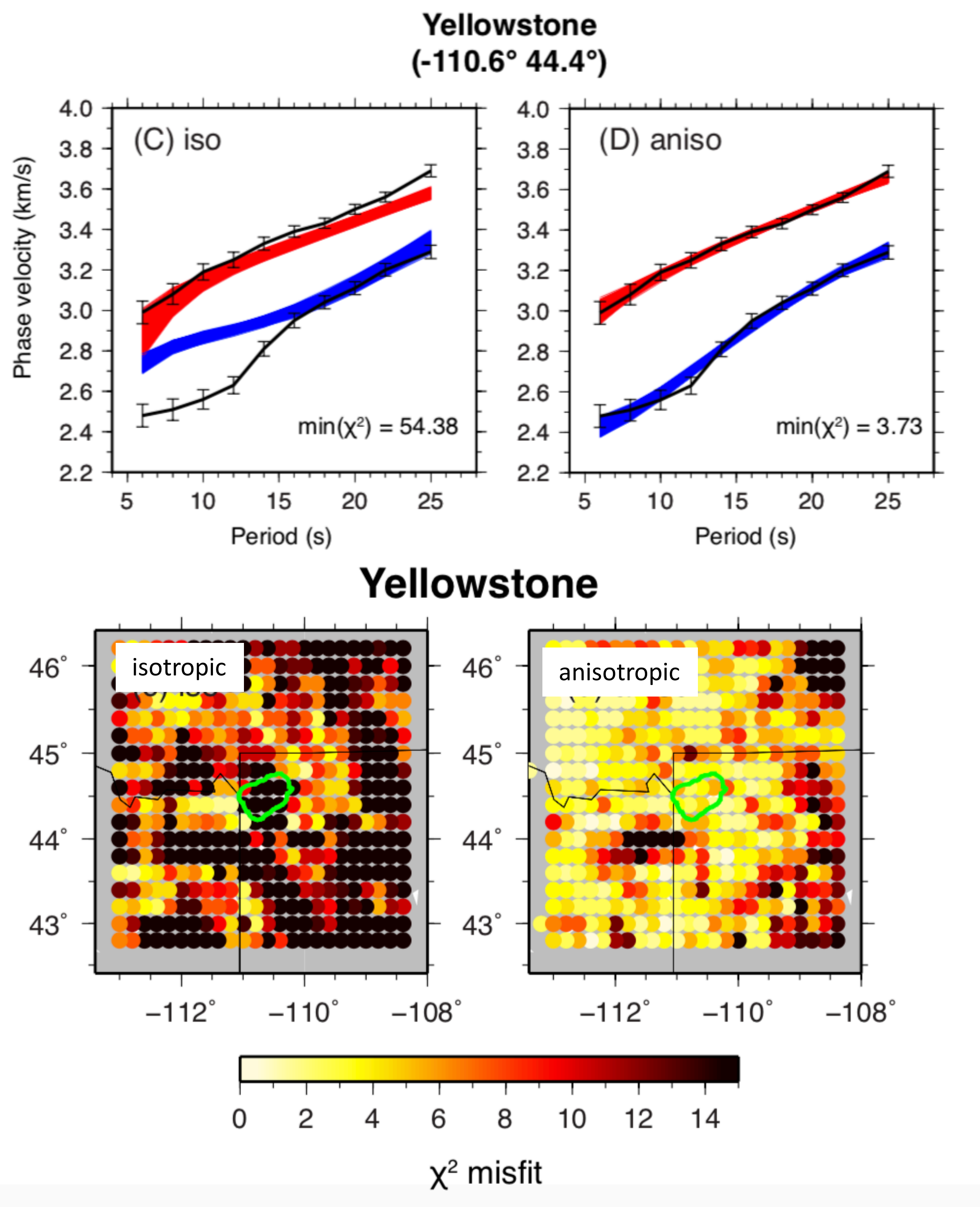

Where is anisotropy required at 1-2 sigma?

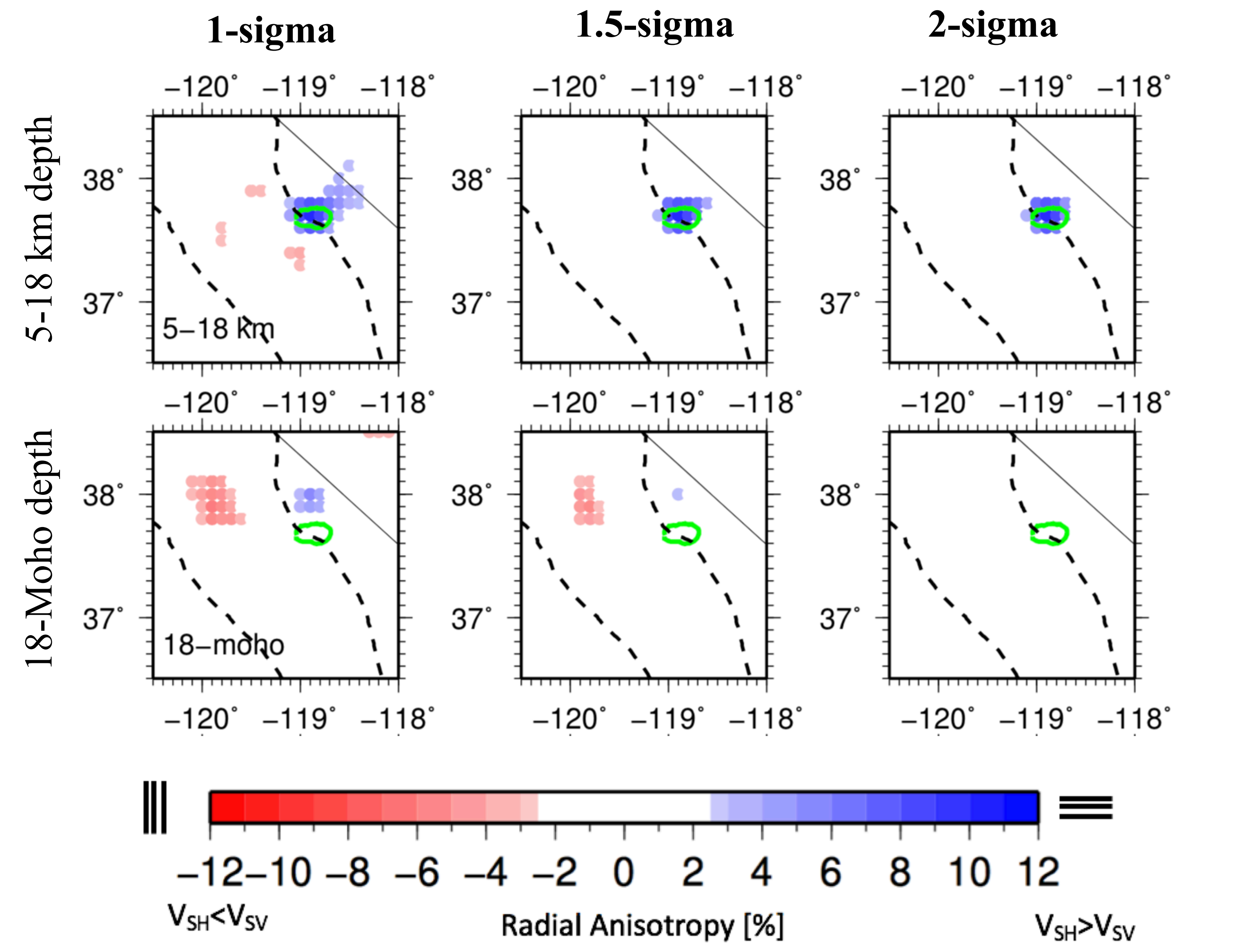

Jiang et al., 2018

Radial anisotropy is most important to fitting middle crustal structure directly beneath the LV caldera

Long Valley region upper, middle, lower crust

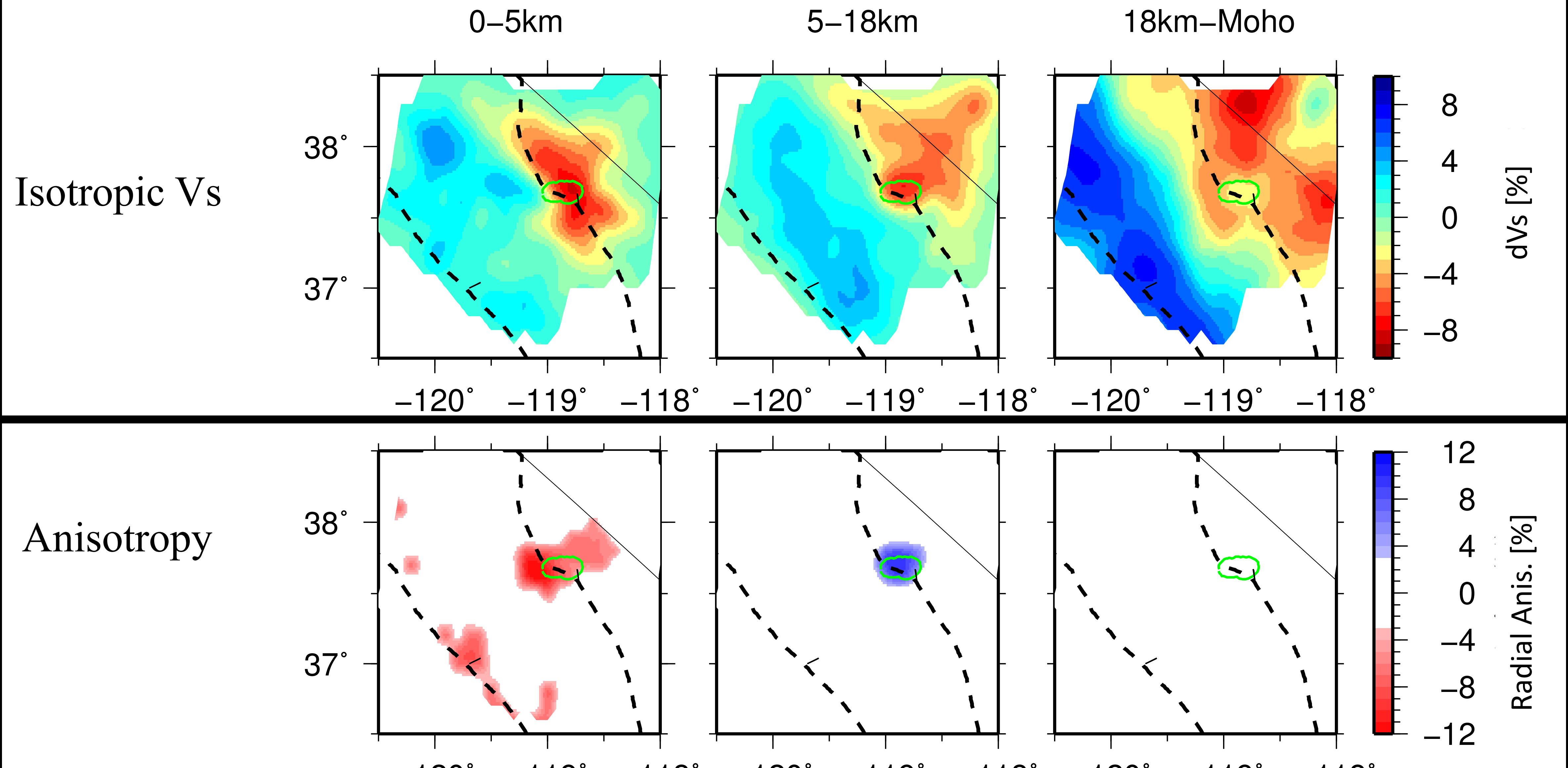

Jiang et al., 2018

Yellowstone region upper, middle, lower crust

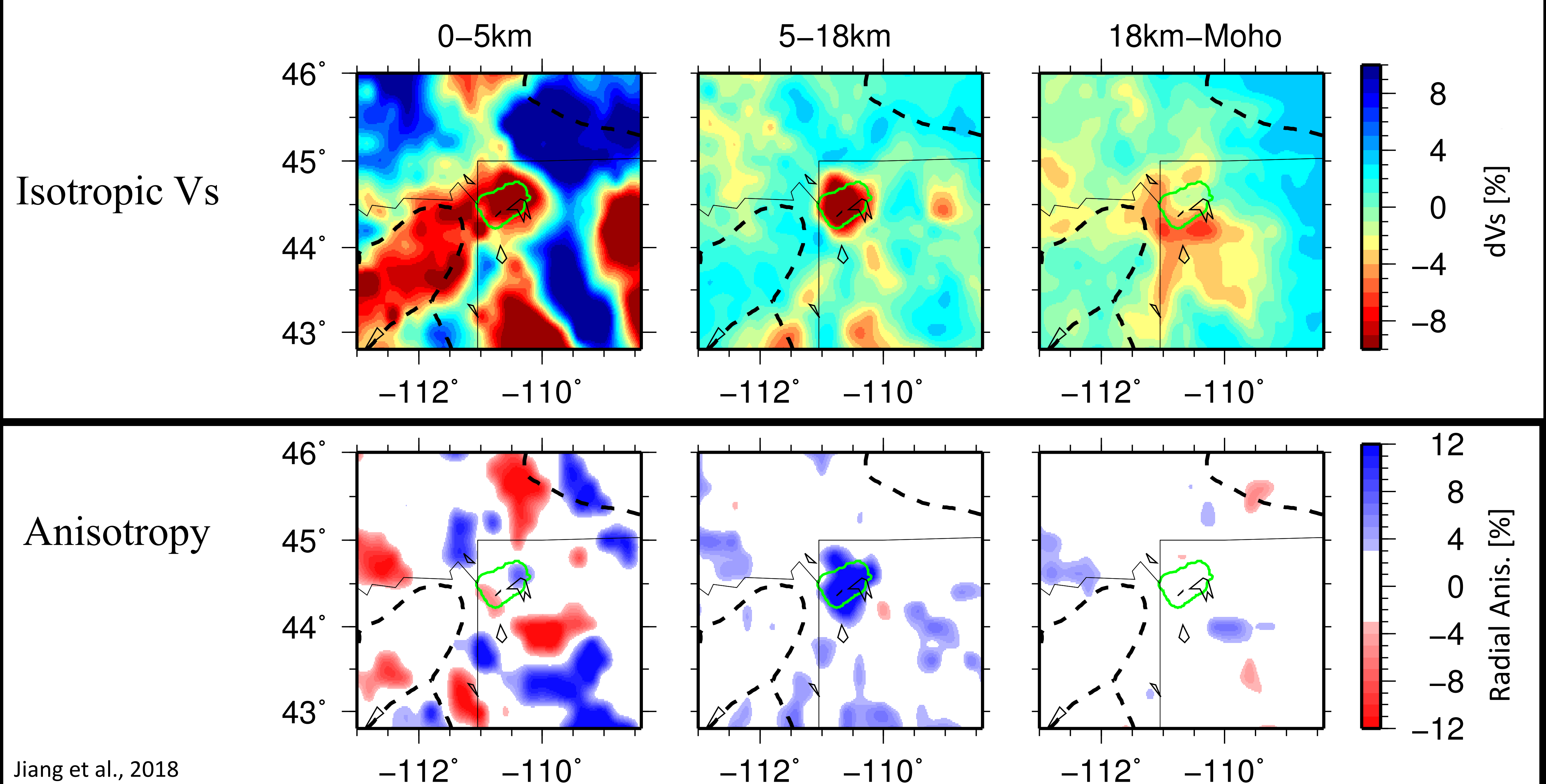

Jiang et al., 2018

Cross sections of anisotropic structures

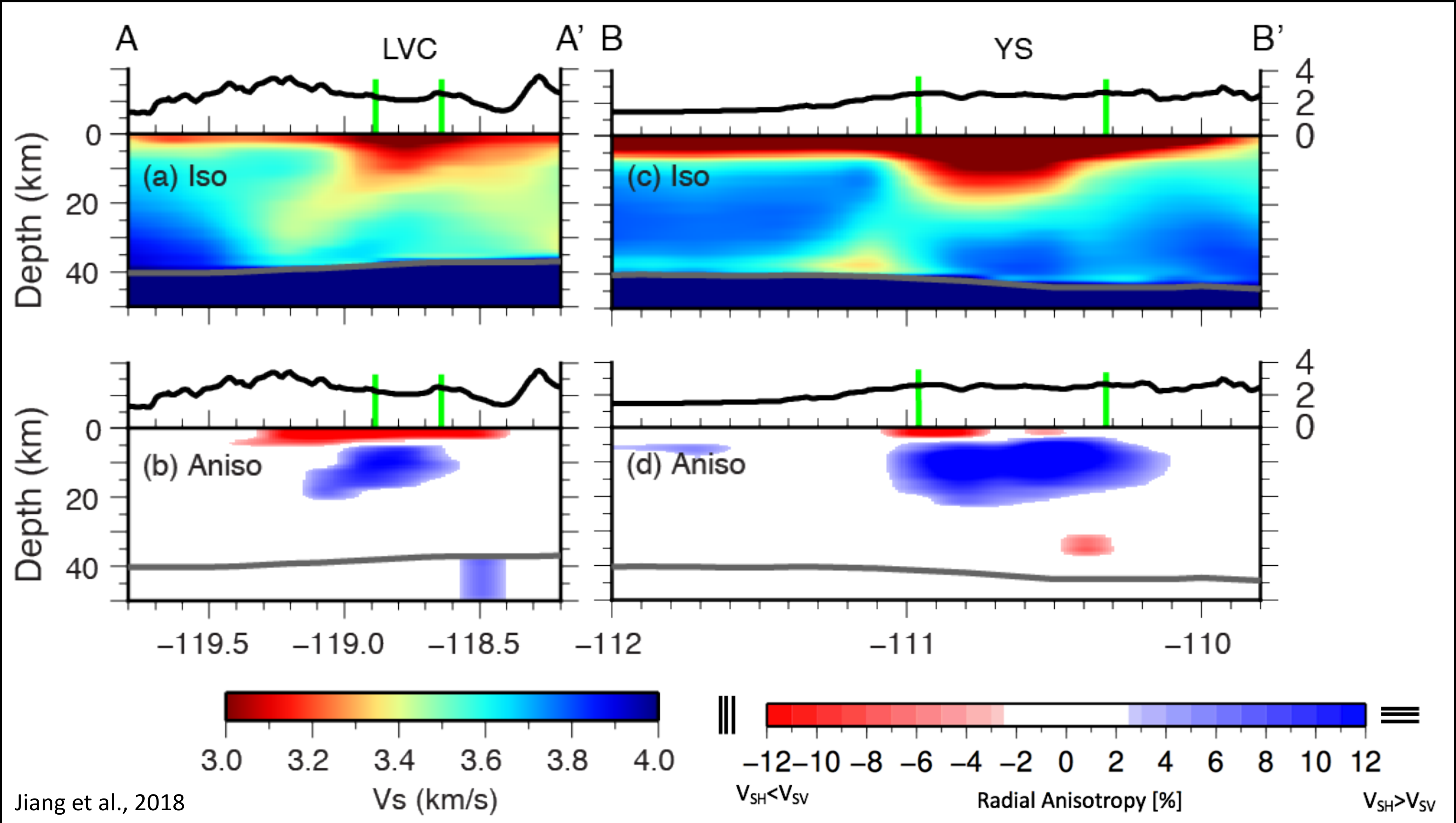

Jiang et al., 2018

Cross sections of anisotropic structures

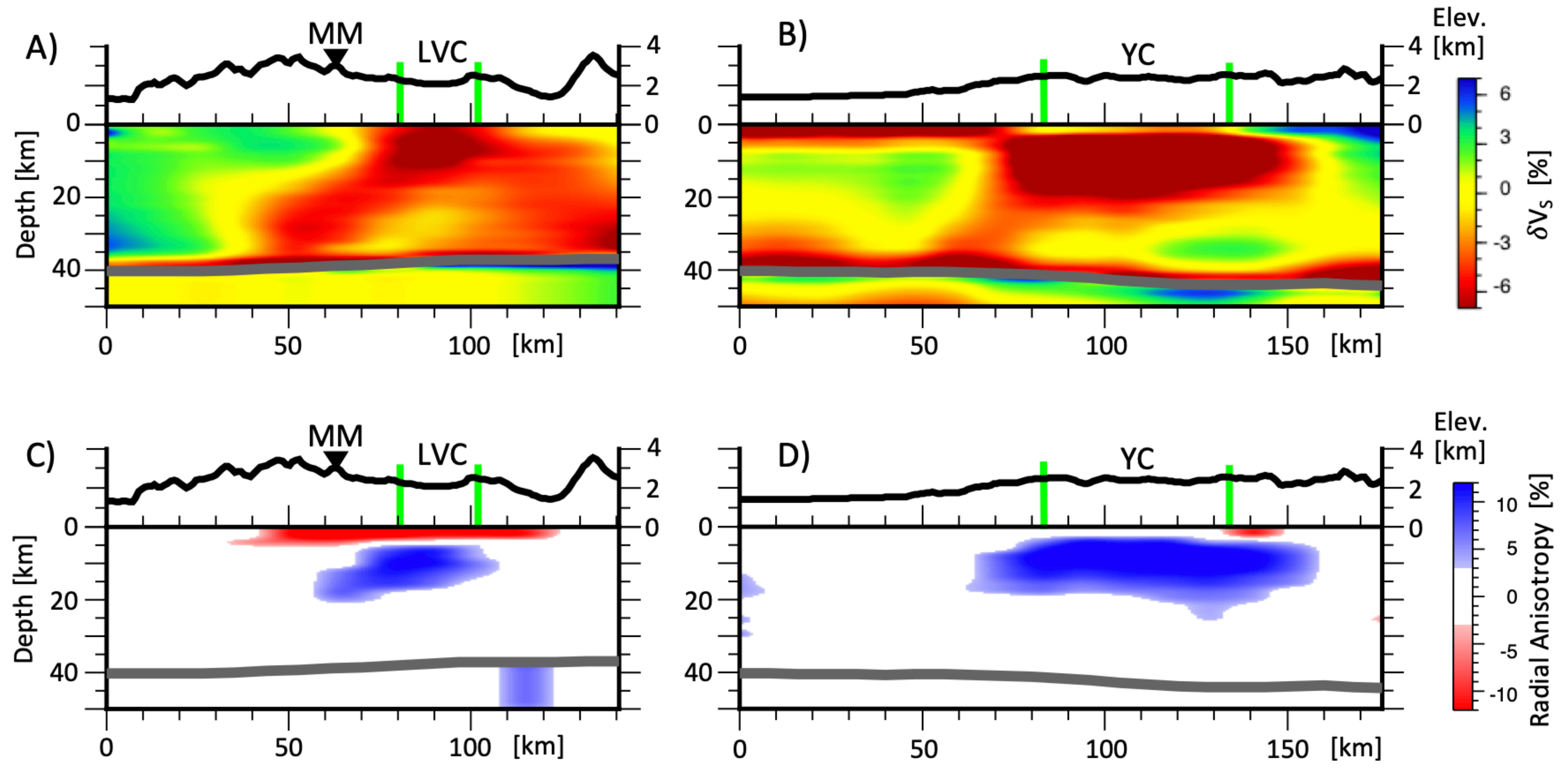

Long Valley cross-sections, different methods

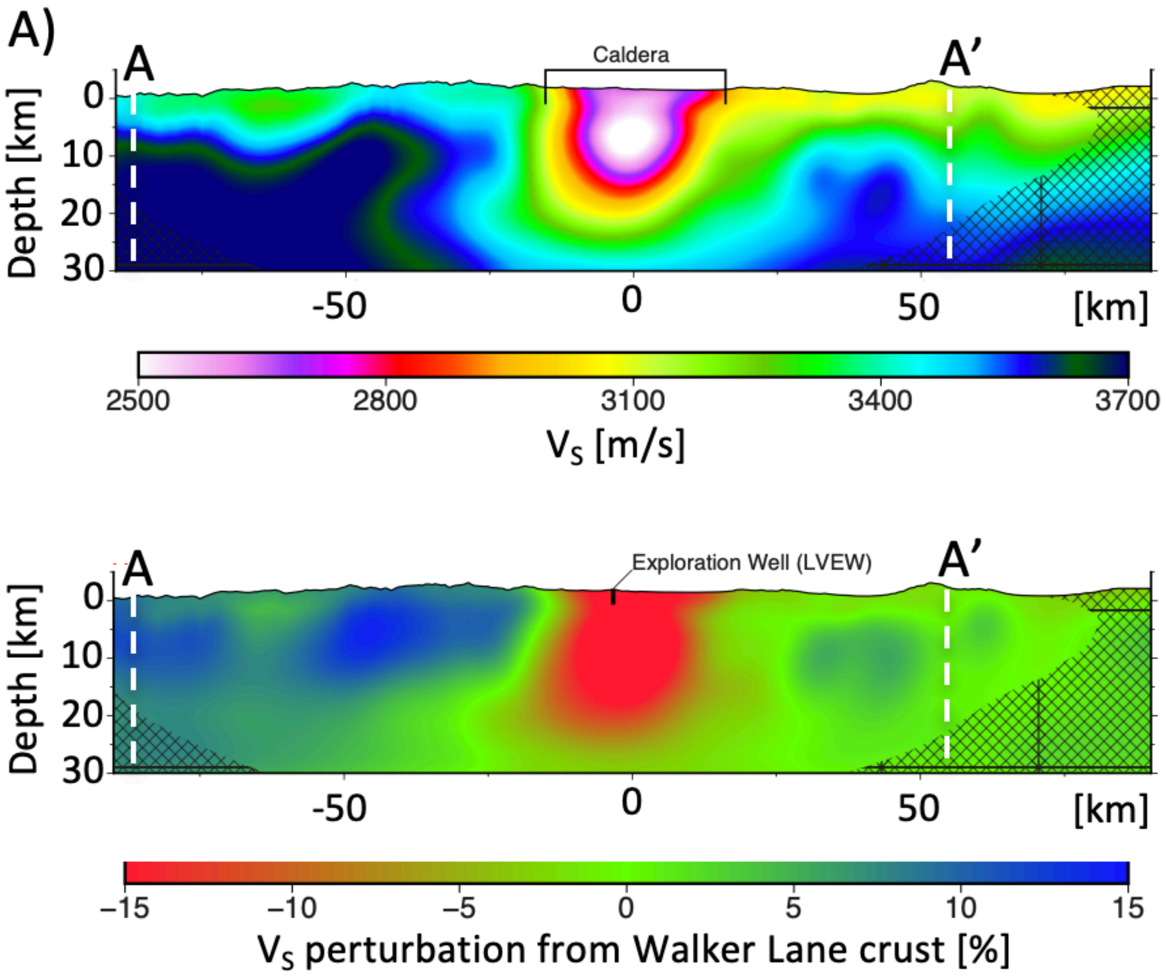

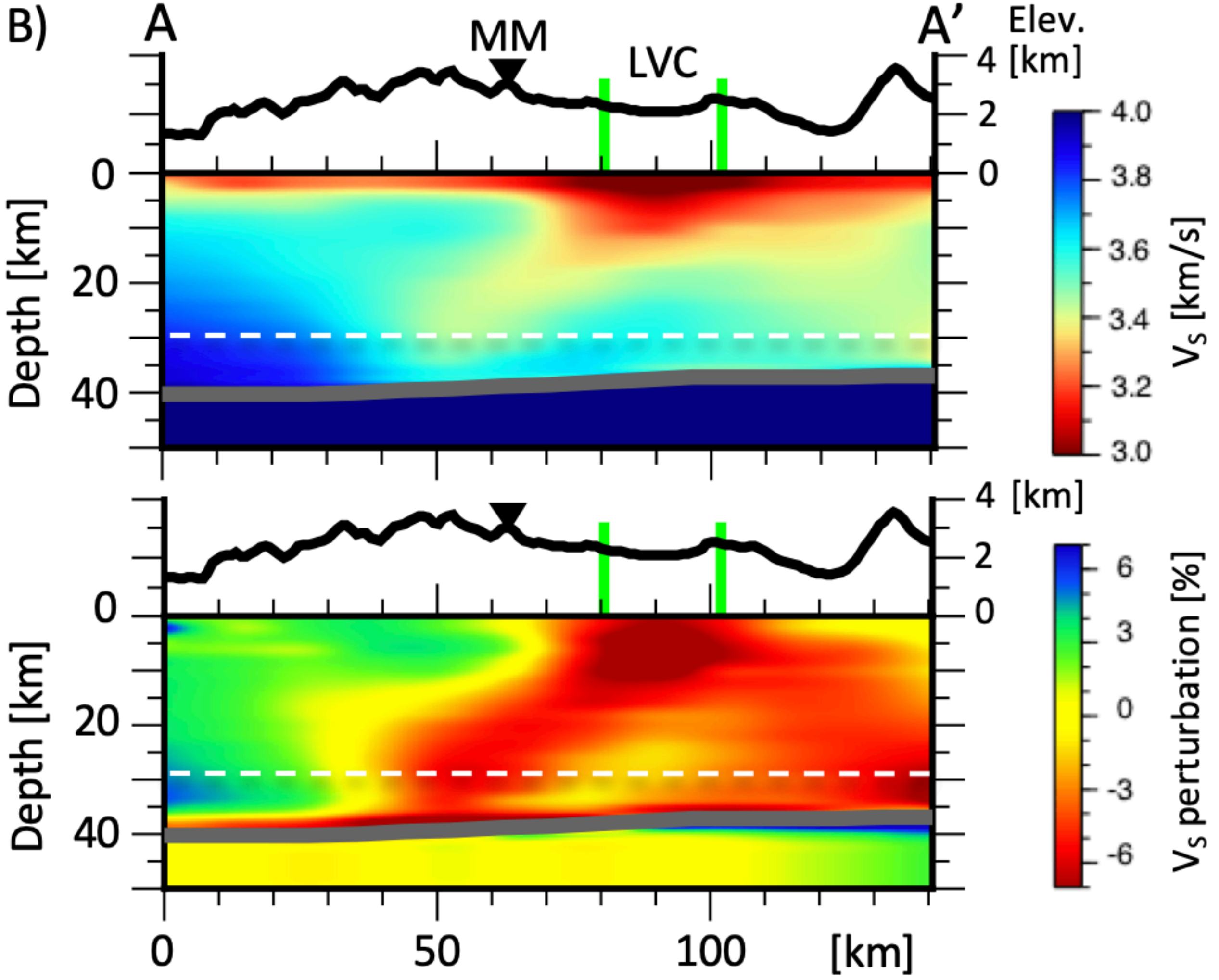

Flinders et al. 2018

Jiang et al., 2018

Origin of positive anisotropy in low-Vs volumes

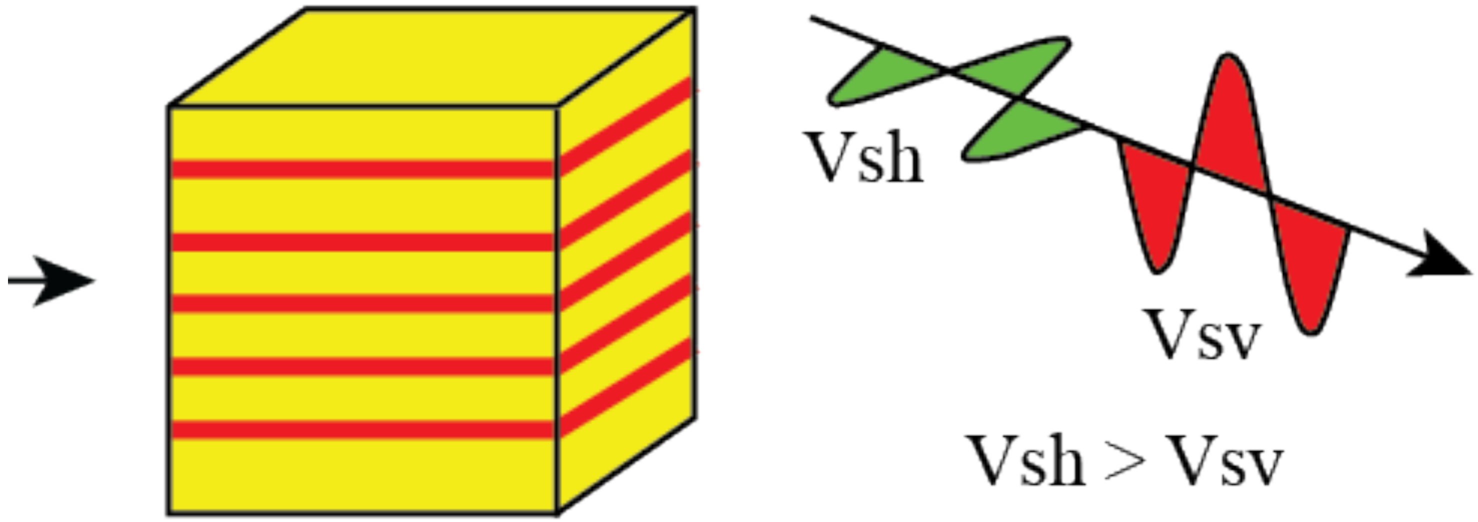

Horizontally elongated volumes of partial melt → magmatic sills/lenses?

Sill geometry tradeoffs

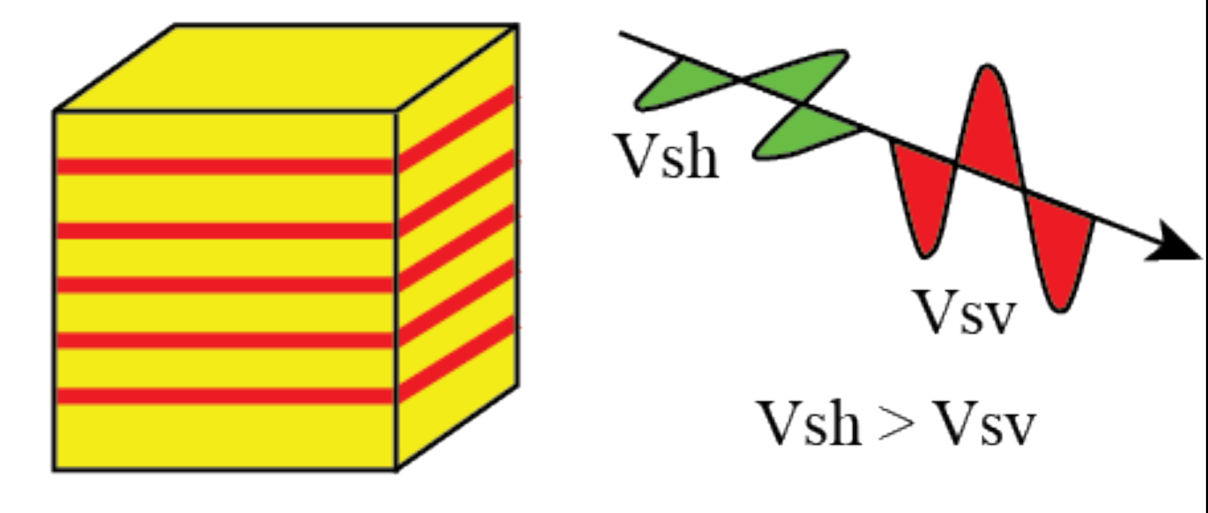

Sills of slow Vs (partial melt) embedded in faster host rock?

Best fit from 5-40% sills and 60-95% host rock
And
1.6 – 2.4 km/s Vs in the sills (could be ~10-25% melt)

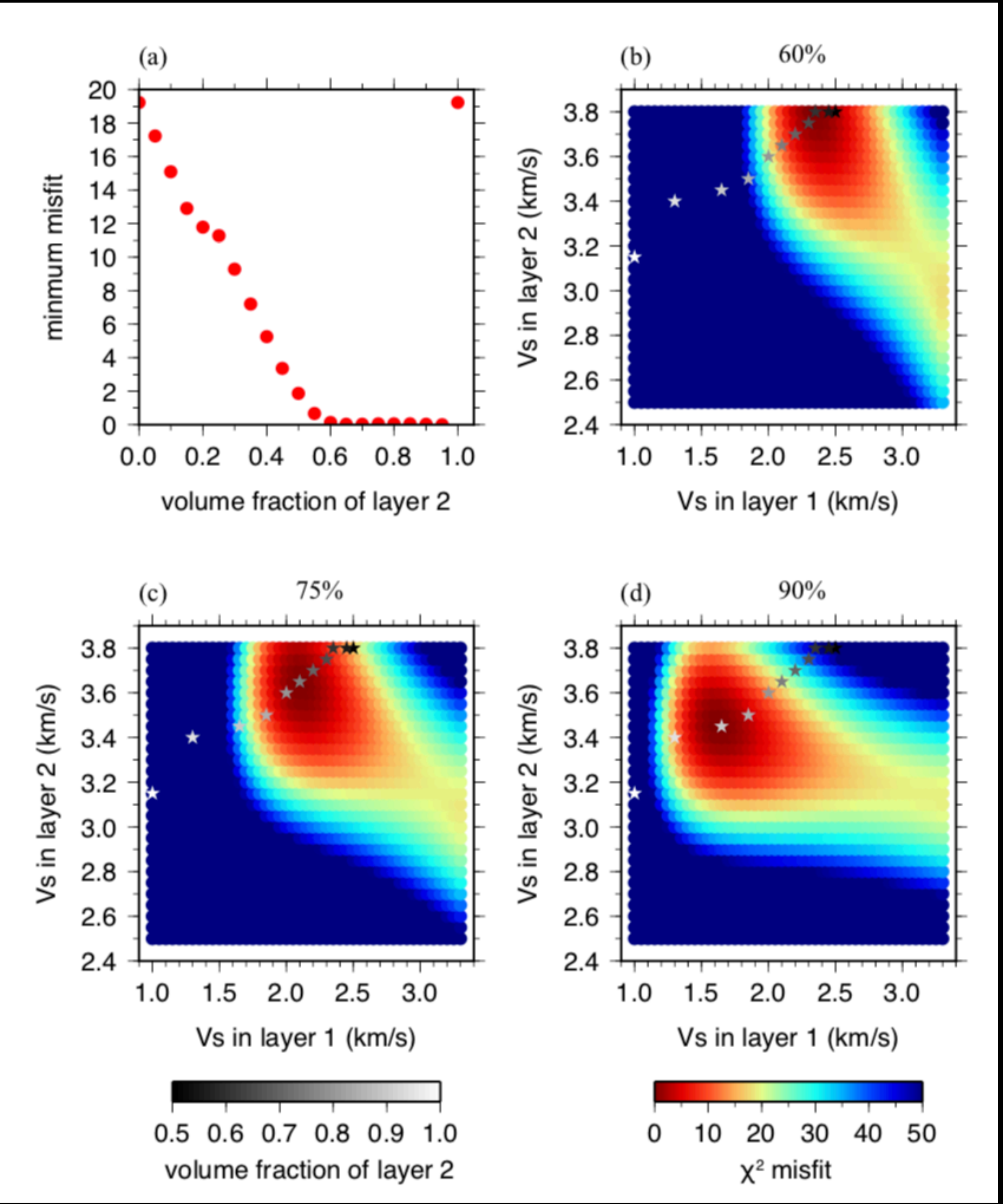

Negligible anisotropy beneath eastern Snake River Plain

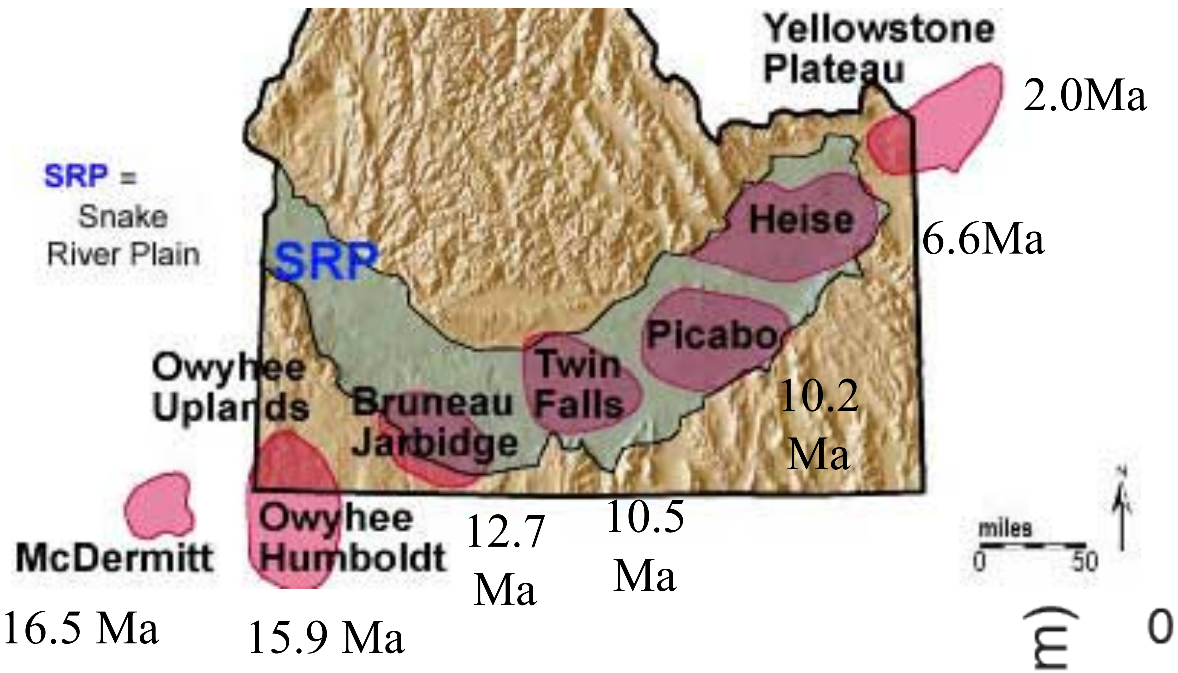

Absence of anisotropic layer beneath Heise indicates that it fades once major melt flux migrates northeast

→ Horizontal layering of evolved melt is likely in the positive radial anisotropy volume

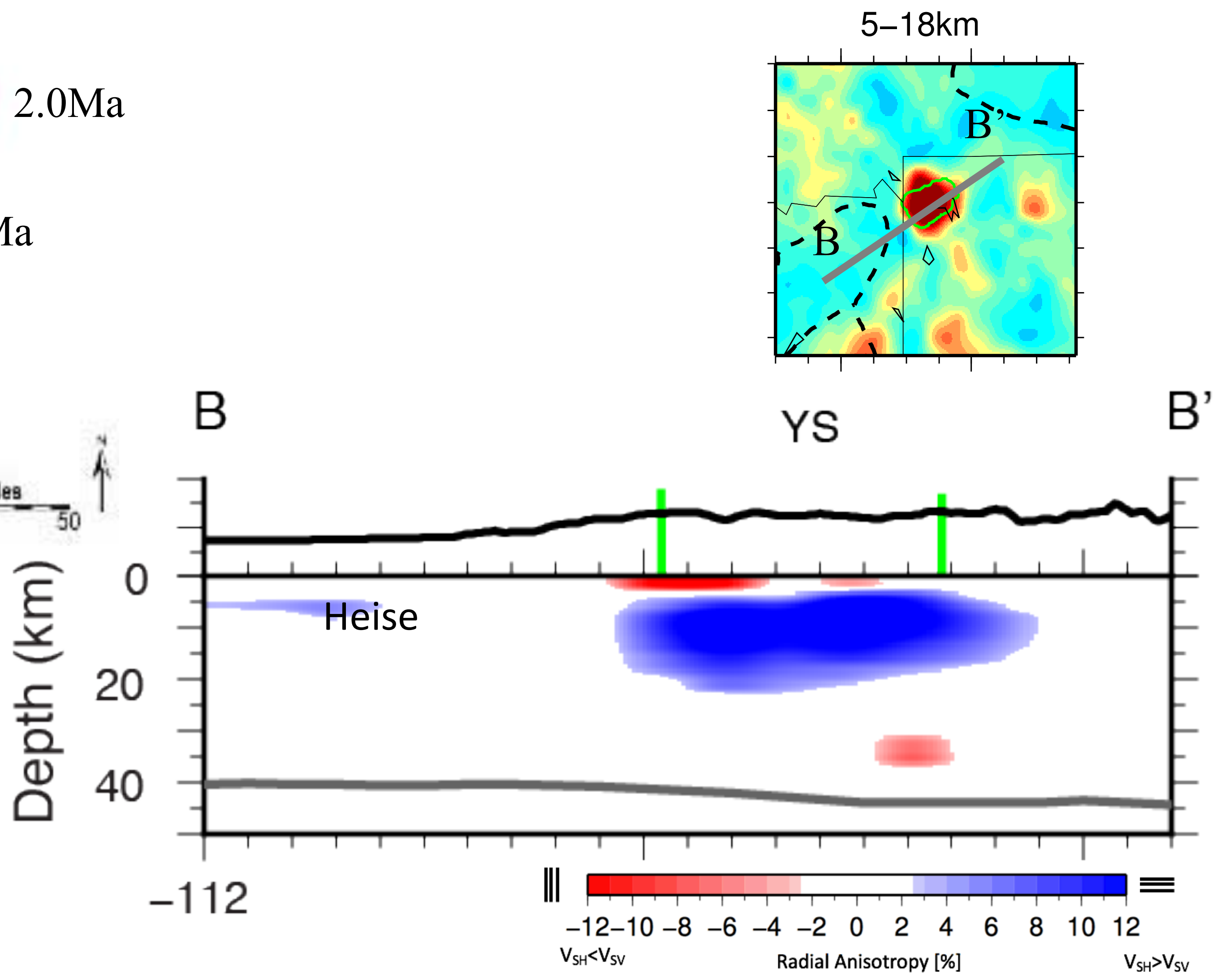

Growing seismic evidence for sill complexes beneath calderas from major silicic eruptions

Toba Caldera

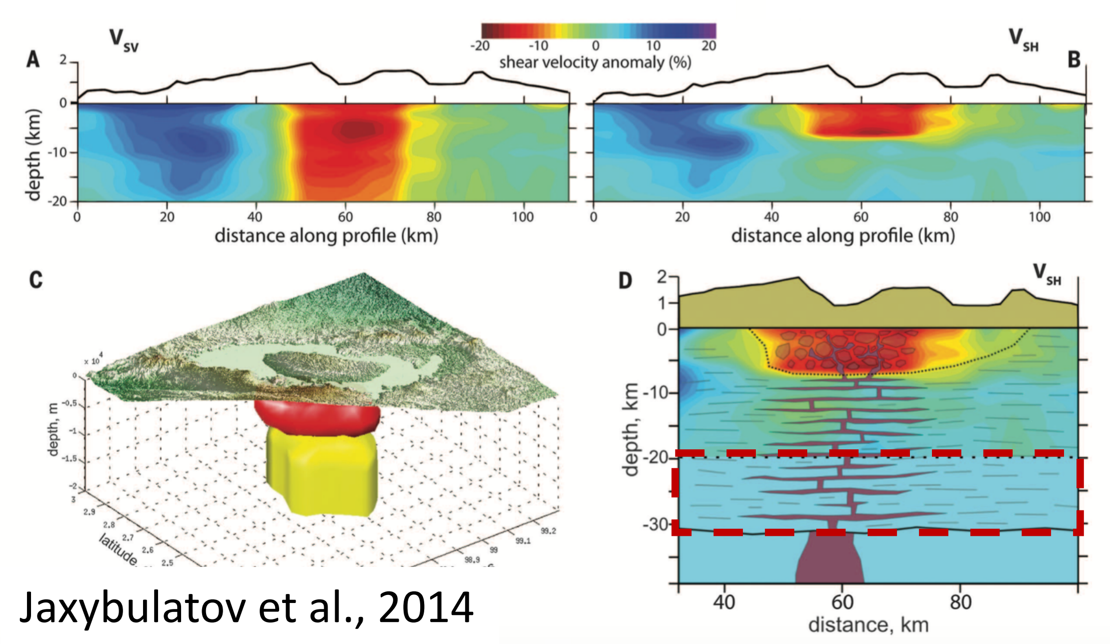

Long Valley Caldera

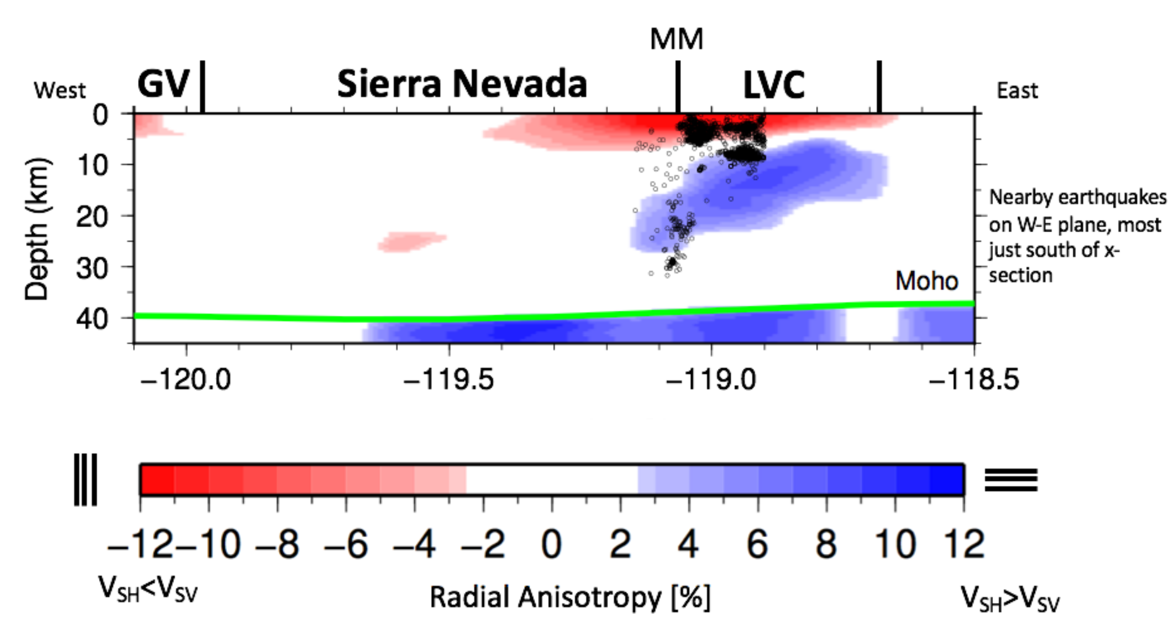

At YS and LVC we can see the bottom of these sill complexes, indicating different reservoir characteristics where primitive melts first intrude the crust.

Very different tectonic/stress setting: active subduction (Toba), thin plate interior in transtension (LVC), craton undergoing slow extension (YS)

LVC Magmatic inflation centered at ~7-8 km

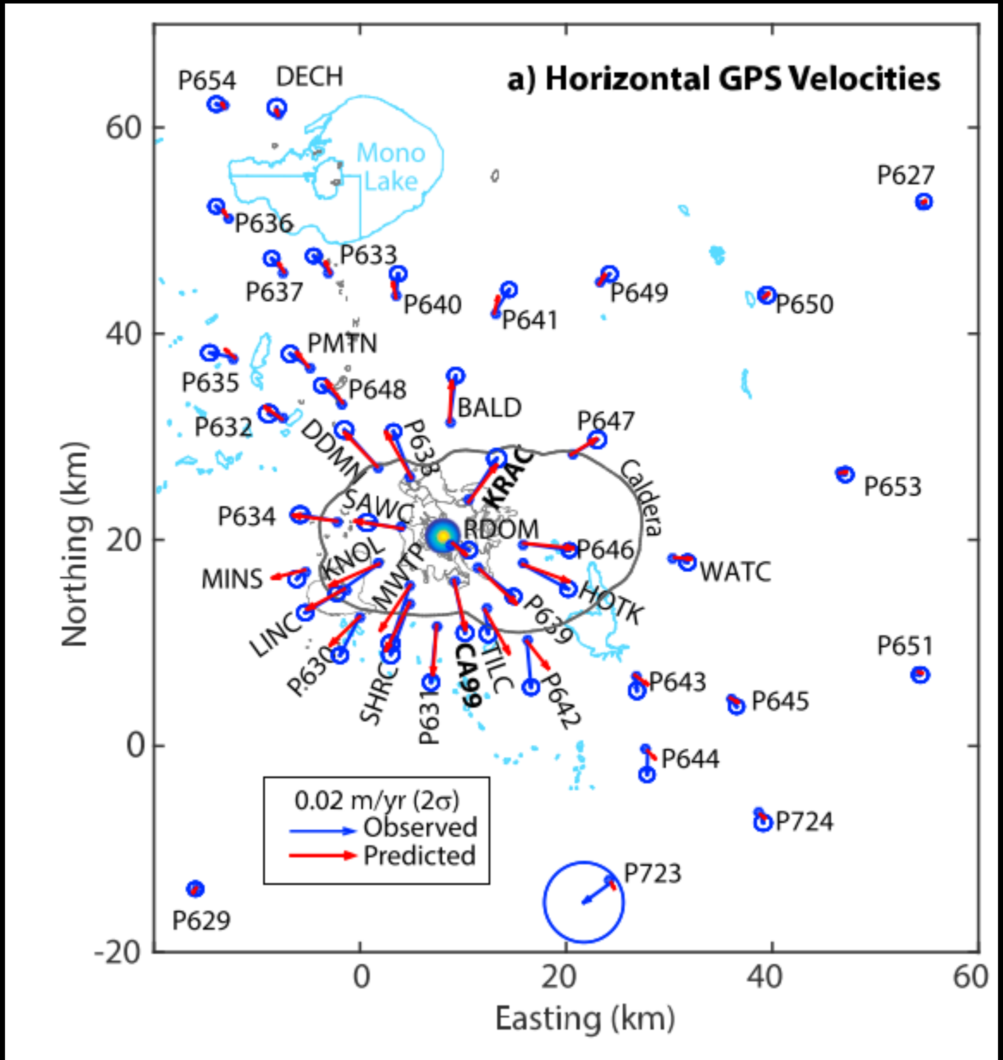

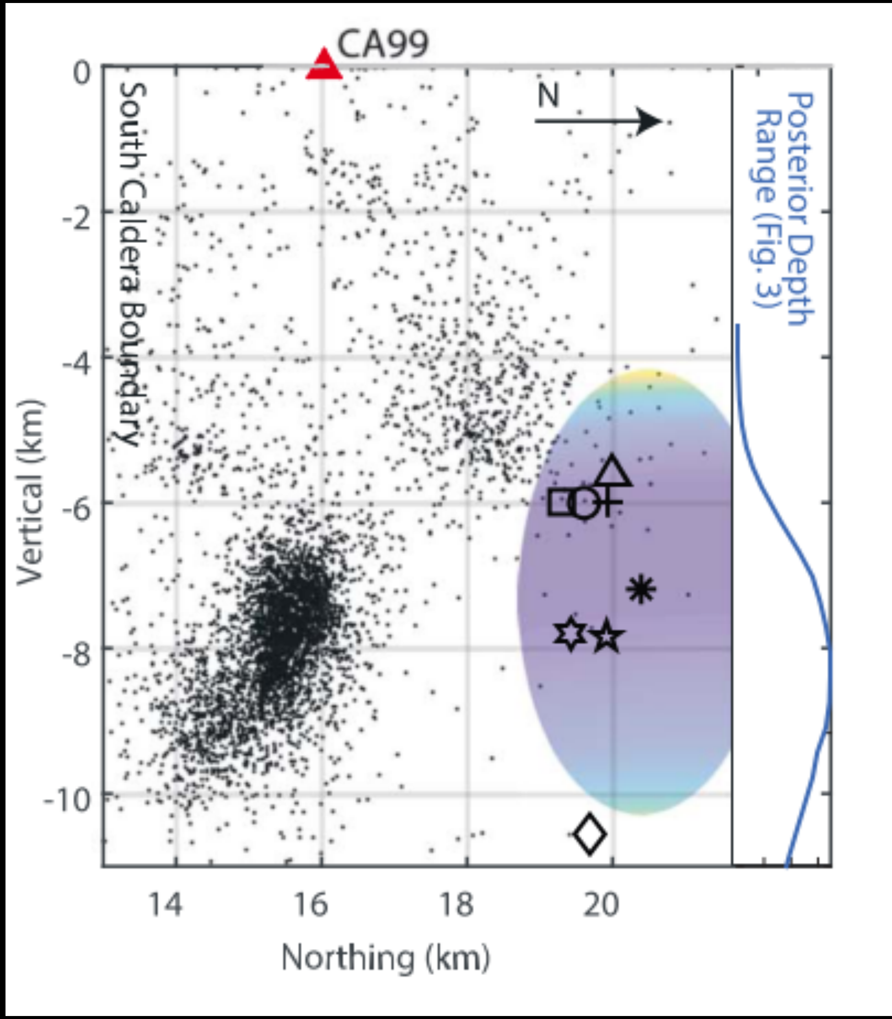

Montgomery-Brown et al., 2015

LVC Magmatic inflation centered at ~7-8 km

Seismic and Geodetic views

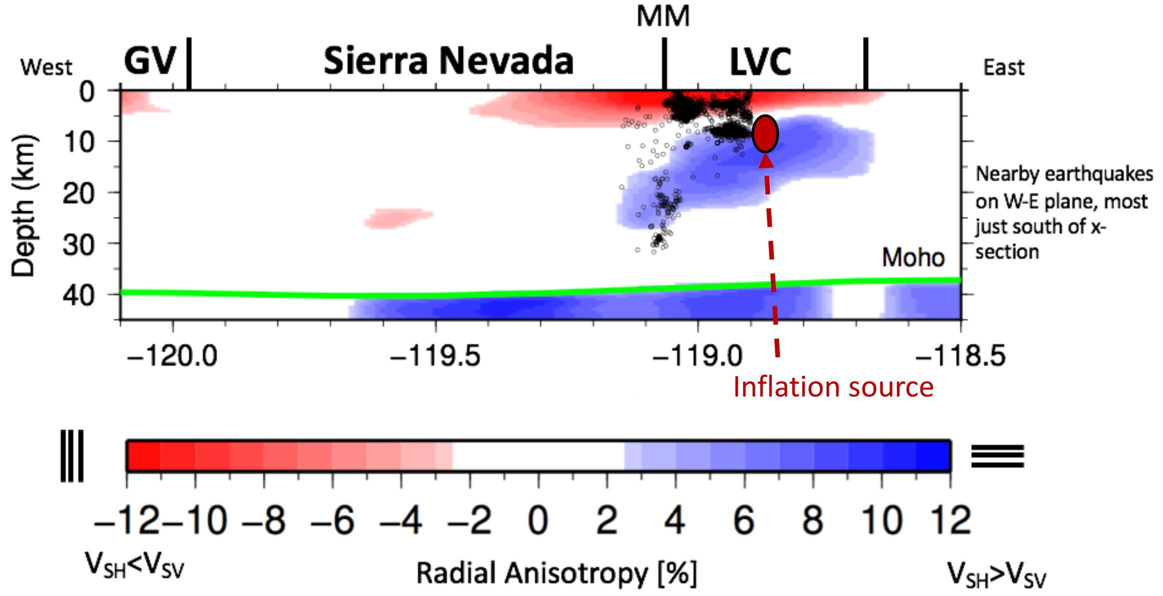

Petrology of Bishop Tuff

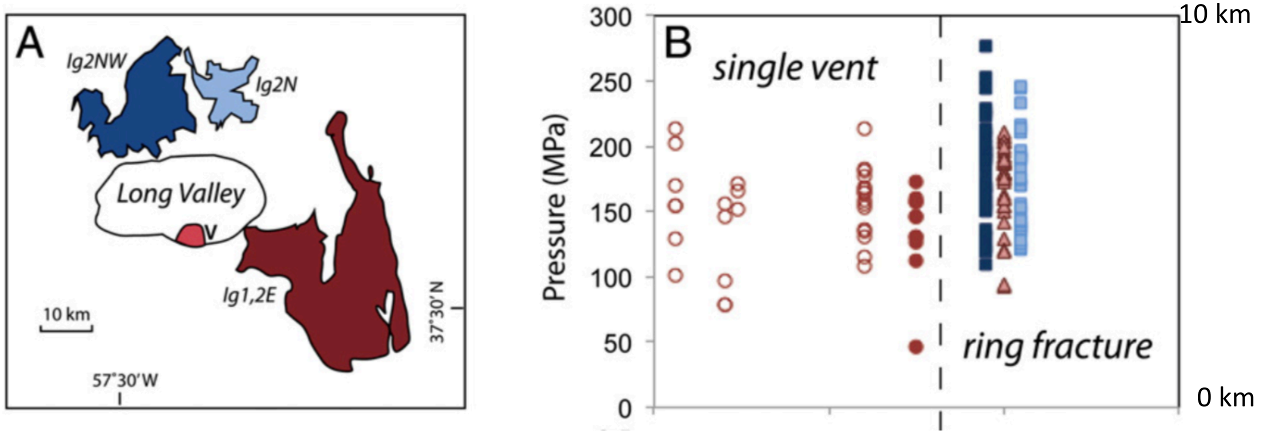

(Wallace et al., 1999;
Cashman and Giordano, 2014)

Are these large sill complexes the long-term magma reservoir, which rapidly mobilize into shallower more crystal-poor reservoirs before eruption (e.g., Rubin et al., 2017; Wotzlaw et al., 2015; Crowley et al., 2007; Till et al., 2015; Matthews et al., 2015)?

Similar depth relationship at Yellowstone, with inflation/deflation near top of sill complex (Chang et al., 2007)

Maintenance of compositional heterogeneity at Yellowstone

Seismic view

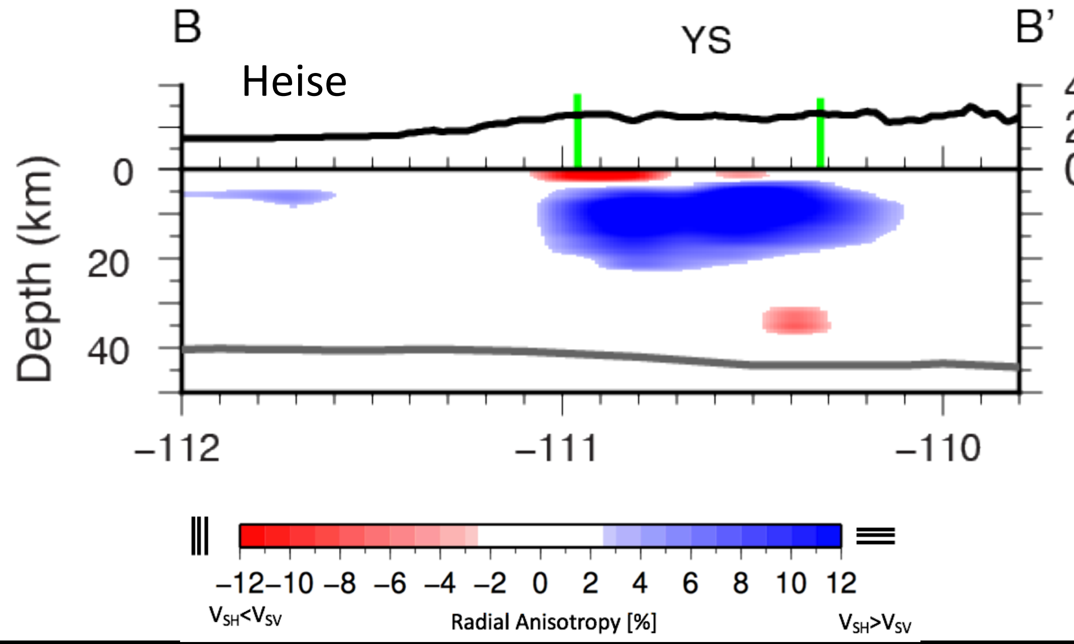

Geochemically distinct batches of magma

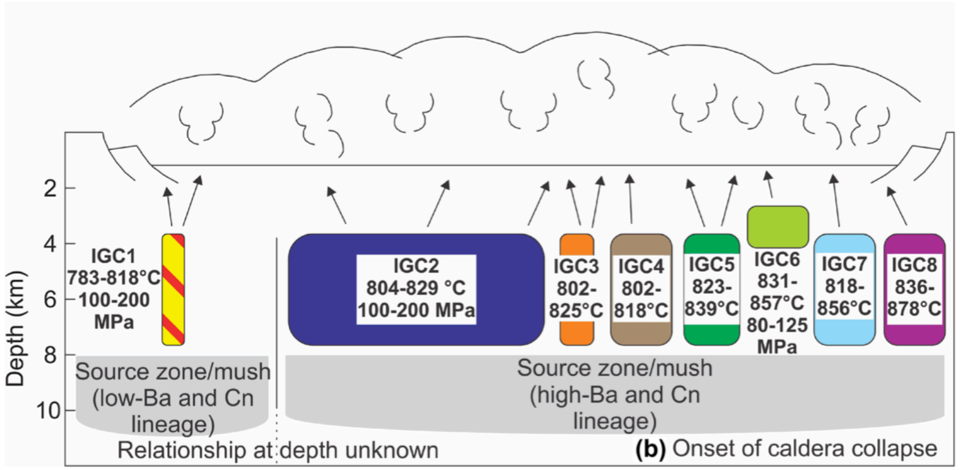

Swallow et al. 2018

Are these large sill complexes the long-term magma reservoir, which rapidly mobilize into shallower more crystal-poor reservoirs before eruption (e.g., Rubin et al., 2017; Wotzlaw et al., 2015; Crowley et al., 2007; Till et al., 2015; Matthews et al., 2015)?

Similar depth relationship at Yellowstone, with inflation/deflation near top of sill complex (Chang et al., 2007)

Maintenance of compositional heterogeneity at Yellowstone

Seismic view

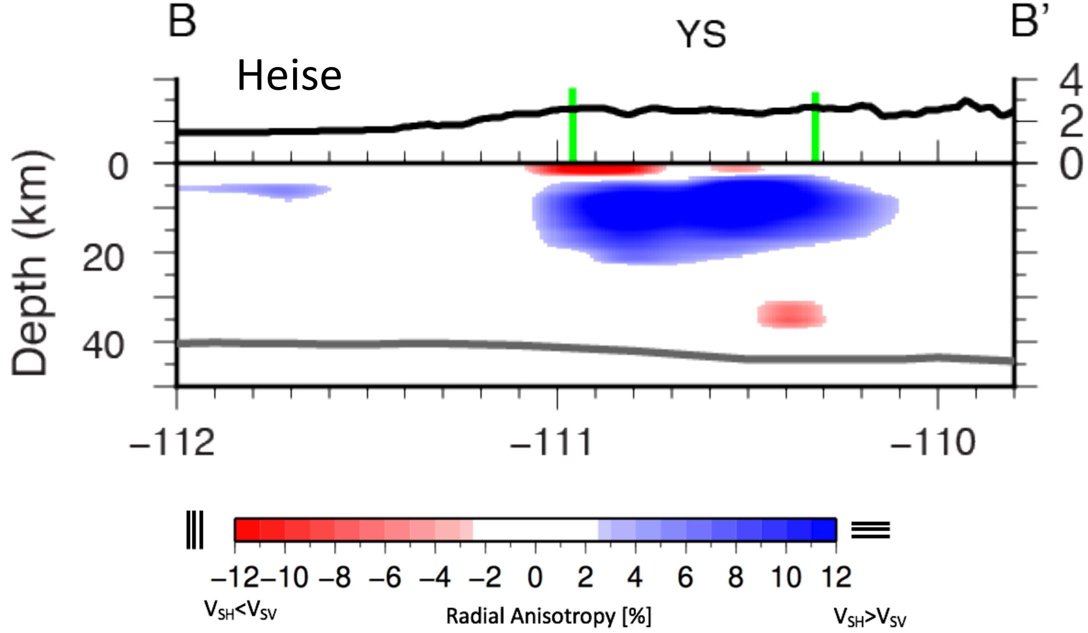

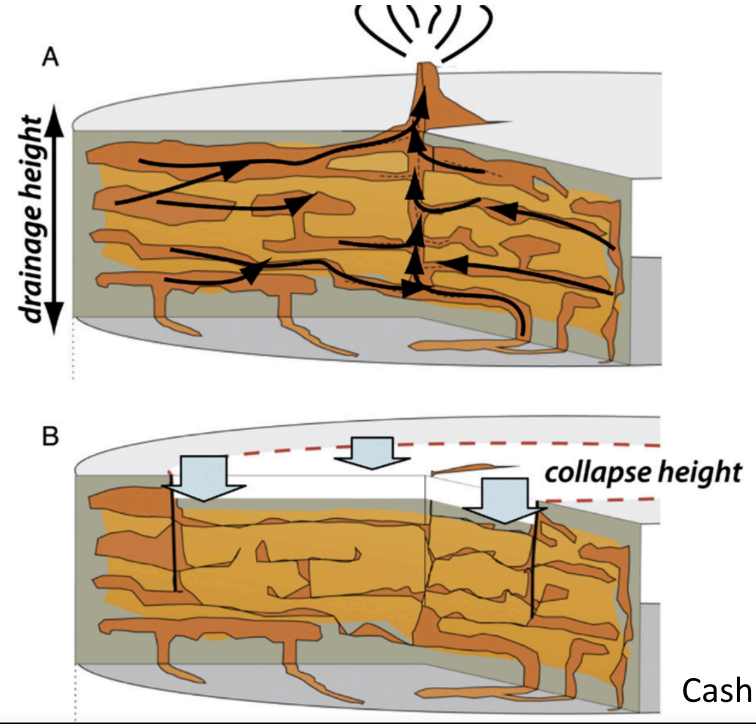

Cashman and Giordano, 2014

Are these large sill complexes the long-term magma reservoir, which rapidly mobilize into shallower more crystal-poor reservoirs before eruption (e.g., Rubin et al., 2017; Wotzlaw et al., 2015; Crowley et al., 2007; Till et al., 2015; Matthews et al., 2015)?

Similar depth relationship at Yellowstone, with inflation/deflation near top of sill complex (Chang et al., 2007)

Updated view for large volume silicic magmatic systems

Strong horizontal fabric consistent with middle-to-upper crustal melts in sill complex (~10-15% anisotropy)

Anisotropy affects estimates of melt volumes. Here, only using V_{SV} would lead to overestimation. But in-situ melt fractions in sills would be higher than the reservoir average.

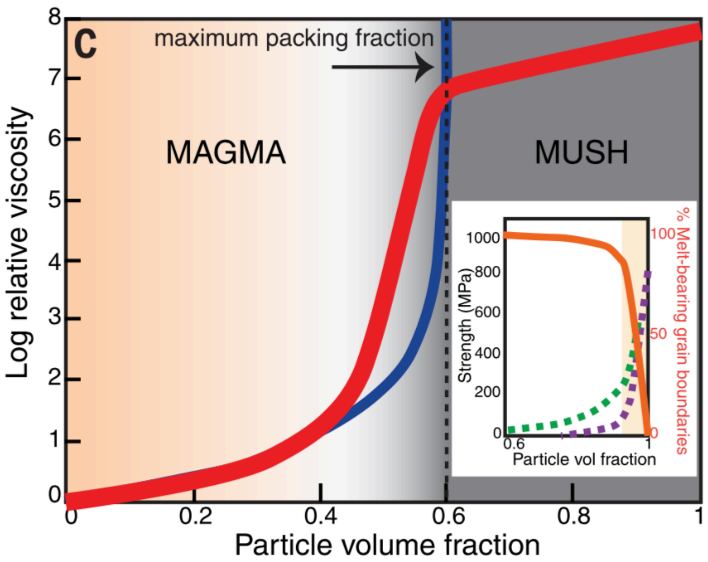

(Cashman et al., 2017; Costa et al., 2009)

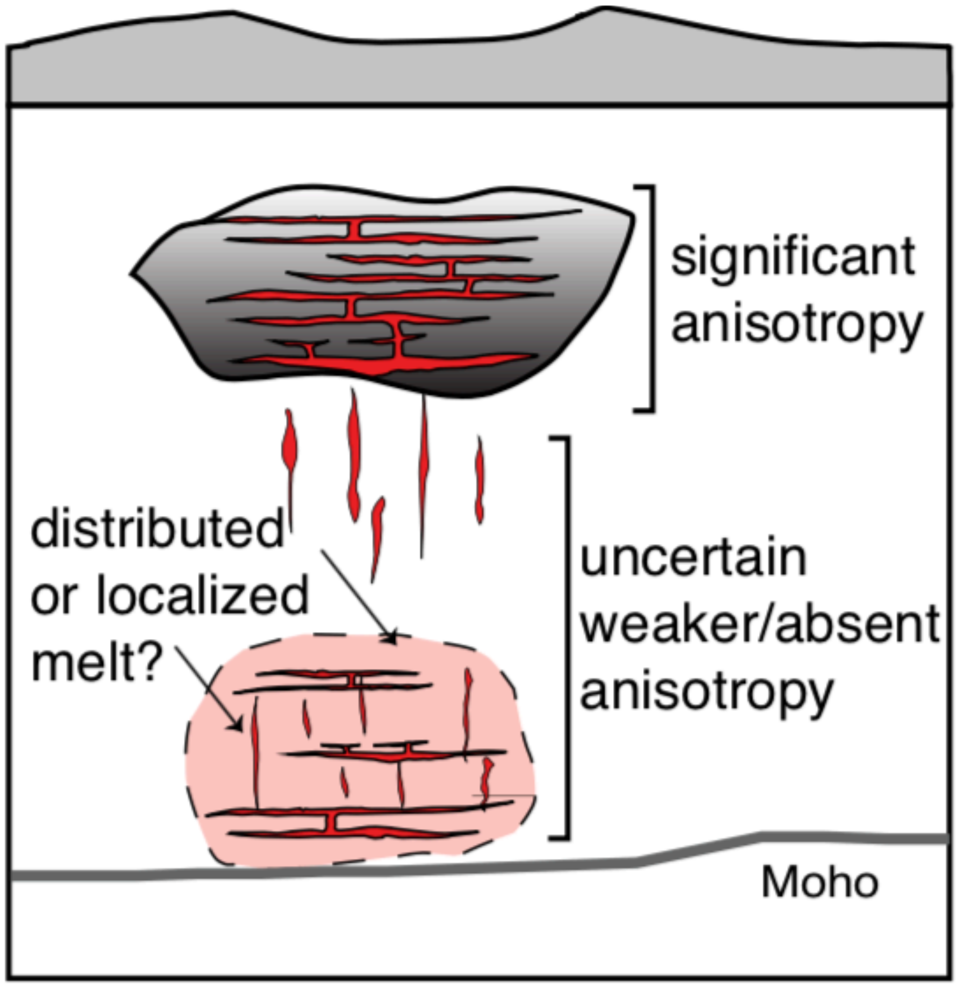

Seismic view of large silicic magmatic systems

Strong horizontal fabric consistent with middle-to-upper crustal melt in sill complexes (~10% anisotropy)

Weaker or absent radial anisotropy in the lower crust indicates different melt storage geometry

Common depth-dependent anisotropic structure in areas with very different tectonic histories suggests dominance of young magmatic processes

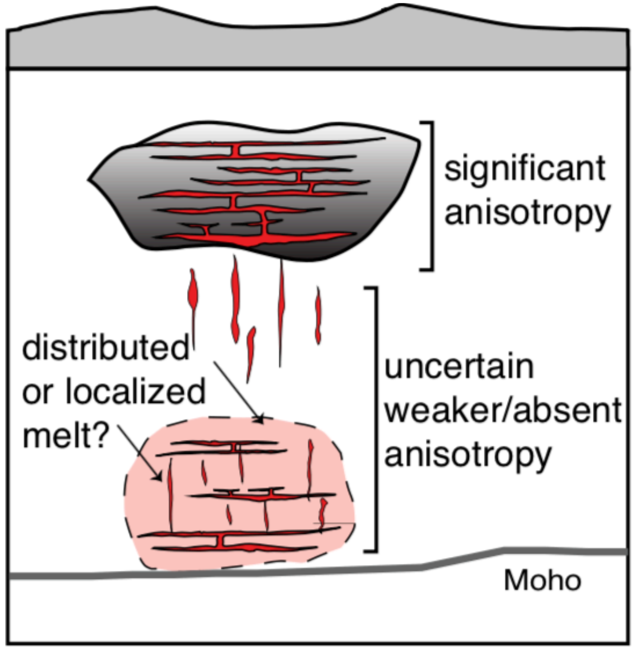

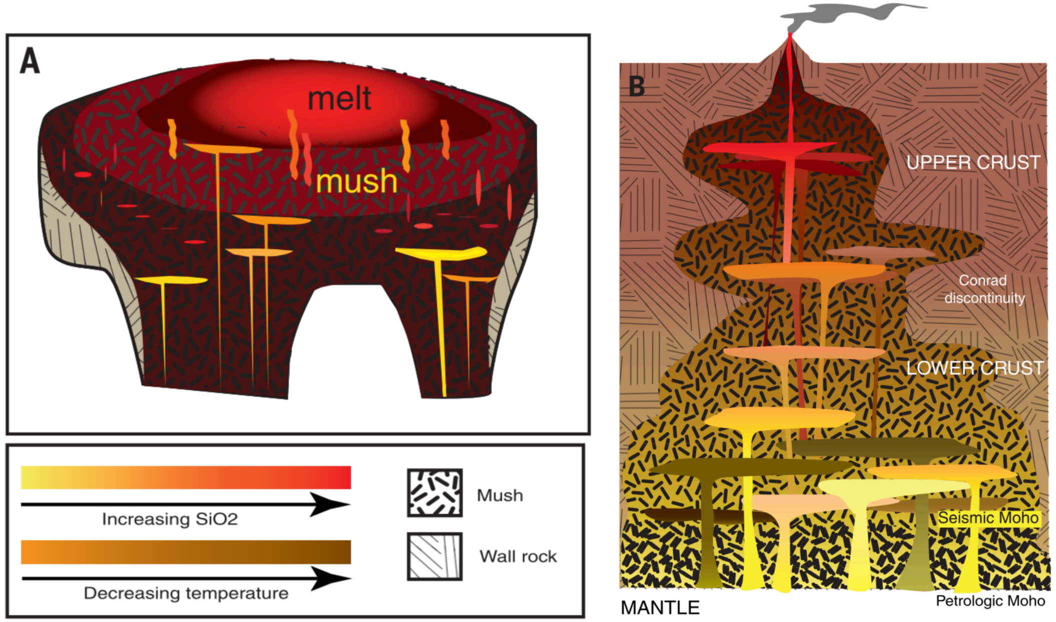

(Cashman et al. 2017;
Hildreth and Wilson, 2007)

Hunting for a relatively small magmatic system with lots of seismographs…

Mount St. Helens

Imaging Magma Under mt. St. Helens (iMUSH)

Seismic Investigators from:

UNIVERSITY of WASHINGTON

RICE

CORNELL UNIVERSITY FOUNDED A.D. 1865

Ken Creager, John Vidale, Geoff Abers, Alan Levander

USGS science for a changing world

Seth Moran, Wes Thelen

Late addition:

THE UNIVERSITY of NEW MEXICO

NODALSEISMIC real cable free data acquisition

NSF

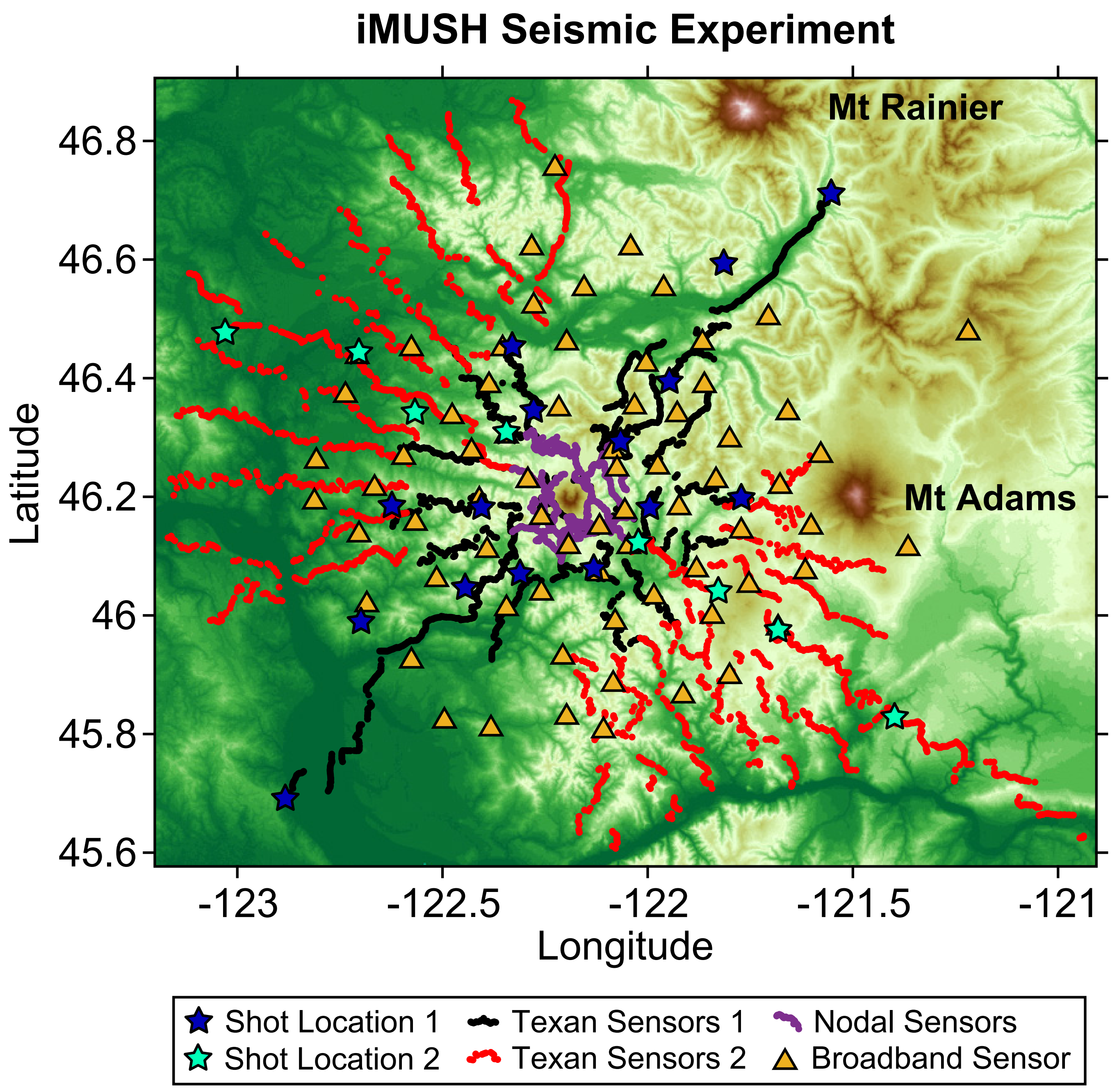

May 18th 1980 – Plinian eruption of MSH

(USGS)

~0.3 km^3 ejected volume of dense rock equivalent

~300 m lower summit

ash/gas plume into stratosphere

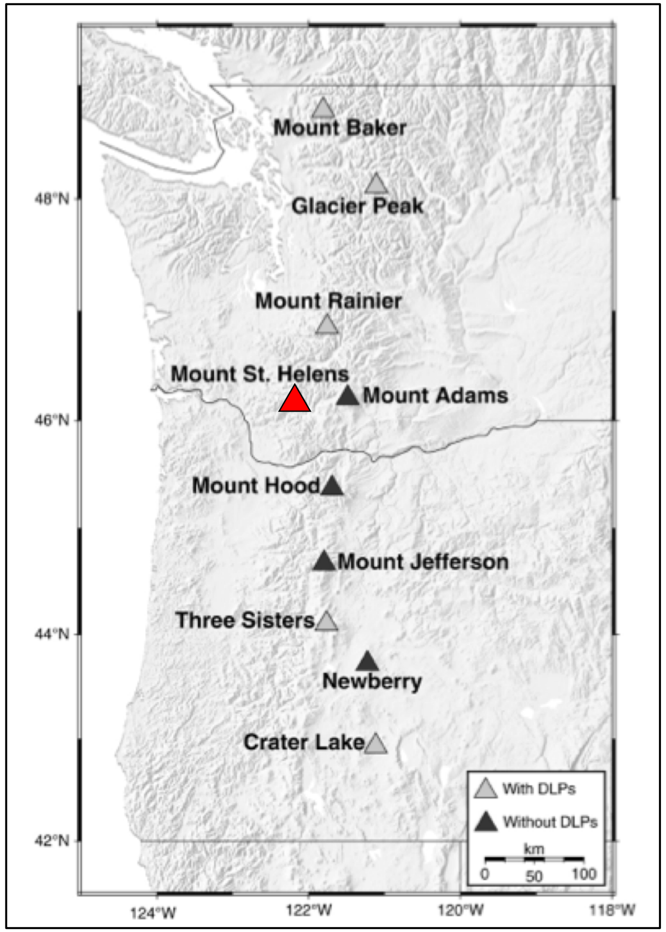

Nichols et al., 2011

Seismicity time and depth distribution 1980-2014




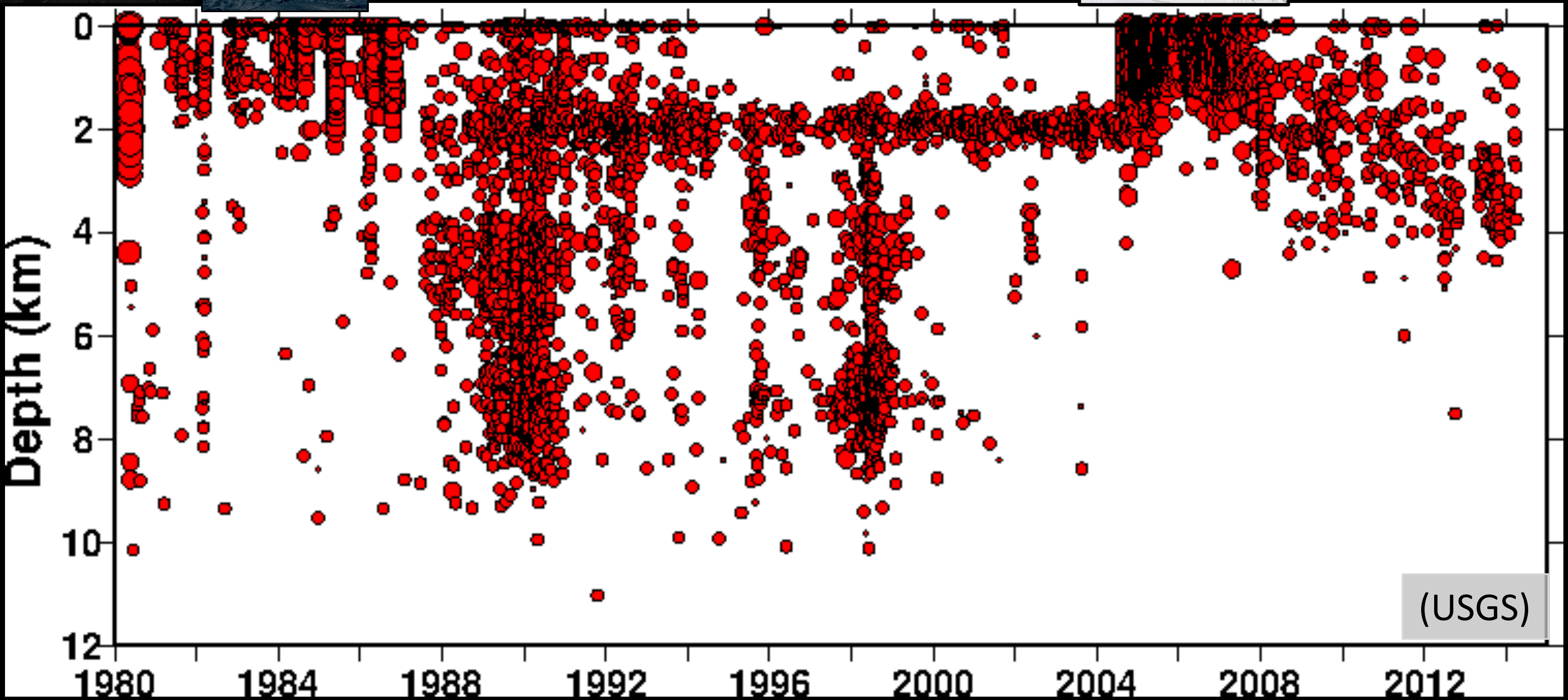

Post-2009 small recharge episodes at Mount St. Helens?

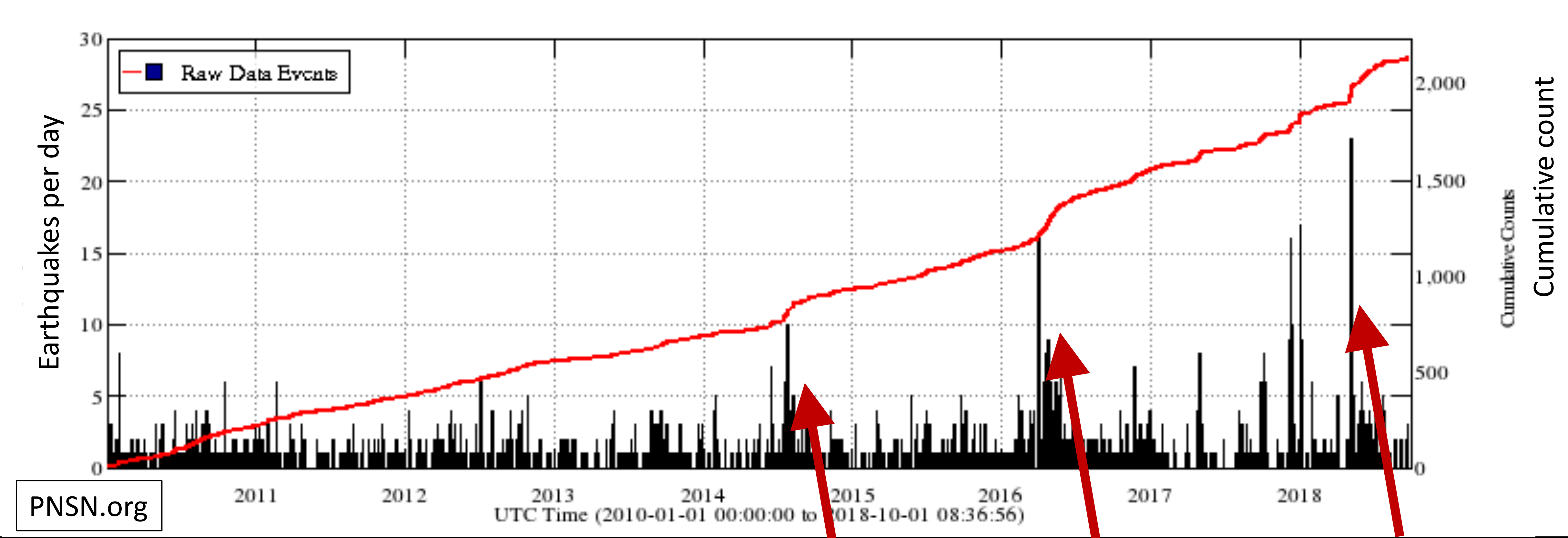

Some iMUSH structural imaging results:

Moho reflectivity - helps constrain magma plumbing location within the subduction system's thermal structure

Earthquake and active source travel time tomography – helps constrain current magma reservoir geometry

More from Geoff Abers this afternoon…

Offset Gathers

- 15-25 Hz bandpass
- 0.2 s short-term
- 1 s long-term
- Binned by distance
- Median trace

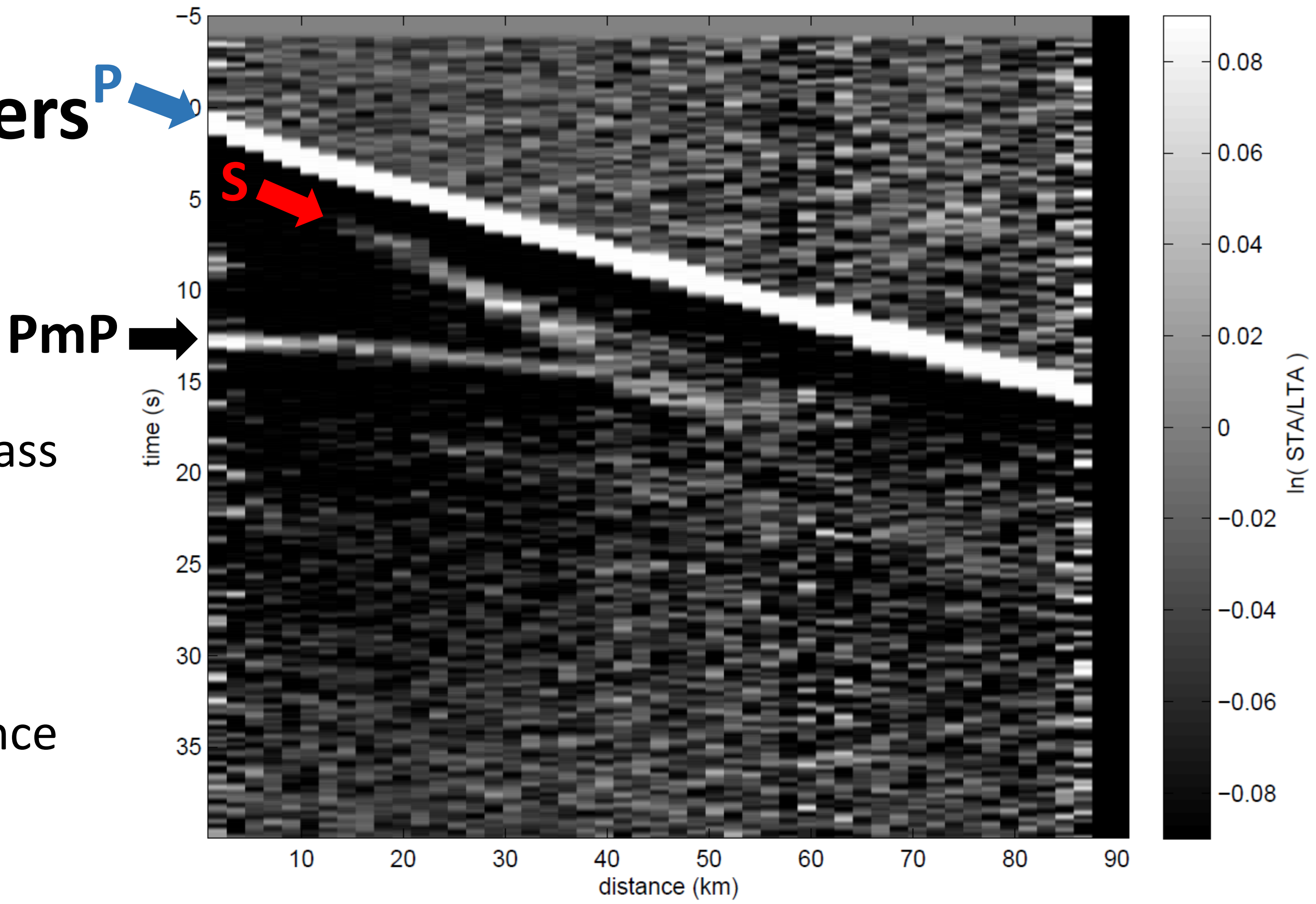

Normal Move Out (NMO) Shot Stacks

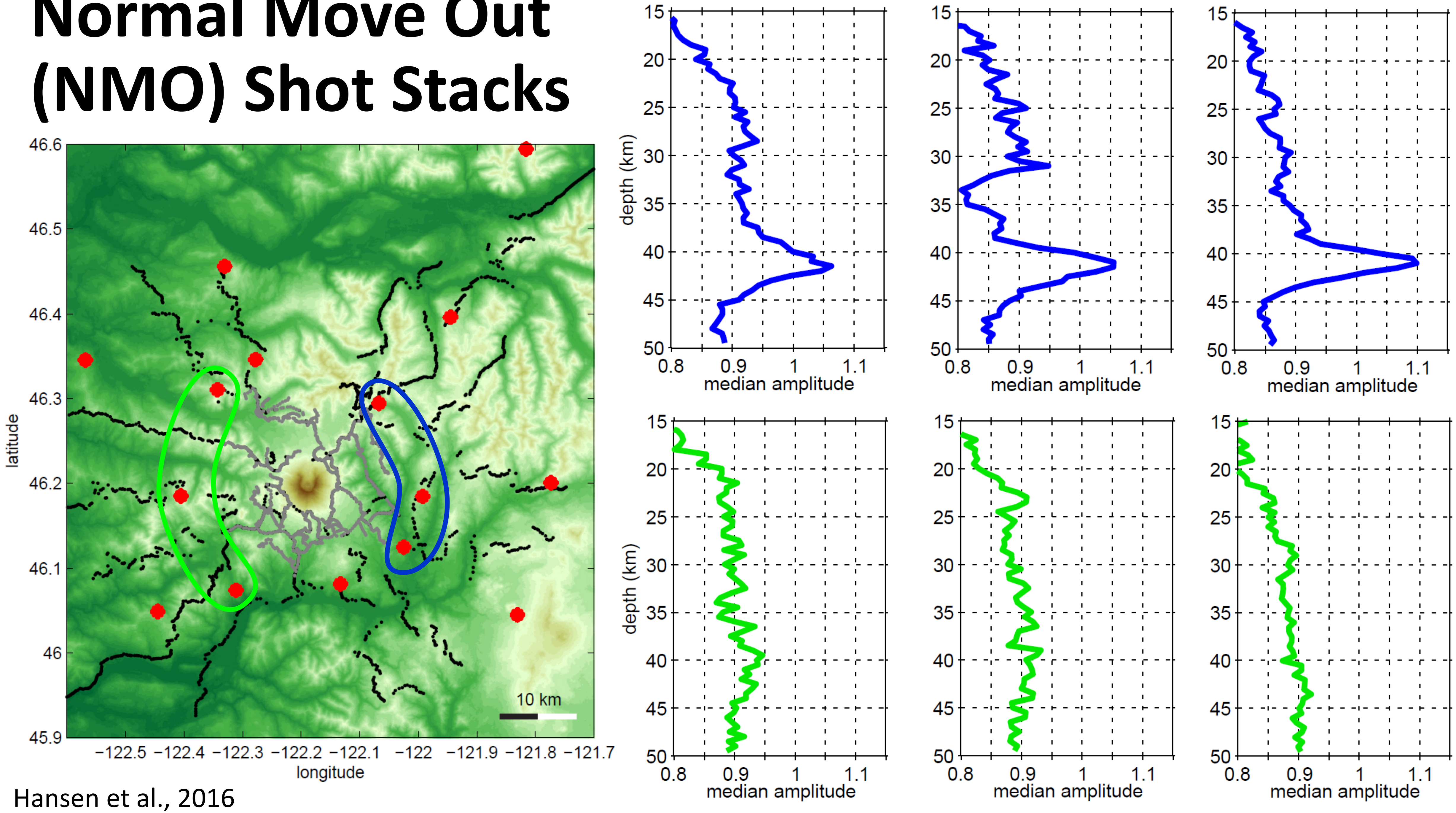

Hansen et al., 2016

Transportable Array Results

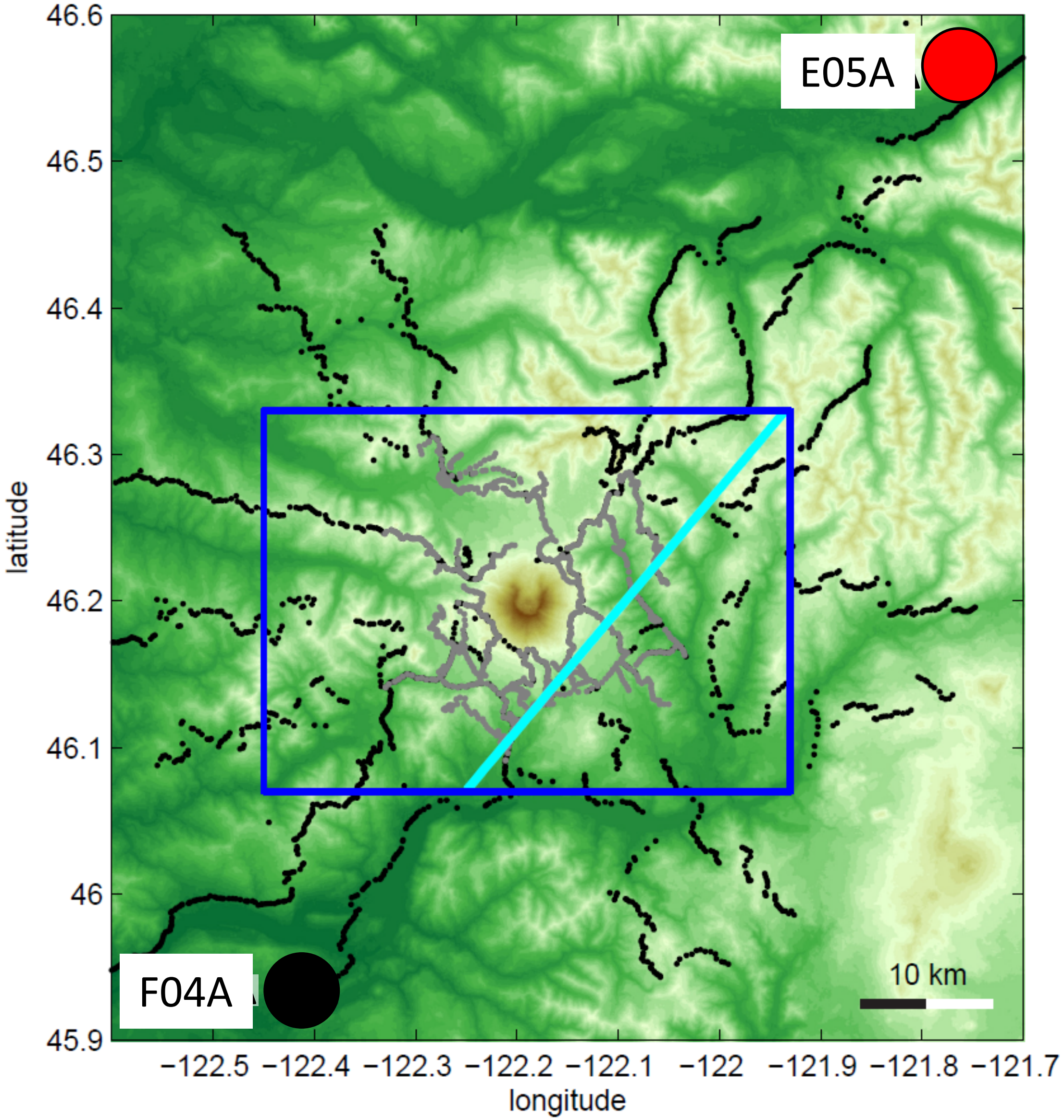

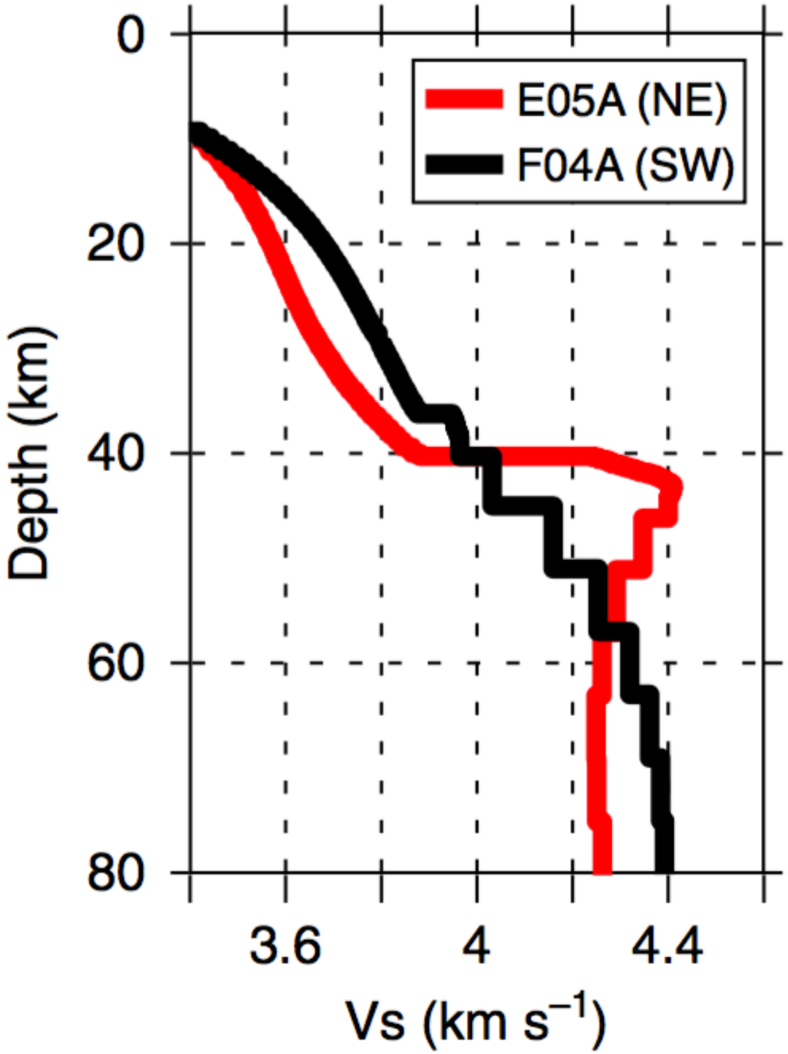

(Shen et al., 2013)

Zooming in on the edge of low reflectivity forearc Moho

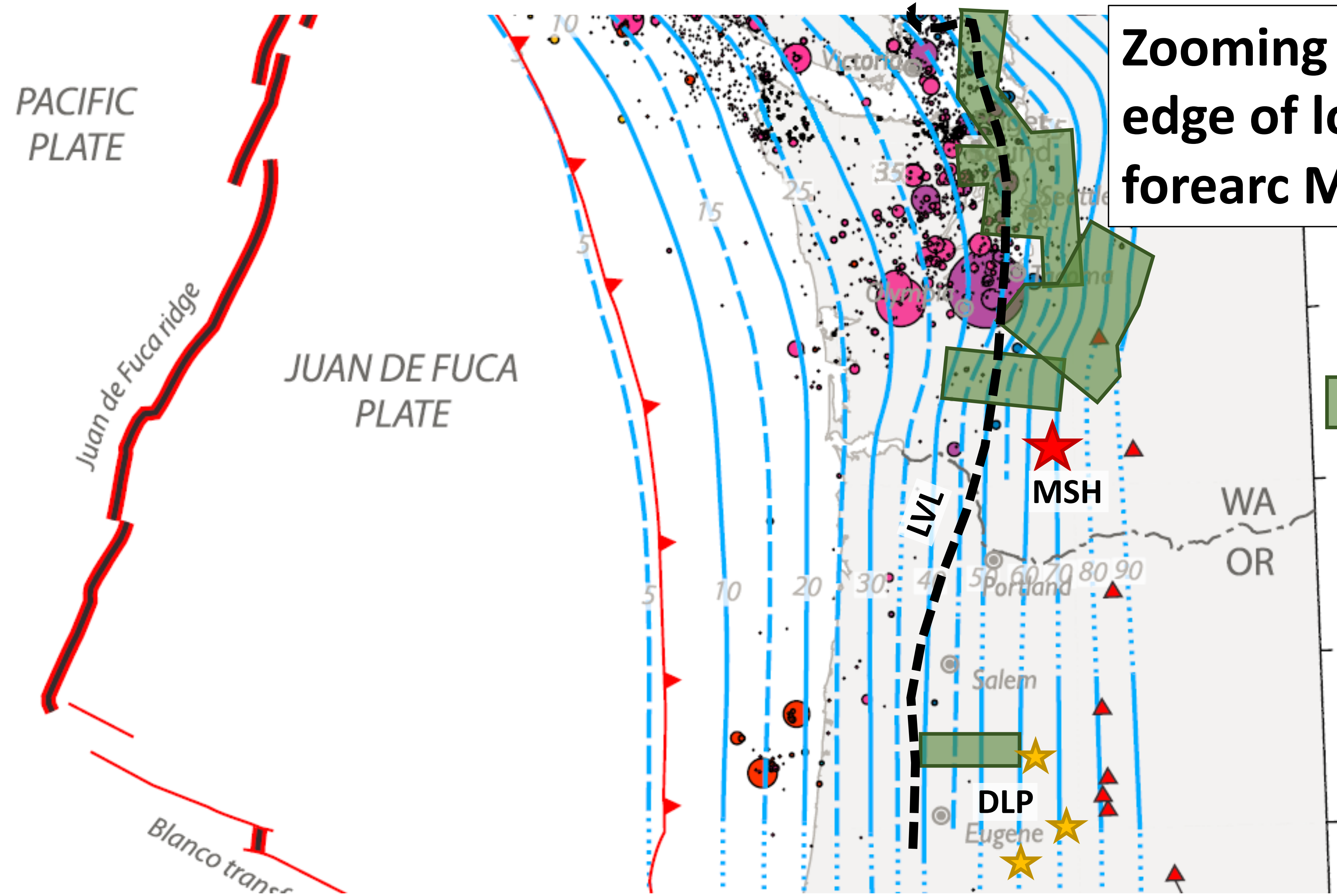

Weak to inverted Moho

Cold hydrated 'nose' of the mantle wedge?

Link to DLP earthquakes?

(McCrory et al., 2012; Audet et al., 2010; Brocher et al., 2003; Obrebski et al., 2015; Vidale et al., 2014)

Mapping the extent of hydrated forearc mantle?

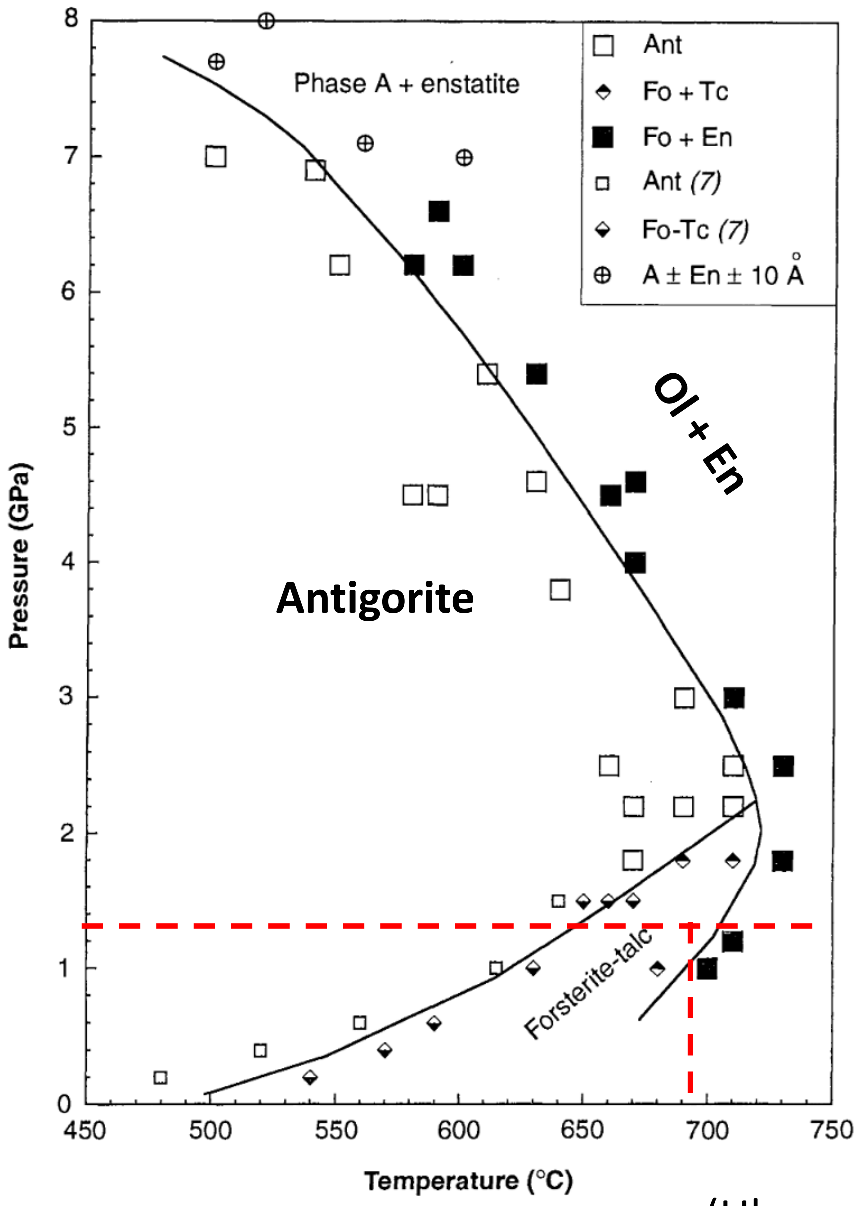

(Ulmer and Trommsdorff, 1995)

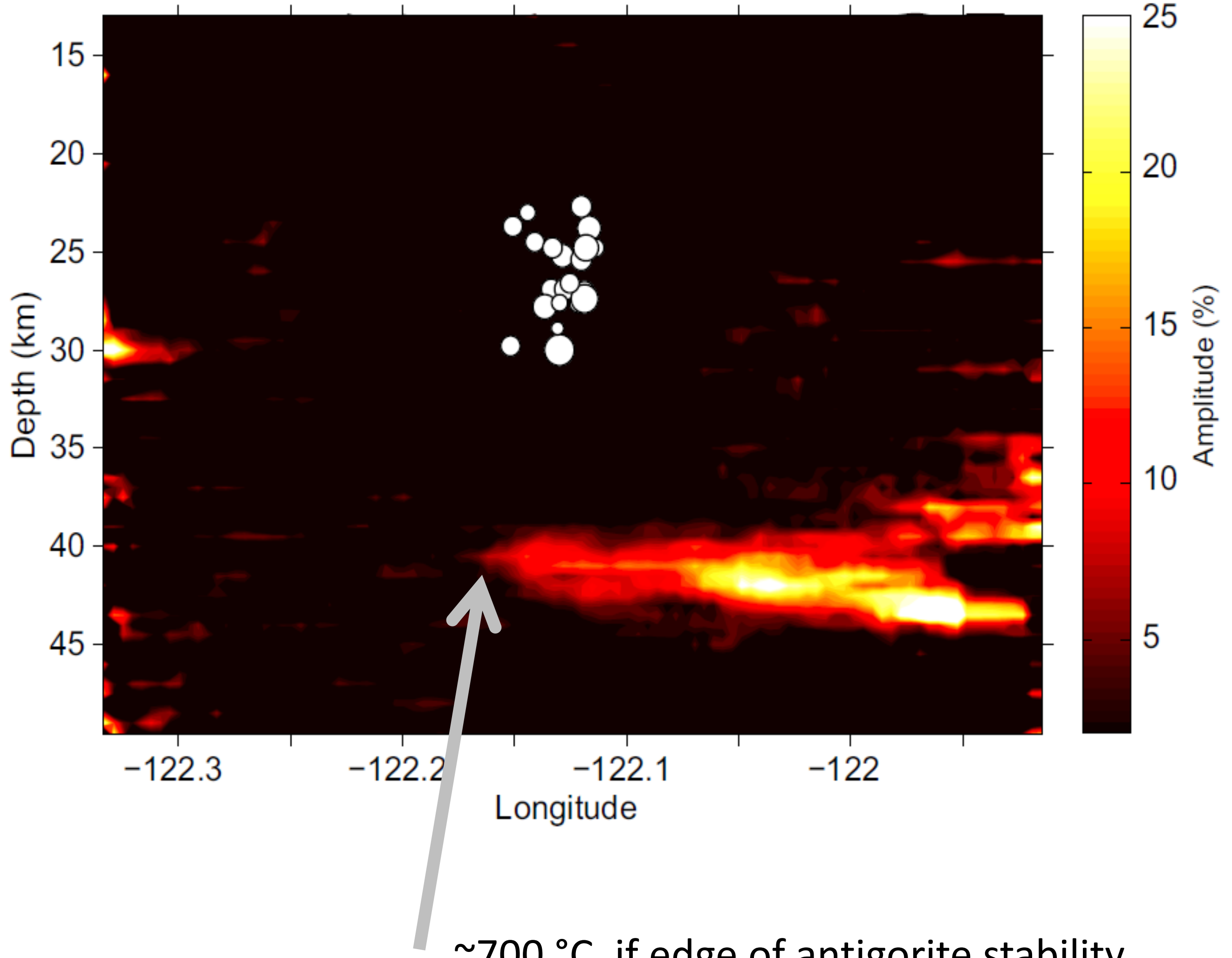

Westward migration of mantle melts beneath Mount St. Helens?

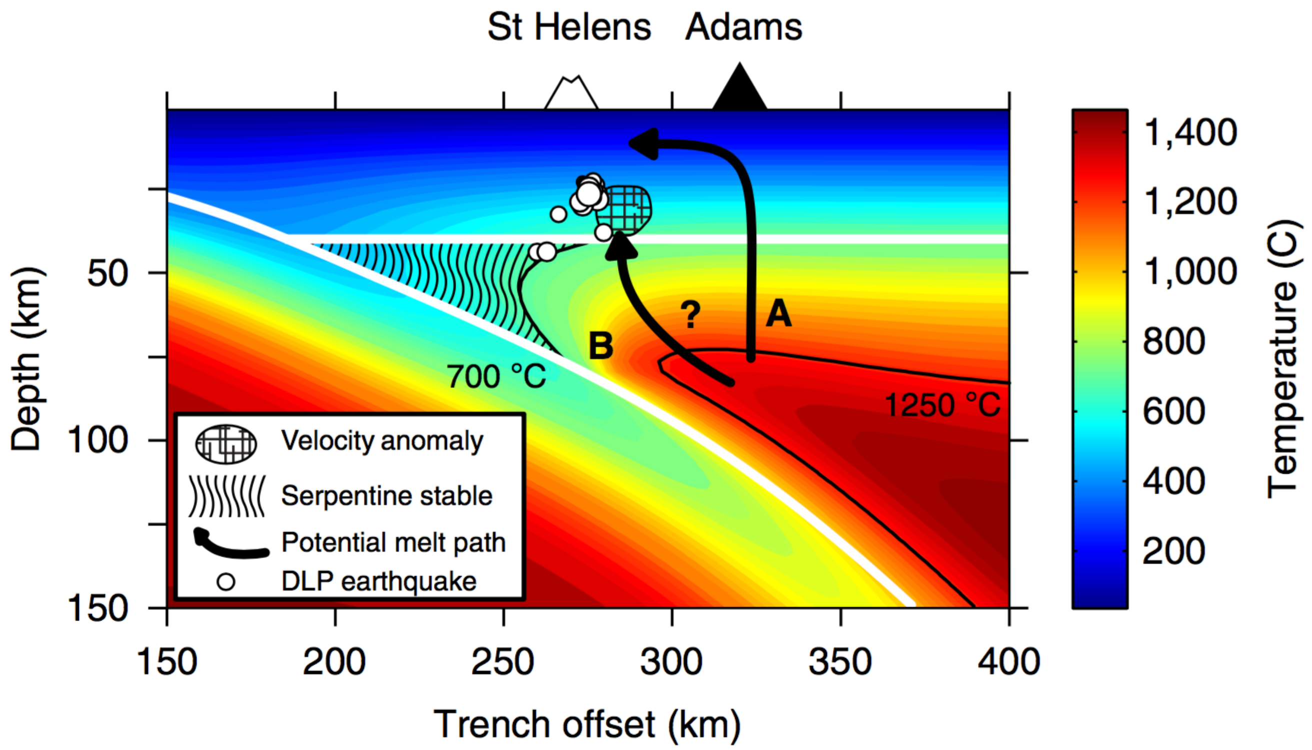

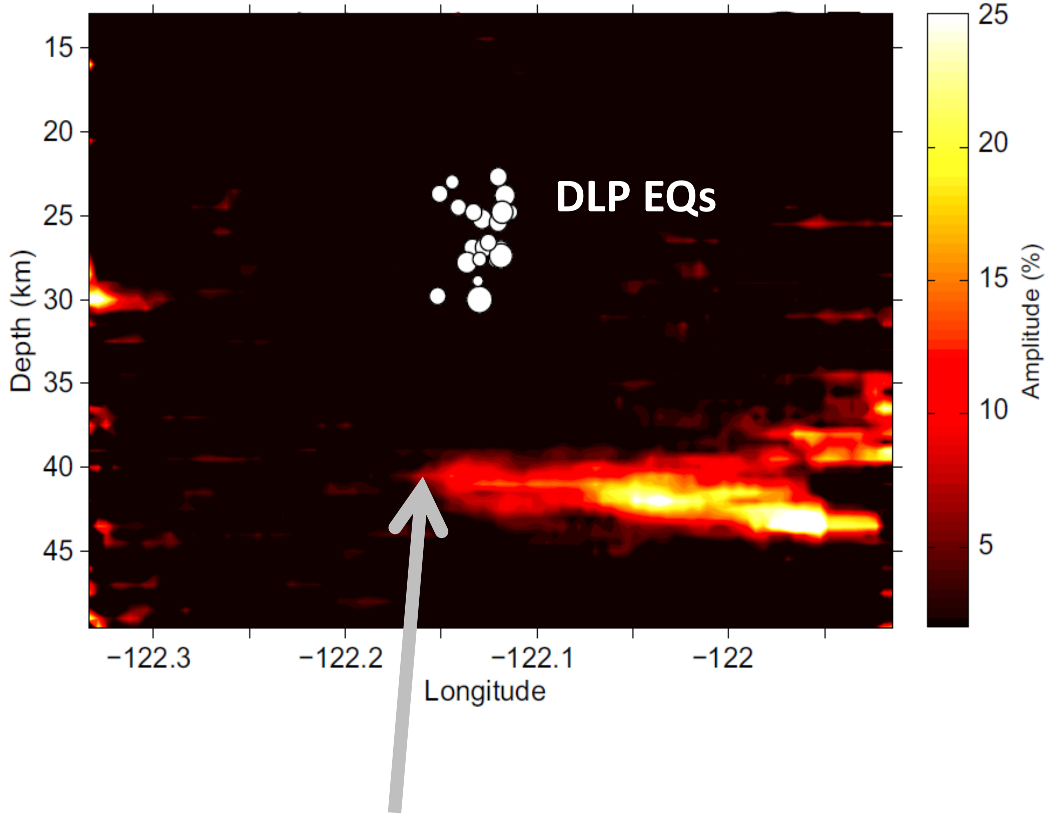

Thermal model from Syracuse et al., 2010
Seismic and Interp. From Hansen et al. 2016

~700 °C, if edge of antigorite stability
~800 °C, if edge of chlorite stability

Controlled source P tomography using short-period array (~5000 geophone sites)

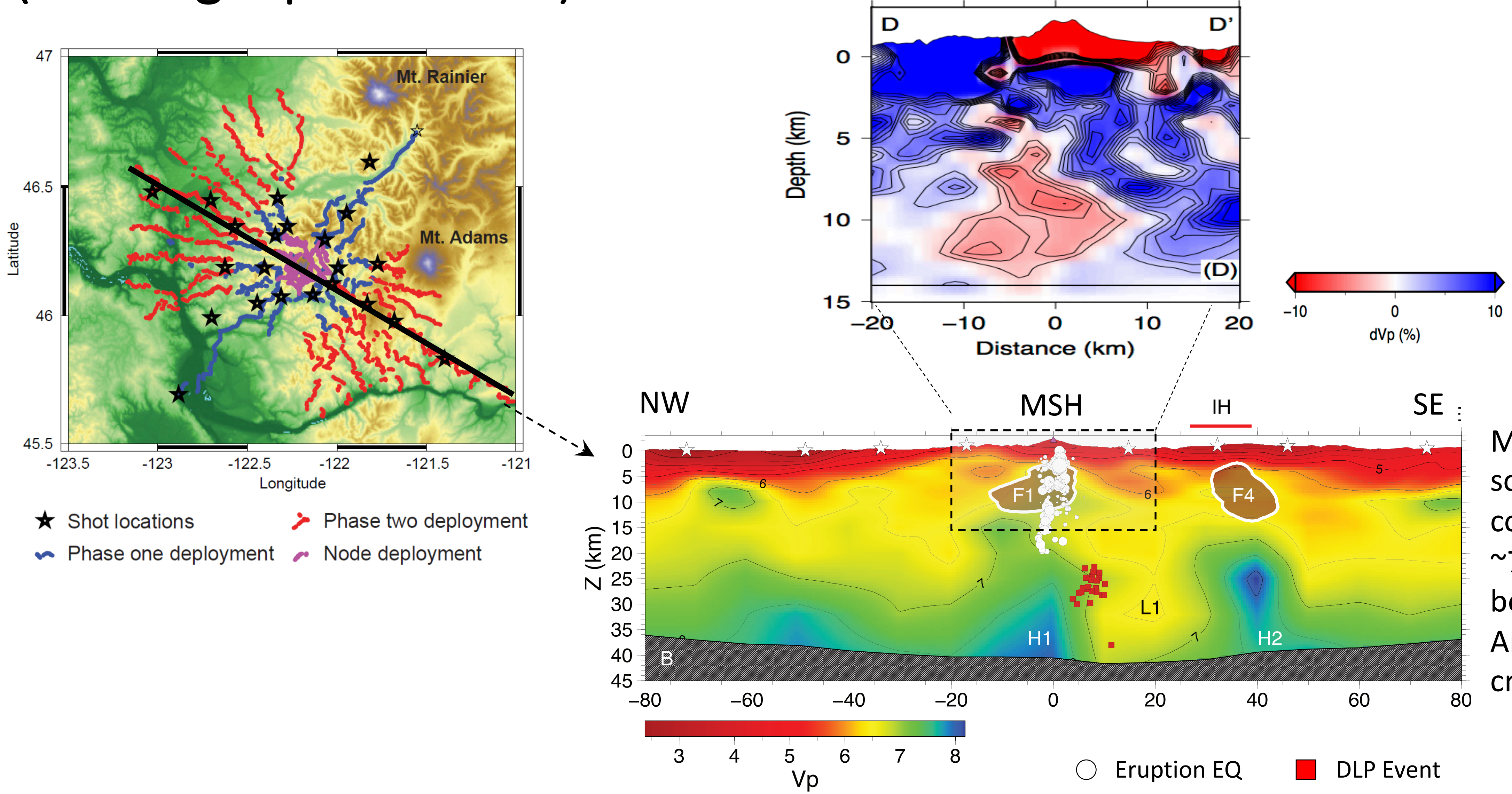

Melt ascent from southeast consistent with low ~700 C temp directly beneath MSH, Anomalous lower crustal Vp

Eric Kiser et al., 2016, 2018 Geology

Pieces of the MSH plumbing system:

Result - Interpretation

Shallow vertical column of seismicity – conduit connecting shallow magma reservoir to surface

Upper crustal high Vp/Vs – shallow dacitic magma reservoir focused at same depths that fueled recent eruptions

Deep crustal low-velocity zone and contrast in Moho reflectivity - marks input of mantle melts east of MSH.

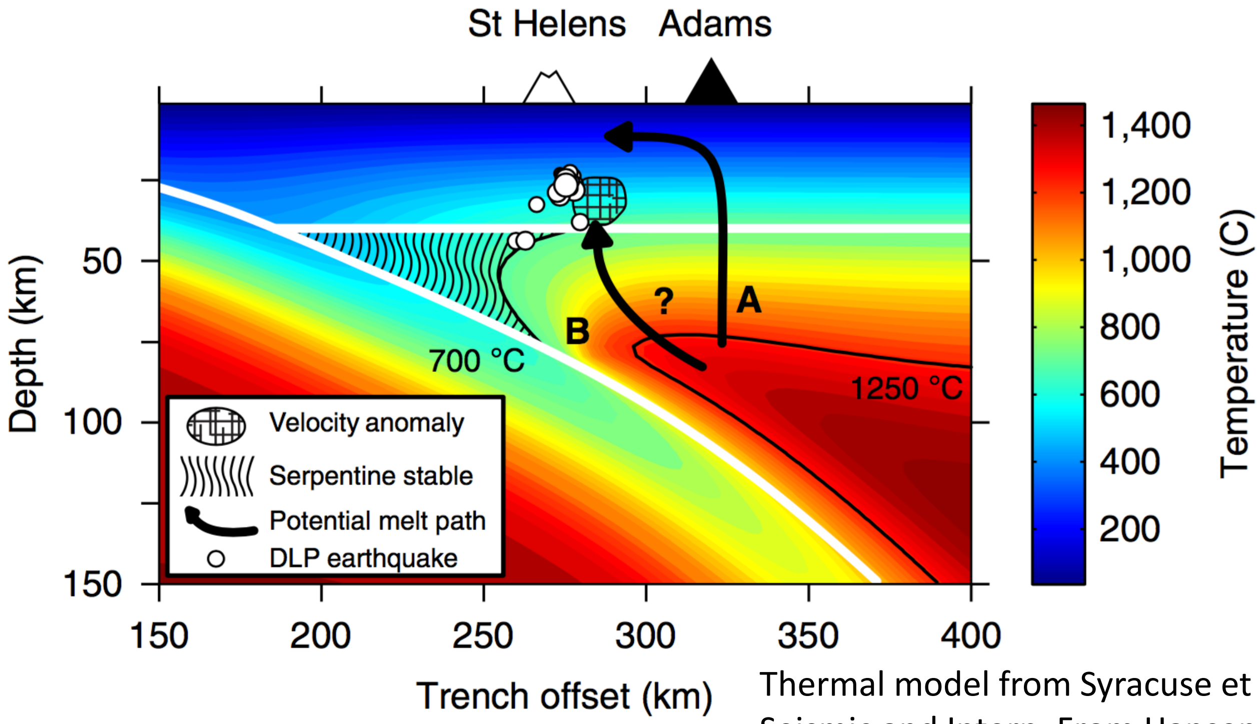

Thermal model from Syracuse et al., 2010
Seismic and Interp. From Hansen et al. 2016

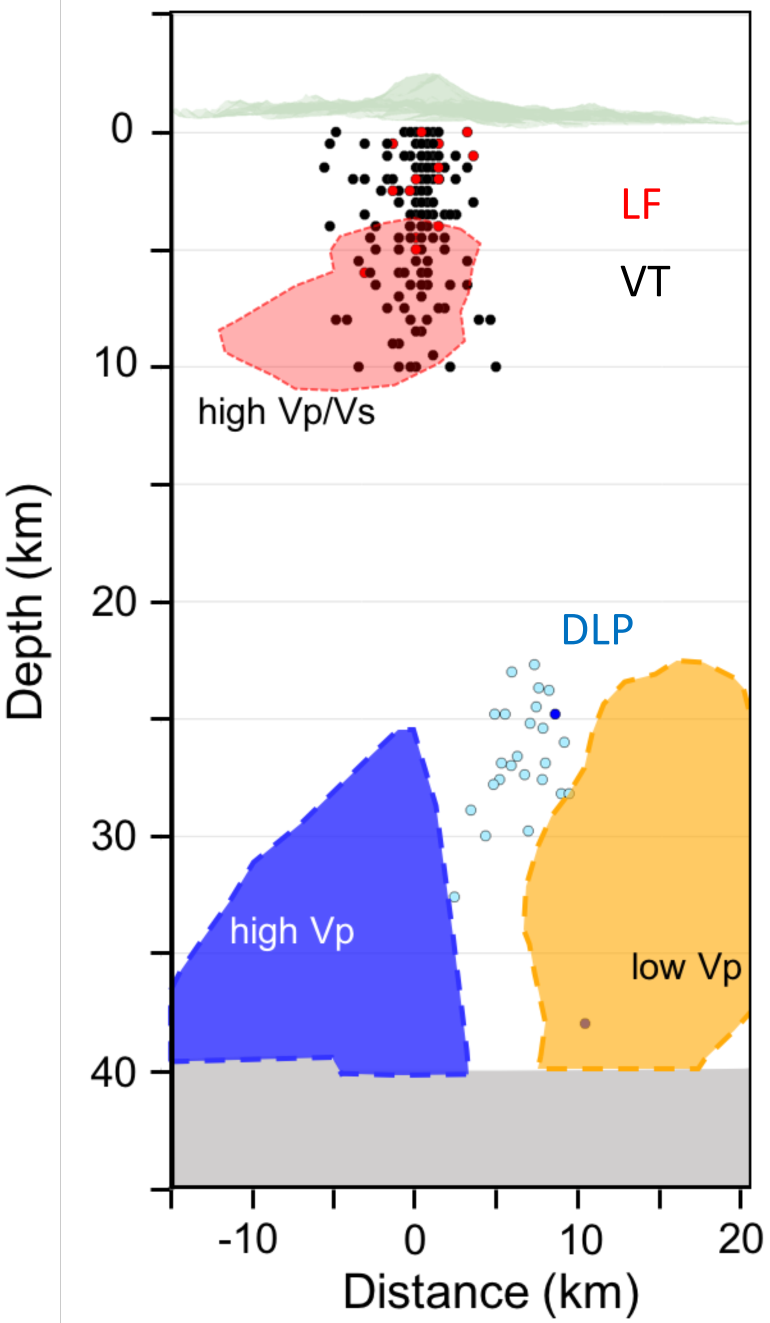

Pieces of the MSH plumbing system:

Result - Interpretation

Shallow vertical column of seismicity – conduit connecting shallow magma reservoir to surface

Upper crustal high Vp/Vs – shallow dacitic magma reservoir focused at same depths that fueled prior eruptions (Kiser et al., 2018)

Deep crustal low-velocity zone and contrast in Moho reflectivity - input of mantle melts east of MSH (Hansen et al., 2016).

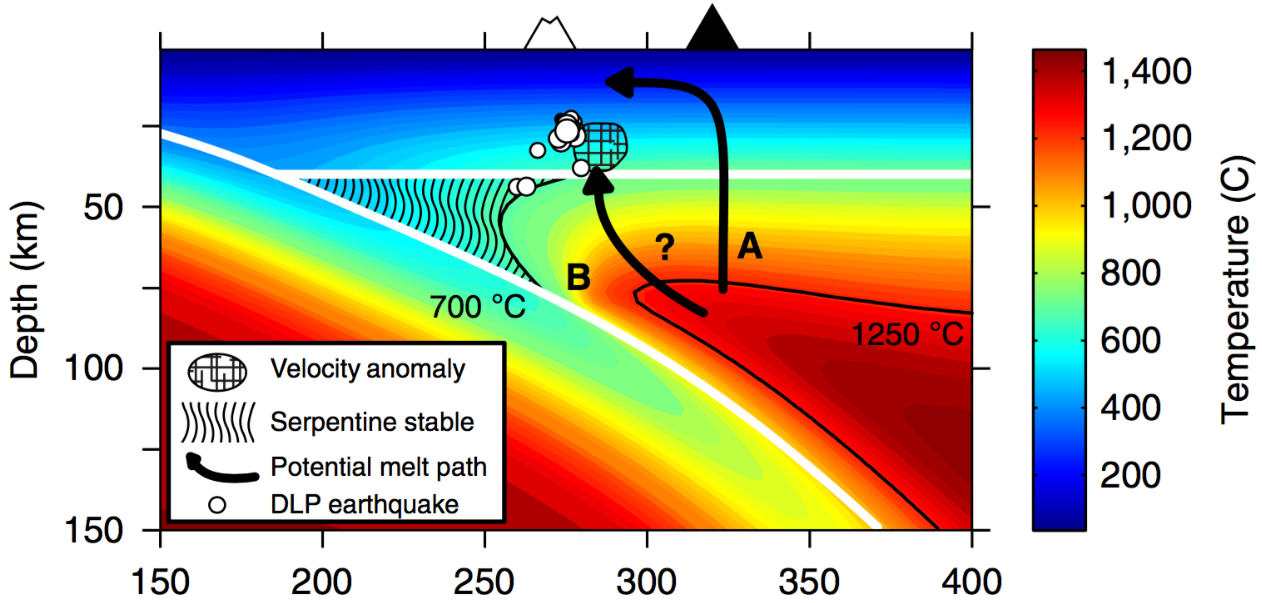

Thermal model from Syracuse et al., 2010
Seismic and Interp. From Hansen et al. 2016

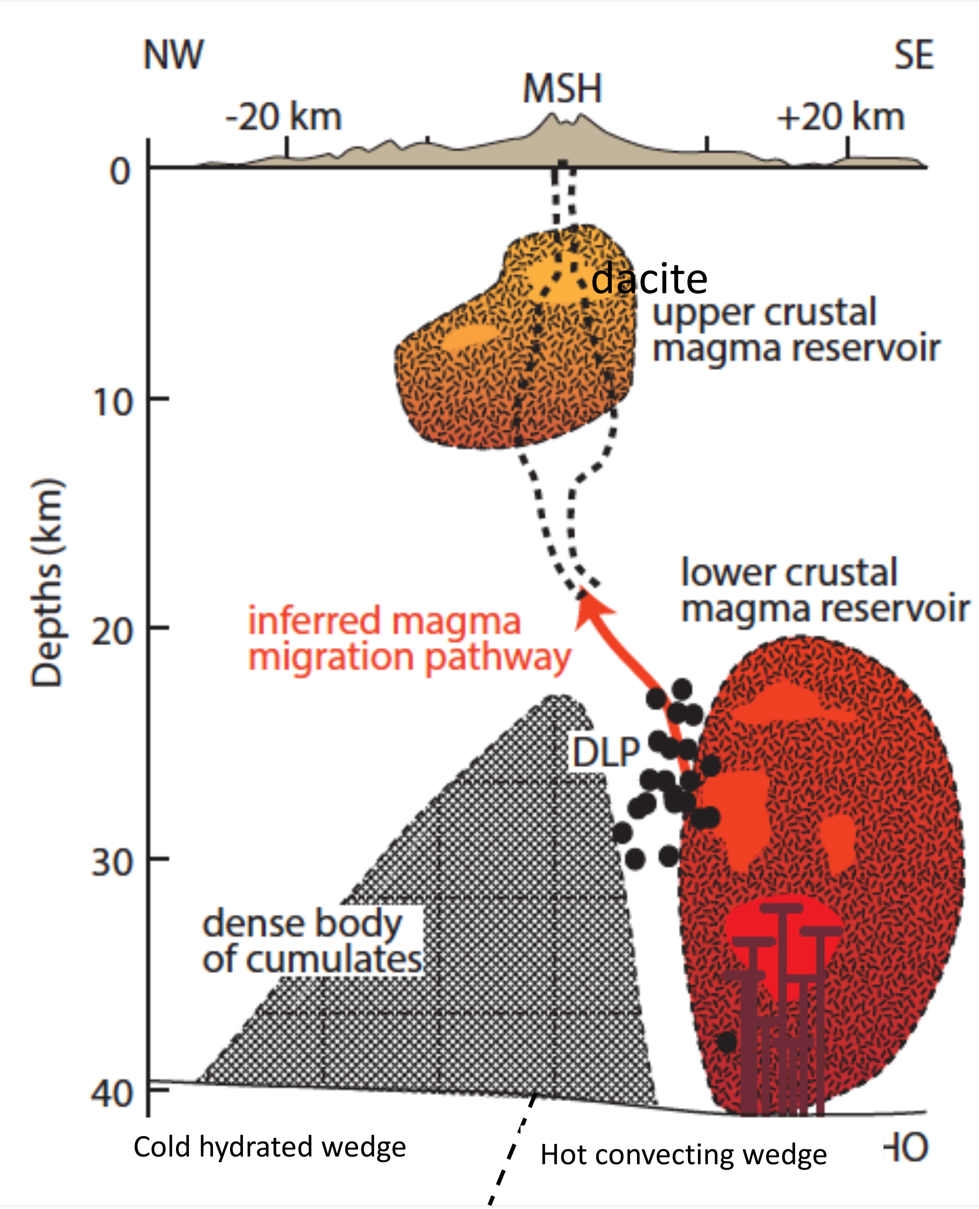

Maren Wanke, Olivier Bachmann et al. at ETH

Questions/Topics

- Magma reservoir depths inferred from geophysical imaging, geodesy, and petrology (links to other lectures this week). How are they sensing different parts of the system or stages of the eruption life-cycle?
- How does melt organization change with depth, longevity of magmatic system, melt flux?
- Relating seismicity to magmatic system structure (more from Greg Waite, Diana Roman, Robin Matoza in later lectures).
- I neglected time-dependent structure constraints, but there are many interesting questions about magmatic sensitivity to small pressure or shear strain perturbations that could be partly addressed with seismology